

Polymers for Battery Applications—Active Materials, Membranes, and Binders

Adrian Saal, Tino Hagemann, and Ulrich S. Schubert*

In the light of an ever-increasing energy demand, the rising number of portable applications, the growing market of electric vehicles, and the necessity to store energy from renewable sources on large scale, there is an urgent need for suitable energy storage systems. In most batteries, the energy is stored by exploiting metals or metal-ion-based reactions. However, nearly every modern battery would not function without the help of polymers. Polymers fulfill several important tasks in battery cells. They are applied as binders for the electrode slurries, in separators and membranes, and as active materials, where charge is stored in organic moieties. This review concentrates on recent research on polymers utilized for every aspect of a battery, discussing state-of-the-art lithium cells, current redox-flow systems, and polymeric thin-film batteries. The focus is on the properties of the polymers applied in different battery systems and how they affect their overall performance.

both large- and small-scale energy storage, ranging from large pumped hydroelectric storage to very small battery cells for hand-held devices.

Secondary batteries are among the more promising energy storage technologies, with a wide range of applications.^[4] Since the development of the lead acid battery in the second half of the 19th century (Gaston Planté, 1860), a broad range of batteries has been invented.^[5] Notable examples are the nickel/cadmium cell (1899)^[6] and the lithium-ion battery, which was developed in the 1970s.^[7] Today, batteries are omnipresent in the everyday lives of a large part of the world's population. They find application in numerous fields, ranging from handheld or portable

1. Introduction

In 2018, the total energy consumption of the world grew by 2.3%, nearly doubling the average growth rate from 2010 to 2017. In the same year, the electricity demand grew by 4%.^[1] A large proportion of the produced energy came from fossil fuels, only 26% of the electricity was generated by renewable sources.^[2] Due to their large environmental impact and the ongoing climate crisis, it is of great importance to reduce the CO₂ emissions in electrical energy production and, thus, to increase the amount of energy generated by renewable sources.^[3] To ensure network stability and reliability with an increasing number of intermittent renewable sources, more suitable storage technologies are required.^[4] Several systems have been developed for

devices to electric vehicles (including vehicles with combustion engines) to large-scale energy storage for renewable sources.^[8] Each field has unique requirements for the applied batteries, therefore different battery types have been developed to meet the demands.

The most dominant type of secondary batteries for modern devices is the lithium-ion battery. Lithium-ion batteries possess high energy densities, good rate capabilities, and a long cycle life. Since their commercialization in 1991, they have been applied in many portable devices, electric vehicles and even in large-scale energy storage systems.^[7] Since 2000, the share of the worldwide produced lithium for application in batteries (35% of the total production in 2015) has increased by 20% per year.^[9]


Another, less known battery type is the redox-flow battery (RFB). With their independent scalability of capacity and power, they are in particular interesting for large-scale storage of renewable energy with regard to grid stability.^[10]

A recent, so far not commercially available type of batteries is the organic battery. Here, an organic compound (small molecule or polymer) is responsible for charge storage. Organic batteries offer high rate capabilities, cheap starting materials, and are less environmentally challenging compared to metal-based batteries. Possible fields of application are small, lightweight, and easily recyclable products.^[11]

None of the above-mentioned batteries would work without polymers. Polymers can be found in the electrodes, where they act as binders, ensuring a good adhesion and contact among the different materials. Furthermore, many membranes are based on polymers. Here, the macromolecules have to be ion-conducting as well as mechanically and chemically robust. In addition, organic batteries rely on polymeric active materials. This review discusses the diverse possibilities polymers have

A. Saal, Dr. T. Hagemann, Prof. U. S. Schubert
Laboratory of Organic and Macromolecular Chemistry (IOMC)
Friedrich Schiller University Jena
Humboldtstrasse 10, Jena 07743, Germany
E-mail: ulrich.schubert@uni-jena.de

A. Saal, Dr. T. Hagemann, Prof. U. S. Schubert
Center for Energy and Environmental Chemistry Jena (CEEC Jena)
Friedrich Schiller University Jena
Philosophenweg 7a, Jena 07743, Germany

 The ORCID identification number(s) for the author(s) of this article can be found under <https://doi.org/10.1002/aenm.202001984>.

© 2020 The Authors. Published by Wiley-VCH GmbH. This is an open access article under the terms of the Creative Commons Attribution License, which permits use, distribution and reproduction in any medium, provided the original work is properly cited.

The copyright line for this article was changed on 28 September 2020 after original online publication.

DOI: 10.1002/aenm.202001984

been applied in batteries and how their properties affect the performance of the different battery types.

Depending on the field of application, different values and parameters are of importance. However, it has to be noted that a direct comparison of values from different studies or publications has to be handled with care, as the experimental setups might differ or because different materials from other sources were applied. The measured parameters can only show trends and qualitative statements. Quantitative and comparative values would have to be evaluated in a single study under constant and well-defined conditions.

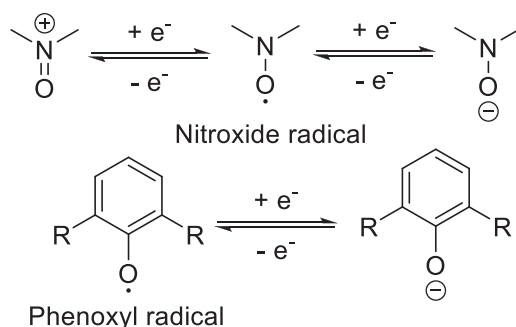
2. Active Materials

While established batteries usually rely on inorganic compounds and metals as charge-storing materials, a new class of redox-active polymers, with organic moieties that are able to reversibly store electrons, has emerged during the last years. The utilization of organic polymers offers several advantages. Polymers can be easily synthesized from basic chemicals and potentially renewable sources, which lowers the price and makes environmentally harmful mining unnecessary. Furthermore, the recycling or disposal at the end of the lifetime is more facile, as polymers can simply be incinerated with regular waste and do not need to be treated separately. Several different concepts have been proposed, ranging from conjugated polymers to organic sulfides and carbonyls to stable organic radicals. Each compound class has its own advantages and disadvantages, which will be shortly discussed in this section.

2.1. Solid-State Batteries

First organic batteries were constructed using conjugated polymers as active materials in the 1980s. The conjugated polymer's backbone can store several delocalized charges.^[12] Namely doped polyacetylene,^[13] polypyrrole, and polythiophene^[14] were applied in those early organic batteries. However, the major drawbacks of this type of battery are the strongly sloping voltage during charge and discharge, caused by the electronically connected, strongly interacting charges, and the limited number of doping sites.^[15] These restrained the application possibilities and commercially available cells were discontinued already after a few years.^[16] To overcome the limitations of conjugated polymers, redox-active units were linked to an insulating backbone. The localized active sites lead to distinct redox potentials, yielding constant charge and discharge voltages. However, the insulating nature of the backbone requires an additional use of conducting (carbon) materials.

One important example for these active materials is the group of stable organic radicals. In 2002 Nakahara et al. reported poly(2,2,6,6-tetramethylpiperidinyloxy methacrylate) (PTMA) as a cathode material and since then a strongly growing field of research has been established.^[11a] Organic radicals can be oxidized to cations and reduced to anions (exemplarily for nitroxide and phenoxy radicals in **Scheme 1**).^[17] As in every other organic active material, electron-withdrawing and electron-donating functional groups strongly influence the redox potential and, thus, the stability of the charged species.^[18]

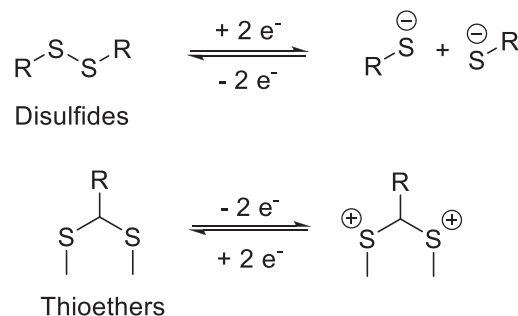


Scheme 1. Schematic representation of the redox behavior of nitroxide radicals.

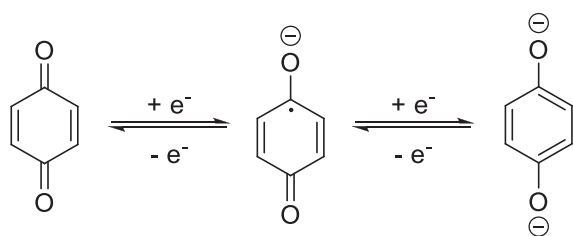
It is advantageous that no highly reactive intermediate species, such as radical cations or radical anions, occur in the redox reactions, in contrast to disulfides or carbonyls. Furthermore, organic radicals possess very fast electron transfer kinetics, making rapid charging and high-power discharging possible.^[19] Another example for organic redox-active materials is organic sulfides, e.g., disulfides or thioethers. In disulfides, the redox state changes between disulfides and thiolate anions (**Scheme 2**). One drawback of disulfides is their low cycling stability due to the constantly occurring bond breaking and reformation of bonds. The slow reaction rates of this reaction also lead to relatively slow charge transfer kinetics.^[20] In thioethers, no bonds are cleaved, but the sulfur itself is oxidized to form a positive charge, thus providing superior kinetics.^[21] As sulfur is an abundant, cheap, and environmentally friendly material, research still targets the overcoming of the drawbacks of organic sulfides to develop commercially usable systems, despite their mentioned disadvantages.

A third type of thoroughly investigated redox-active materials is the class of carbonyl compounds, in particular the quinone family. The members of this class of compounds can reversibly be reduced to alkoxide groups in a two-electron process, in case of aldehydes and ketones (**Scheme 3**).^[22] In quinones, the driving force of the reduction is the aromatization of the system. Several derivatives have been published, ranging from quinones to imides to structures that possess alternative, electron-withdrawing substituents, such as malononitrile, in place of the carbonyl oxygen.^[23]

Furthermore, viologen-based structures can be applied as redox active moieties.^[24] The quaternized bipyridinium units can be reduced to radical cations in one-electron processes.



Scheme 2. Schematic representation of the redox reactions of organic sulfides.



Scheme 3. Schematic representation of the redox reaction of quinones.

Further reduction (often an irreversible process) leads to a charge-neutral structure (**Scheme 4**). Due to its low redox potential, an application on the anodic side is usually preferable.

As comprehensive overviews on organic battery active materials were published recently, this review will not contribute to this topic in further detail. Interested readers are referred to the reviews of Friebe and Schubert in 2017^[25] and Friebe et al. in 2019,^[26] and Muench et al. from 2016,^[27] for all-organic polymer-based batteries. Furthermore, the reviews of Bhosale et al. from 2018^[28] and Shea and Luo from 2020^[29] discuss organic active materials (polymeric and nonpolymeric) for metal ion batteries.

2.2. Polymer-Based Redox-Flow Batteries

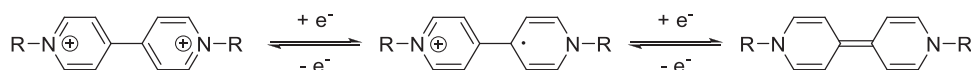
Besides thin-film batteries, polymeric active materials can also be used in RFBs, where they are applied in dissolved form in liquid electrolytes. Generally, the same active units as for thin-film batteries can be utilized, but, in contrast to solid-state batteries, the solubility of the polymer has to be as high as possible. In addition, the overall viscosity of the polymer solution represents an important performance parameter.^[30] To tackle the challenges of too high viscosities and too low solubilities, different approaches were studied, e.g., dendrimeric or micellar structures,^[31] the introduction of tailor-made comonomers that increase the solubility with a simultaneous decrease in viscosity,^[30b,32] and polymeric nanoparticles that can be suspended in the electrolyte solvent to minimize the internal viscosity.^[33]

This review only covers the most recent literature on polymeric active materials in RFBs. For more information and publications, readers are referred to the comprehensive reviews by Lai et al.,^[34] Winsberg et al.,^[30b] and by Ding et al.^[35]

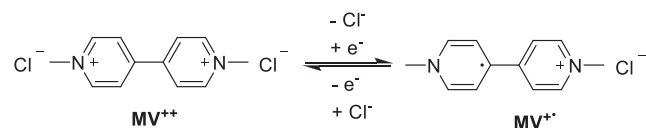
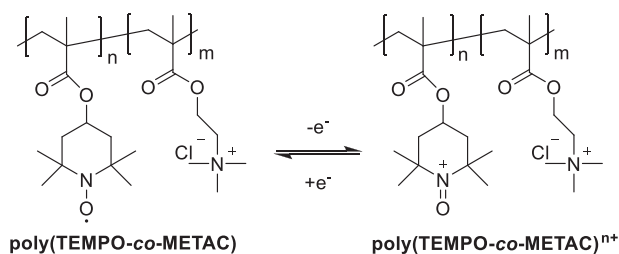
2.2.1. (2,2,6,6-Tetramethylpiperidin-1-yl)oxyl (TEMPO)

Polymeric TEMPO derivatives were first applied in organic batteries by Nakahara et al. in 2002.^[11a] The fast redox kinetics and easy synthesis of the stable radical make the system very interesting for battery research. Thus, it has been thoroughly investigated in both solid-state and redox-flow batteries.^[36]

In 2018, Hagemann et al. fabricated an aqueous all-organic RFB, utilizing for the first time a small molecule as well as a



Scheme 4. Schematic representation of the redox chemistry of viologen.

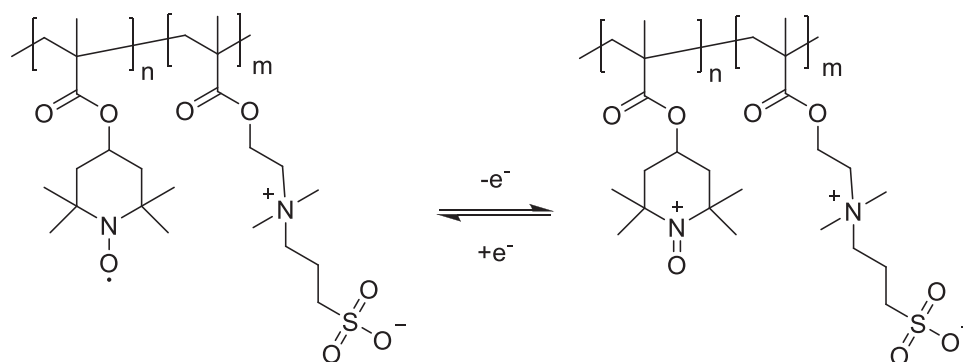


Scheme 5. Schematic representation of the structure and (applicable) redox reaction of the TEMPO-containing copolymer poly(TEMPO-co-METAC) and of MV. Adapted with permission.^[37] Copyright 2018, Elsevier.

polymeric charge-storage material.^[37] In this proof-of-concept investigation, the already evaluated active materials *N,N'*-dimethyl-4,4'-bipyridinium dichloride (MV) and poly(2,2,6,6-tetramethylpiperidinyloxy-4-yl methacrylate-co-[2-(methacryloyloxy)ethyl] trimethylammonium chloride (poly(TEMPO-co-METAC)) (**Scheme 5**), an aqueous sodium chloride solution and an affordable anion-exchange membrane (AEM) were used.

A stability test over 100 consecutive cycles at a constant current density of 5 mA cm⁻², with 0.5 M anode and cathode material concentration (each in 1.5 M NaCl_{aq}) was performed. The battery exhibited a maximum discharge capacity of 4.44 Ah L⁻¹, which corresponds to a material utilization of 66% and an energy density of 3.6 Wh L⁻¹, and a capacity loss of 0.13% per cycle.

In a subsequent study, Hagemann et al. synthesized a zwitterionic TEMPO-containing copolymer (**Scheme 6**), which featured a high solubility in aqueous electrolytes (volumetric capacity > 20 Ah L⁻¹ in 1.5 M NaCl_{aq}).^[32] At the same time, a relatively low absolute viscosity was achieved. To investigate the basic usability of this polymer as active cathode material, symmetric galvanostatic battery studies, applying either a cellulose-based dialysis membrane (molecular weight cut-off (MWCO) of 1 kDa) or an anion-exchange membrane, were performed. In long-term stability tests over 1000 consecutive charge and discharge cycles at a constant current density of 8 mA cm⁻², polymer concentrations which are equal to a charge-storage capacity of 5 Ah L⁻¹ in 1.5 M NaCl_{aq} were utilized. Independently from the membrane type, both cells exhibited an initial discharge capacity of 47 mAh (corresponding to a material utilization of 93%) and a capacity fading of 0.08% per cycle. Afterward, using a combined polymer-/small-molecule-based setup, an aqueous all-organic RFB with MV as anolyte and an anion-exchange membrane was tested. Active material concentrations of the TEMPO-containing polymer and MV equal to a charge-storage capacity of 10 Ah L⁻¹ in 1.5 M NaCl_{aq} were applied. During 125 consecutive cycles at a constant current density of 8 mA cm⁻², a discharge capacity of 88 mAh (equal to a material utilization of 88%) and a capacity decay of 0.29% per cycle were achieved.



Scheme 6. Schematic representation of the structure and redox reaction of the TEMPO-containing zwitterionic copolymer. Adapted with permission.^[32] Copyright 2019, The American Chemical Society.

In 2019, Nishide and co-workers reported on TEMPO-, viologen- and quinone-containing redox-active nanoparticles.^[38] Because of the hydrophilic molecular design, a high dispersibility was achieved and the restricted solubility of the used polymers was overcome (**Figure 1**). The polymer dispersions displayed fast redox kinetics, due to fast electron propagation within the particles. Furthermore, high concentrations of the redox moiety of over 1 M could be used in RFB experiments. In a first study, TEMPO- and viologen-containing nanoparticles were dispersed in aqueous 3 M NaCl solutions to obtain the catholyte and anolyte with a concentration of the redox-active moiety of 0.66 and 0.4 M, respectively. As a separator a conventional cellulose-based dialysis membrane with a pore size of 5 nm was utilized. A long-term stability test over

100 cycles at a current density of 1.5 mA cm^{-2} revealed a volumetric charging capacity of 7.2 Ah L^{-1} , which correlates to a material utilization of 66%, and a rather limited coulombic efficiency (CE) of 80%. However, a low capacity loss of only 0.07% per cycle was observed. To achieve a higher cell voltage (1.3 V instead of 1.1 V) and higher coulombic efficiencies in a subsequent battery test, a diazaanthraquinone-containing nanoparticle dispersion (1.5 M) was utilized as anolyte. With a current density of 4 mA cm^{-2} , a similar capacity decay of 0.08% per cycle was achieved during 50 consecutive charge/discharge cycles. However, despite the significantly higher concentration, a lower volumetric charge capacity of $\approx 6.3 \text{ Ah L}^{-1}$ was observed, corresponding to a poor material utilization of only 15%.

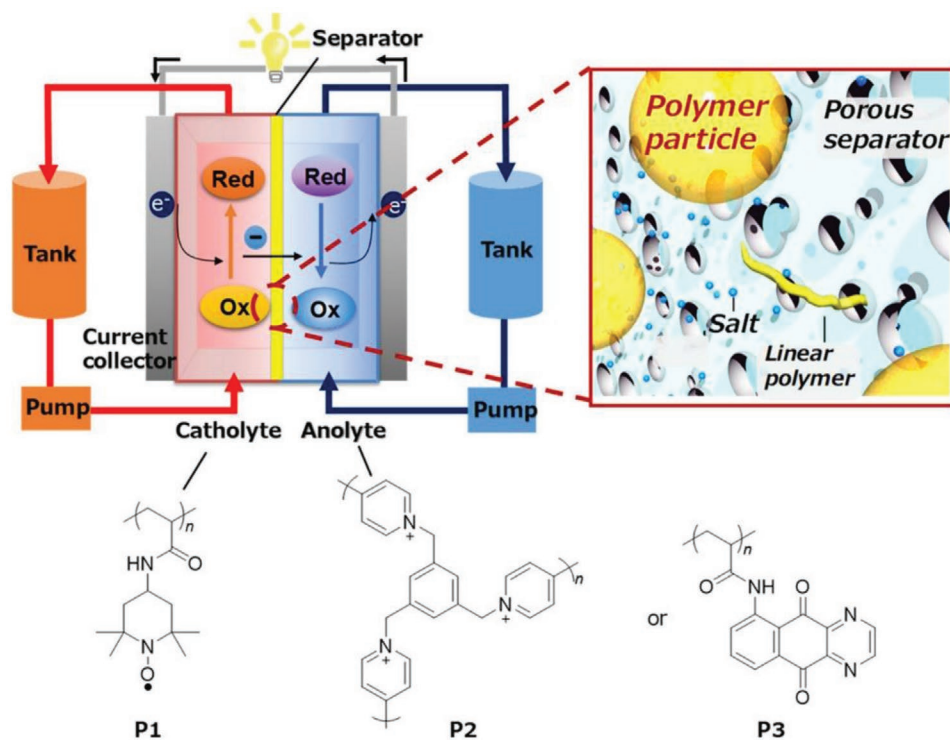
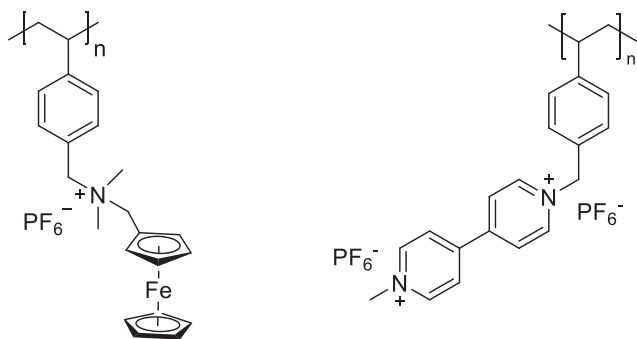


Figure 1. Schematic representation of the used active materials and the concept of the nanoparticle-based RFB. Reproduced with permission.^[38] Copyright 2019, American Chemical Society.



Scheme 7. Schematic representation of the structure of the ferrocene- and viologen-containing polymers. Adapted with permission.^[41] Copyright 2017, IOP Science.

2.2.2. Ferrocene (Fc)

Fc is a widely studied organometallic compound, which exhibits a reversible redox chemistry. The di(cyclopentadienyl) iron sandwich compound can be reversibly oxidized to the ferrocenium cation.^[39] Therefore and due to its very fast redox kinetics, ferrocene has been applied in polymeric batteries, demonstrating good performances.^[40]

In 2017, Montoto et al. utilized ferrocene- and viologen-containing redox-active polymers, as catholyte and anolyte, respectively (**Scheme 7**).^[41]

Both polymers were chosen due to their facile availability by one-step syntheses, their electrochemical stability, and their fast transfer kinetics. Both polymers revealed high molar masses ($M_N = 271$ kDa for the ferrocene-based and 318 kDa for the viologen-based polymer). As separators, two hydrocarbon-polymer-based porous membranes (Celgard 2325 and Daramic 175) with differing porosity were used. In a proof-of-concept cell test utilizing effective concentrations of the redox-active moieties ferrocene and viologen of 0.01 M, over 50 charge/discharge cycles at a current density of 0.58 mA cm⁻² were conducted. Both porous membranes exhibited a material utilization of around 75%. However, after 15 cycles, a capacity decay of around 12%, equal to a loss of 0.8% per cycle, was observed.

Only recently, Borchers et al. published a copolymer of a ferrocene substituted methacrylamide and the water-soluble comonomer METAC, for an application in RFBs.^[42] The synthesized copolymer exhibited high solubilities in water and the active units reveal reversible redox reactions in 0.1 M NaCl. In battery tests, very high CEs of over 99% were achieved with a capacity fade of 10% over 100 cycles at 4 mA cm⁻². When cycling the active material at an elevated temperature of 60 °C, higher capacities were observed, due to the decreased viscosity of the solution and increased diffusion coefficients. Electrochemical cycling at 60 °C revealed a stable redox process over 100 cycles at 4 mA cm⁻², again with CEs above 99%. Open-circuit voltage experiments show little self-discharge of the system at elevated temperatures. These results might expand the range of application of RFBs to warmer climates and conditions and might decrease the usage of expensive cooling systems.

2.2.3. Imides

Imides have been intensively studied for electrochemical purposes. Usually, each imide functional group can be reversibly reduced two times. Thus, the commonly used naphthalene or perylene diimides are able to store up to four electrons.^[43] In general, an enolization reaction of the carbonyl groups takes place, promoted by conjugated groups.^[44] Multiple polymeric imide structures have been applied in thin-film batteries.^[45]

In 2018, Winsberg et al. evaluated phthalimide-containing copolymers with varying comonomer composition regarding their usability as anode material in a nonaqueous RFB.^[46] To enhance the solubility in organic solvents, (vinylbenzyl) triethylene glycol monomethyl ether (TEGSt) was used as a comonomer. The polymer exhibited a quasi-reversible redox behavior with a potential of -1.89 V versus Ag/AgNO₃ in *N,N*-dimethylformamide (DMF). The principal applicability of poly(*N*-vinylbenzyl phthalimide-*co*-TEGSt) was investigated in a nonpumped setup, utilizing poly((2,2,6,6-tetramethylpiperidin-1-yl)oxyl-*co*-polyethylenglycol methacrylate) as catholyte. During ten consecutive cycles with a concentration of the redox-active repeating units of 0.01 M, a capacity fading of around 4.5% per cycle was observed in both DMF and dimethoxyethane (current densities of 0.5 and 0.4 mA cm⁻², respectively). Because of the high capacity fading, this phthalimide-containing copolymer is not suitable for an application as anode material in RFBs.

Yan et al. described a polymer-based RFB utilizing aqueous-dispersed particulate slurry electrolytes, namely polyhydroquinone as catholyte and a polyimide as anolyte.^[47] In contrast to the polymers used in previous studies, the redox-active moieties are located on the main-chain aromatic rings (**Figure 2**). For the flow-battery studies, particulate slurries with redox-active-unit concentrations of 1 M in 2 M H₂SO₄ for both anolyte and catholyte and a dialysis membrane (MWCO of 1 kDa, Viskase) were utilized. In a first test, a polymeric naphthalene diimide was employed as catholyte and a discharge capacity of 8.95 Ah L⁻¹, a moderate capacity loss of 0.36% per cycle and coulombic efficiencies of 87% were achieved during 50 cycles at a current density of 5 mA cm⁻². In a second, long-term stability test over 300 charge/discharge cycles using the same electrolytes but at a higher current density of 20 mA cm⁻², significantly different results were observed. The maximal discharge capacity dropped to 4.95 Ah L⁻¹, the capacity loss per cycle decreased to 0.1% per cycle, and the coulombic efficiencies increased to 100%. Finally, the usability of a dianhydride-*p*-phenylenediamine derivative of the polyimide as active cathode material was investigated. A battery test, conducted over 50 consecutive cycles at a current density of 5 mA cm⁻², exhibited significantly less favorable performance parameters, such as a lower discharge capacity of 5.38 Ah L⁻¹ and a higher capacity decay of 1.1% per cycle.

2.2.4. Viologen

Due to its reversible reduction to form a radical anion, viologens have found their way in various polymers for applications in both thin-film and redox-flow batteries.^[24b,c,36b,48]

One approach was presented by Rodríguez-López and co-workers.^[33] The authors investigated polymeric redox-active

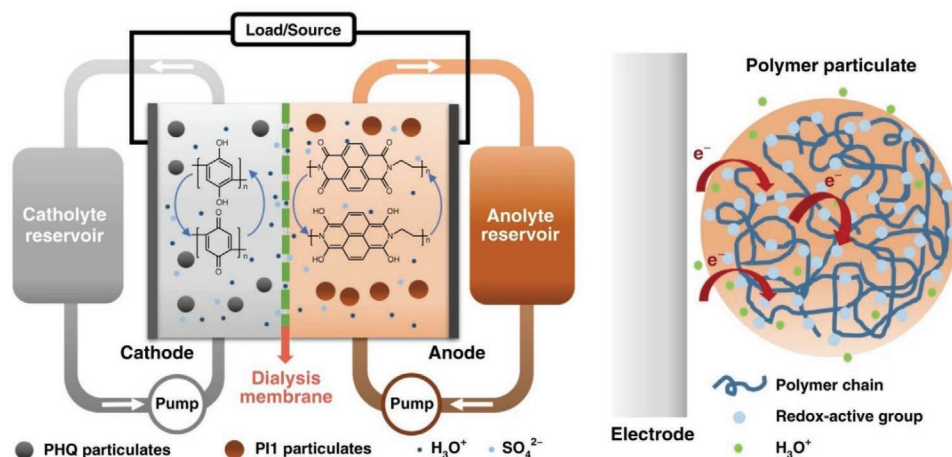


Figure 2. Schematic representation of the used polymer particulate and the developed all-polymer particulate slurry RFB. Reproduced with permission.^[47] Copyright 2019, Springer Nature.

colloids whose combination of a defined spherical structure, size tunability, and high charge capacity makes them interesting candidates for improved RFBs.^[33,49] However, the reported nonaqueous polymeric redox-flow battery (pRFB), utilizing ferrocene- and viologen-based colloidal particles with 10 M redox-active units as catholyte and anolyte, respectively (**Figure 3**), exhibited only moderate performance parameters, such as a low material utilization of 21%, and a useable current density of 0.2 mA cm^{-2} , but revealed stable cycling at a capacity of 55 mAh L^{-1} over 11 consecutive cycles.

In a subsequent study, Rodríguez-López and co-workers investigated the impact of charge dynamics and conditioning on the cycling efficiency.^[50] Therefore, a crosslinked polystyrene-based viologen polymer ($\approx 830 \text{ nm}$ in diameter) was fabricated. During charge/discharge experiments, the electrolyte with a 1 M solution of the redox-active colloid could be cycled in a stable manner only for eight cycles. In the first cycle, a low coulombic efficiency of 60% was observed, increasing to 100% during the following cycles. Furthermore, a material utilization of 72% was achieved. Over the ten cycles, a massive capacity loss of nearly 88%, equal to a decay of 11% per cycle, was observed.

2.3. Conclusions, Challenges, and Perspectives

In summary, polymeric active materials exhibit many advantageous properties. Usually, their synthesis is straightforward and provides a lower environmental impact as observed for battery relevant metals. In addition, the resources required for the preparation is available worldwide (based on oil, gas (fracking), renewable resources or power-to-x technologies), independent of regional conflicts and the irregular distribution of raw materials and metal ores. This makes the overall synthesis less expensive and less susceptible to price changes on the global market. Furthermore, the molecular structure can easily be modified to accommodate to the needs of the particular battery system. The redox potential can be tuned or solubility-enhancing groups can be introduced for an application in flow batteries. In electrochemical tests, most active polymeric materials perform well, often displaying very high charge and discharge capabilities.

Polymeric flow batteries are able to rely on water as an electrolyte solvent, making use of sulfuric acid (as is the case in vanadium redox-flow batteries) obsolete. This lowers the environmental impact of the whole battery system. Moreover, cheap and easily producible size-exclusion membranes can be utilized. After the lifetime of the battery, polymeric active materials can be easily recycled, as no environmentally challenging metals or metal oxides are present in the cells. On the other hand, the current volumetric and in some cases gravimetric capacity is inferior to lithium-ion batteries. Furthermore, the cycling stability has to be improved and also the shelf-life of polymeric materials still needs to be evaluated in more detail. In case of the flow-battery applications, the viscosities of polymer solutions represent a major challenge. For further exploration of the subject, modifications of the polymeric structure are necessary to enhance the solubility and, at the same time, to decrease the viscosity.

In our opinion, a great potential lies in the exploration of green active materials and solvents, to make the application of in particular flow batteries more appealing to a wider community and public, which might be concerned about safety issues of vanadium redox-flow batteries (VRFBs). This also applies for polymeric solid state batteries. Furthermore, the high viscosities of polymeric flow batteries might be overcome by utilizing branched polymers or small molecules instead of polymers. In the latter case, size exclusion membranes would have to be replaced by more expensive ion-exchange membranes (IEMs). On the other hand, the overall operation costs might stay constant, as less powerful pumps would be required. This would have to be evaluated in detail for the different systems. In case of polymeric solid state batteries, electrode optimization is crucial. While numerous active materials have been published, more effort has to be placed in identifying the optimal ratios of electrode material, binder and carbon additive and to find the correct combinations of the aforementioned.

3. Membranes and Separators

The separator plays a crucial role in a battery. As the separating medium between the two electrodes, it has to meet certain

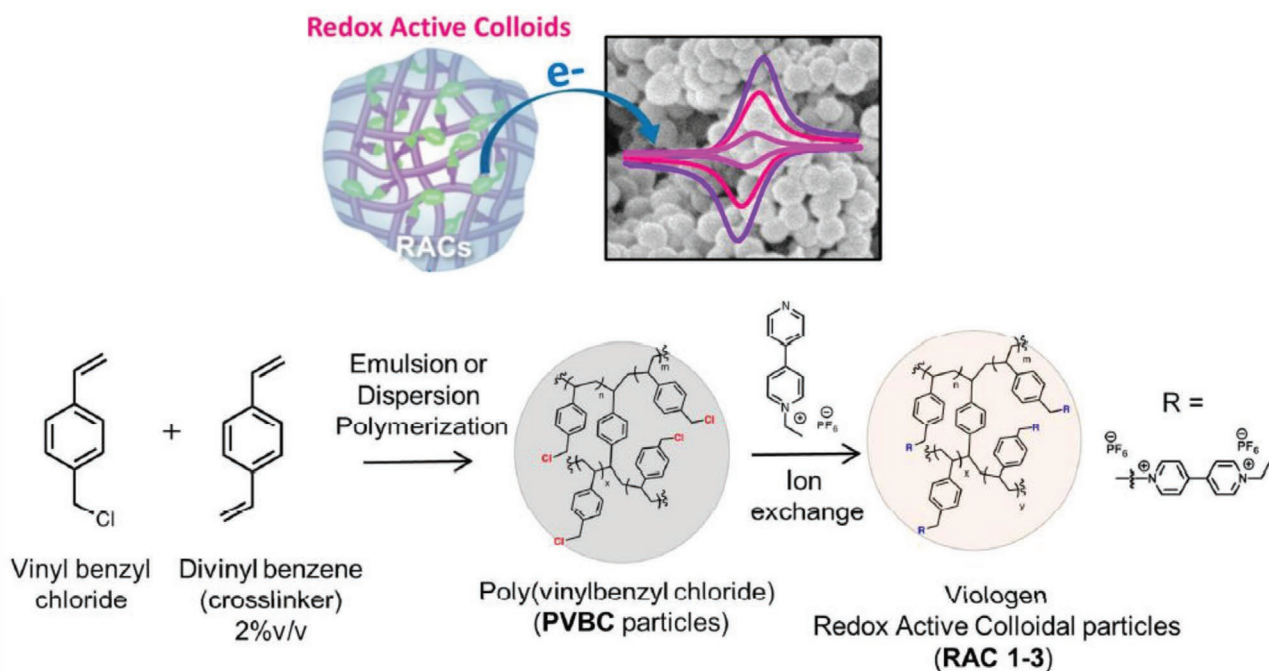


Figure 3. Preparation of the redox-active colloids (RAC) via an emulsion or dispersion polymerization and subsequent polymer analog reaction with viologen as potential charge-storage materials for RFB application. Reproduced with permission.^[33] Copyright 2016, American Chemical Society.

requirements to enable a stable working cell. A separator has to be 1) electronically insulating to avoid short circuits between the electrodes, it has to be 2) ionically conducting for charge compensation during cycling, it needs to offer 3) a good wettability and interaction with the electrolyte solvent, to further increase the ionic conductivity and to decrease the internal resistance and it must 4) exhibit good thermal and mechanical stabilities to avoid shrinkage at higher temperatures and to withstand mechanical stress and tension during assembly.^[51] One of the most significant challenges a separator has to match when working with bare metal electrodes, such as lithium, sodium or zinc, is dendrite formation. This difficulty can be tackled by either improving the uniformity of the solid–electrolyte interphase (SEI) or by increasing the mechanical strength of the separator.^[52] Another challenge is the undesired shuttling of redox products, for example polysulfides in Li–S batteries or Mn²⁺ in spinel-type lithium manganese oxides, which can be mitigated or completely inhibited by properly designing the separator.^[53] To meet all these occurring challenges with current separators and membranes requires an intelligent design.

Several parameters are important when describing and comparing the performance of battery separators. The thickness determines both ionic conductivity and mechanical stability. Here, a trade-off has to be made as thinner membranes possess higher ionic conductivity but lack of mechanical stability. The ratio of the resistance of the separator immersed in an electrolyte and the resistance of the electrolyte alone is the MacMullin number, which should be as low as possible. The wettability defines the interactions between the membrane and the electrolyte solvent and is determined by the contact angle of a drop

of water (or electrolyte solvent) on the separator surface. A good wettability usually correlates to a high affinity between separator and solvent and, thus, higher conductivities. The air permeability is determined by the Gurley value. Furthermore, pore size and porosity determine the ionic conductivity and should be designed to accommodate the electrolyte but no particles, which were blended into the electrode slurry. Thermal, mechanical and chemical stability should all be as high as possible to prevent malfunction of the system at high temperatures, due to stress during manufacturing or because of reactive species inside the cell. A list of the desired parameters with selected target values can be found in **Table 1**.^[54]

When ionic polymers are used as membrane material, the term IEM or single-ion conducting polymers (SICP) is used. The working principle of ion-exchange membranes was first described by Ostwald in 1890, who observed that certain ions could not pass semipermeable membranes due to electrostatic repulsion.^[55] Furthermore, the Donnan exclusion effect, which describes equilibria of semipermeable membranes states that only the corresponding counter-ions can permeate the membranes, while species of the same charge are repelled.^[56] The integrated ionic functional groups, depending on the membrane type negatively or positively charged, form an electrostatic bond with the contrary charged ions, which can be exchanged by ions with the same charge. The effectiveness of this reversible and stoichiometric process depends on the strength of the electrostatic bond.^[57] SICPs can be divided into cation-exchange membranes (CEM) and AEMs. CEMs contain negatively charged pendant groups, such as sulfonate, carboxylate or phenolate, and AEMs possess positively charged functional groups, such as quaternary ammonium. CEMs are

Table 1. Important performance parameters of a separator in lithium-ion batteries and target values for commercially available separators.^[54]

Parameter	Target
Thickness [μm]	<25
MacMullin number	<8
Gurley [$\text{s}/10\text{ cm}^3$]	\approx 25
Pore size [μm]	<1
Porosity [%]	\approx 40
Shear strength [9.8 mN/25.4 μm film]	>300
Melt integrity [$^{\circ}\text{C}$]	>150
Chemical stability	High, long-term
Thermal stability	<5% shrinkage (60 min, 90 $^{\circ}\text{C}$)
Tensile strength	<2% offset at 69 bar
Skew [mm m^{-1}]	<2

preferably applied in cells where cations or protons are necessary charge carriers and permeating anions cause undesirable side reactions. Furthermore, cation- or proton-exchange membranes are utilized in proton-exchange-membrane fuel cells (PEMFC).^[58] AEMs are applied in cells where anions compensate occurring charges, e.g., in aqueous, basic media. Notable examples are alkaline zinc and zinc–air batteries and hydroxide-exchange membrane fuel cells (HEMFC).^[58,59] When compared to CEMs, AEMs usually possess higher electrical resistance and a lower conductivity, due to the lower anion mobility.^[60] Furthermore, CEMs are mostly commercially available and exhibit a high variability in structure and good chemical stabilities.^[61]

In general, polymer electrolytes can be divided in different categories, depending on the applied electrolyte solvent, salt and polymer backbone. The categories used in this review are listed below and are adopted from current literature and a review by Hallinan and Balsara^[62]

- 1) Gel polymer electrolyte (GPE): A polymer swollen in an electrolyte solution, forming a stable gel.
- 2) Solid polymer electrolyte (SPE): A polymer film containing an electrolyte salt and no electrolyte solvent. However, in some cases plasticizers may be present.
- 3) Ionic-liquid-based polymer electrolyte (IL-PE): A polymeric separator containing an ionic liquid as electrolyte.
- 4) SICP: A class of polymers where either the backbone itself or a side-chain or pendant group carries a charge. A special case is the class of polymerized ionic liquids (PIL).

This review cannot cover the vast amount of literature on separators, membranes and polyelectrolytes in this chapter in all details. It will solely focus on highlights of the most recent timespan of 2016 to 2019. Therefore we recommend other, more detailed reviews on this topic, for interested readers. A very detailed review on commercial separators and their parameters was published by Celgard researchers, Arora and Zhang in 2004.^[54b] Comprehensive reviews on the design and characterization of separators are available from Zhang et al.^[51] and Lagadec et al.^[63]

3.1. Separators for Lithium-Based Batteries

The most common separators in commercially available lithium battery applications are polyolefin-based, such as polyethylene (PE) and polypropylene (PP). Advantages of this type of separator are the good mechanical stability and the ability to inhibit thermal runaways. On the downside, the hydrophobicity limits the wettability by electrolyte solvents and these membranes possess rather high production costs.^[64] As these are both commercially available and already described and investigated excessively,^[54b] the focus of this chapter will be on alternative polymers and on recent progress in separator research.

The above listed disadvantages led to more advanced separator designs, which are able to overcome the observed limitations and raise the performance of the membranes. Popular alternatives to PE and PP are polyvinylidene fluoride (PVdF), poly(acrylonitrile) (PAN), poly(methyl methacrylate) (PMMA), and cellulose.^[65] As each of the mentioned polymers has its own drawbacks, blends or copolymers are often utilized, or inorganic additives are used to improve the physical properties of the separators.

3.1.1. PVdF

PVdF and poly(vinylidene fluoride-*co*-hexafluoropropylene) (PVdF–HFP) have been widely studied as separators for different battery types.^[64–66] PVdF possesses a high electrolyte uptake, leading to high ionic conductivities of swollen polymers.^[67] However, the application of PVdF separators is limited by the low stability of electrolyte solvents in PVdF matrices and the low intrinsic ionic conductivity of the pure polymer, resulting from a high crystallinity.^[68] Of PVdF and PVdF–HFP, the latter possesses the lower crystallinity, due to its pendant side groups. Thus, it exhibits a higher electrolyte uptake and, hence, a higher ionic conductivity in the swollen state.^[69]

Kang et al. investigated the properties of an electrospun membrane consisting of a blend of cellulose acetate (CA) and PVdF.^[65e] By mixing CA and PVdF in an optimized ratio of 2:8, the electrolyte uptake, ionic conductivity and mechanical strength could be increased in comparison to pure PVdF. Higher amounts of CA lead to a decrease in both electrolyte uptake and mechanical strength. This effect was observed due to less available fluorine atoms, which are able to coordinate Li^+ , and a drop of the crystallinity with a simultaneous rise of the porosity of the manufactured membranes. As well, the thermal stability was increased. When assembling a cell with a Li anode, the described separator and a LiCoO_2 cathode, the initial (204 mAh g^{-1}) and overall capacity was increased by 47% compared to pristine PVdF, while also displaying better rate capabilities.

PVdF and polyvinyl alcohol (PVA) were mixed in a 5:1 ratio and immersed in an ionic liquid (*N*-methyl-*N*-butylpiperidine-bis(trifluoromethylsulfonyl) imide) by Ma et al.^[70] By incorporating 46 wt% of IL, high ionic conductivities of $1.19 \times 10^{-3}\text{ S cm}^{-1}$ were achieved. The lithium-ion transference numbers were determined to be 0.45 (with IL) and 0.29 (without IL). The authors suggested that t_+ might be further increased by utilizing larger, less mobile cations for the IL or by

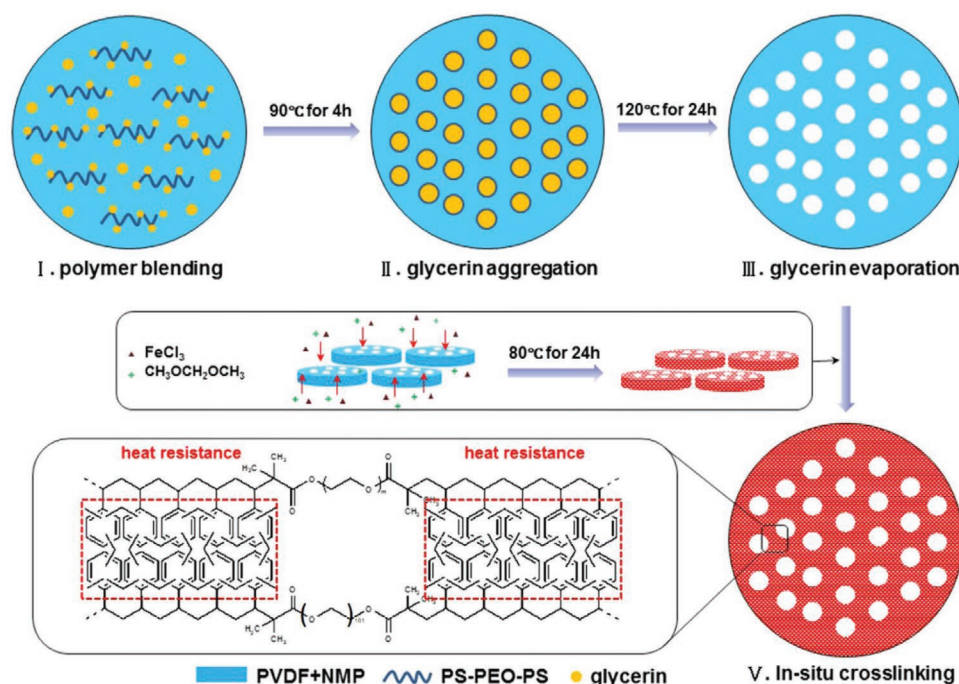


Figure 4. Schematic representation of the membrane forming by phase-inversion technique of the temperature-stable, hyper-crosslinked polymer. Reproduced with permission.^[71] Copyright 2016, American Chemical Society.

utilizing anions with lower coordination constants for lithium, increasing the diffusivity of Li⁺. A cell with Li/IL-PE/LiFePO₄ was constructed and revealed good discharge capacities of 105 mAh g⁻¹ after 99 cycles at 0.2 C (88% capacity retention).

Xiao et al. presented a separator with PVdF and an in situ crosslinked polystyrene–polyethylene oxide–polystyrene (PS–PEO–PS) triblock polymer, exhibiting high ionic conductivities and excellent thermal stability.^[71] PVdF was blended with different block copolymers and precursor membranes were formed by utilizing the phase-inversion technique (Figure 4). The in situ crosslinking was performed by a Friedel–Crafts reaction with formaldehyde dimethyl acetal and FeCl₃. In high-temperature experiments, a low shrinkage up to 260 °C was observed, making the membrane suitable for high-temperature applications. For weight ratios of about 60:40 (PEO:PS), high ionic conductivities of 1.38 × 10⁻³ S cm⁻¹ were achieved. When applied in Li/GPE[EC:DMC:EMC 1:1:1 w/w/w, 1 M LiPF₆]/LiFePO₄ cells, 100% capacity retention after 40 cycles at 0.1 C and an initial capacity of 138 mAh g⁻¹ was reported. The good ionic conductivity is attributed to the PEO block, which is also responsible for a uniform blending of the triblock polymer with PVdF. The crosslinking of the PS-block stabilizes the membrane at high temperatures.

3.1.2. PEO

PEO has been widely applied in polymer membranes and separators, mainly due to its ability to complex and conduct cations, such as Li⁺, in its amorphous regions.^[72] As a consequence, large efforts were devoted to decrease the crystallinity of PEO in order to increase the ionic conductivity. This was mostly

realized by adding nanofillers or applying polymer blends and copolymers.

Li et al. prepared a PEO-based gel polymer electrolyte with an in situ UV-crosslinked polyacrylate network.^[73] The membrane possesses a high ionic conductivity of 3.3 × 10⁻³ S cm⁻¹ and a high value for t₊ of 0.76. Compared to pristine PEO and commercially available separators, the thermal stability at up to 200 °C is significantly improved. Combustion tests revealed better flame retardation abilities. Applied in a Li/GPE/LiFePO₄ cell setup, an initial discharge capacity of 150 mAh g⁻¹ at 0.1 C was observed. Cycling at 0.5 C for 500 cycles revealed 81% capacity retention. The authors proposed that the improved properties arise from the high electrolyte uptake of the membrane.

Polyacrylate backbones with branched side-chains of PEO were evaluated in solid polymer electrolytes by Fu and Kyu^[74] By copolymerizing polyethylene glycol methyl ether acrylate (PEGMEA) and polyethylene glycol diacrylate (PEGDA), a crosslinked network with pendant PEG-groups was synthesized. A higher amount of PEGMEA reduces the glass transition temperature and raises the ionic conductivity of the SPE. At room temperature, a conductivity of up to 1.54 × 10⁻³ S cm⁻¹ was reached for pure PEGMEA electrolytes (20% PEGMEA, 40% succinonitrile, 40% Li bis(trifluoromethane)sulfonimide (LiTFSI)). In cell tests, SPEs with ratios of 10% PEGMEA and 10% PEGDA were applied (σ = 1.16 × 10⁻³ S cm⁻¹ at room temperature) with lithium anodes and LiFePO₄ or Li₄Ti₅O₁₂ cathodes. Both cells revealed virtually no capacity loss after 50 cycles at C/4.

A blend of PEO and poly(vinylpyrrolidone) (PVP) was used as an SPE in Mg-ion batteries by Anilkumar et al.^[75] PVP is able to lower the crystallinity of PEO, thus enhancing the ionic conductivity. At room temperature, the sample with

30 wt% of $\text{Mg}(\text{NO}_3)_2$ possesses a high ionic conductivity of $5.8 \times 10^{-4} \text{ S cm}^{-1}$, which outperforms previously reported Mg^{2+} -conducting SPEs. The cationic transference number was determined to be $t_+ = 0.33$ and the separator was applied in $\text{Mg}/\text{SPE}/\text{MgMn}_2\text{O}_4$ cells, which were, however, only investigated through CV.

A mesoporous organic polymer network, based on crosslinked triphenylamine, was integrated into a PEO matrix, which was used as a separator by Liu et al.^[76] The SPE, with LiTFSI as a filler salt, exhibited an ionic conductivity of $4.4 \times 10^{-3} \text{ S cm}^{-1}$ at 63 °C. Dendrite formation was hindered by the membrane and the authors suggested that the high conductivity arose from a lowered crystallinity, induced by the added mesoporous polymer. In full cells with $\text{Li}/\text{SPE}/\text{LiFePO}_4$ a capacity retention of 84% was observed after 300 cycles at 0.5 C.

3.1.3. PAN

PAN has been widely studied as a promising separator material for battery applications. Compared to commercial polyolefinic separators, it exhibits better ionic transport, good thermal, mechanical, and chemical stabilities, can take up more electrolyte, and achieves long cycling lifetimes.^[77] As well, suppressed dendrite formation was observed, due to its high mechanical stability. On the other hand, electrolyte leakage in long-term application decreases the performance of PAN.^[77b]

To improve the morphology of PAN membranes prepared via nonsolvent-induced phase separation, He et al. introduced a mixture of PAN and PVA and effectively increased the ionic conductivity and the cycling stability.^[78] When applying a PVA-to-PAN ratio of 10:90 or 20:80, a good porous morphology was achieved compared to pristine PAN, which exhibited a dense, nonporous structure using this method of preparation. Due to the high electrolyte uptake of 500 wt% (Celgard 2320: 68 wt%), higher ionic conductivities were achieved. In cell tests ($\text{Li}/\text{GPE}[\text{EC}:\text{DMC}:\text{EMC} 1:1:1 \text{ w/w/w}, 1 \text{ M LiPF}_6]/\text{LiCoO}_2$), capacity retentions of 95% after 200 cycles at 1 C were observed, compared to only 60% for the commercial Celgard 2320 membrane.

Huang et al. synthesized copolymers of acrylonitrile (AN) and maleic anhydride (MAH), which increased the performance of the separator (prepared via phase inversion (Figure 5)), compared to pure PAN membranes.^[79] The incorporation of MAH increased the electrolyte uptake, the ionic conductivity and the lithium transference number due to weaker interactions among the nitrile groups inside the copolymer and due to stronger interactions of electrolyte anions and carbonyl groups of maleic anhydride. The copolymer exhibited an ionic conductivity of $3.03 \times 10^{-3} \text{ S cm}^{-1}$ and a transference number of $t_+ = 0.57$ for a ratio of 4:1 acrylonitrile to MAH. Additionally, the contact angle between electrolyte solvent and separator was decreased. In cells of $\text{Li}/\text{GPE}[\text{EC}:\text{DMC}:\text{EMC} 1:1:1 \text{ w/w/w}, 1 \text{ M LiPF}_6]/\text{LiFePO}_4$ good cycling stability with 92% capacity retention after 50 cycles at 2 C was achieved, outperforming PAN separators.

Liu et al. performed two similar studies on PAN and P(AN-MAH) and the effect of polyhedral oligomeric silsesquioxane (POSS) on the morphology and electrochemical properties of the prepared membranes.^[80] In the first study, PAN was grafted from the vinyl-group-containing POSS, obtaining a

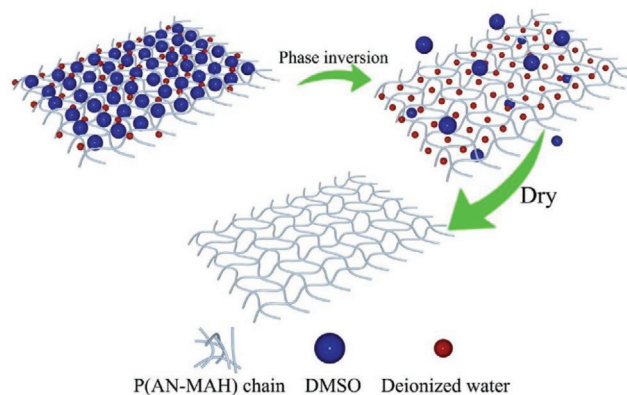


Figure 5. Schematic representation of the phase-inversion mechanism, applied for the synthesis of a P(AN-MAH) copolymer. Reproduced with permission.^[79] Copyright 2018, Elsevier.

membrane with an ionic conductivity of $6.06 \times 10^{-3} \text{ S cm}^{-1}$ for 8% POSS, a lithium-ion transference number of 0.59, a high porosity and electrolyte uptake, and an increased thermal stability, outperforming PAN without POSS. In cell tests ($\text{Li}/\text{GPE}[\text{EC}:\text{DMC} 3:7 \text{ w/w}, 1 \text{ M LiPF}_6]/\text{LiFePO}_4$), a capacity retention of 94% at 0.2 C after 80 cycles was observed. In case of the P(AN-MAH), POSS was only blended with the polymer to obtain the hybrid separator structure. All in all, a lower conductivity ($2.51 \times 10^{-3} \text{ S cm}^{-1}$), a lower porosity, a lower electrolyte uptake, and a lower lithium transference number were observed for separators with 5% POSS. In addition, the capacity retention (89% after 80 cycles at 0.2 C) was lower, indicating that the copolymer of PAN-(vinyl-POSS) outperformed the blend of P(AN-MAH) and POSS in all categories.

3.1.4. PMMA

Beside the above described polymers, PMMA is likewise suitable for an application in separators. Due to its carbonyl groups, excellent interactions with carbonate solvents are observed, which leads to a high electrolyte uptake.^[81] On the other hand, PMMA gel-polymer electrolytes suffer from poor mechanical properties at higher plasticizer or electrolyte contents due to gel-like mechanical behavior, which makes it difficult to produce free-standing films.^[82]

A Celgard PE membrane was coated with a mixture of poly(propylene carbonate) (PPC) and PMMA by Huang et al. to improve its interactions with the electrolyte and the ionic conductivity.^[83] PPC has a high affinity to carbonate electrolytes and is able to transport lithium ions. PMMA mechanically stabilizes the PPC film and is, in contrast to polyolefinic additives, compatible with the liquid electrolyte, while the Celgard PE membrane provides a mechanically stable foundation for the separator. By coating the PE separator, the ionic conductivity at room temperature was raised from $0.66 \times 10^{-3} \text{ S cm}^{-1}$ for PE to $1.71 \times 10^{-3} \text{ S cm}^{-1}$ for a ratio of 8:2 PPC to PMMA. Higher ratios of PPC to PMMA led to lower conductivities. In cells ($\text{Li}/\text{GPE}[\text{EC}/\text{DMC} 1:1 \text{ v/v}, \text{LiPF}_6]/\text{LiFePO}_4$) a 95% capacity retention was observed after 100 cycles at 0.1 C, and the rate capabilities outperformed pure PE separators.

PMMA was copolymerized with vinyl-containing POSS to improve the thermal and electrochemical properties of PMMA by Liu et al.^[84] GPEs with a 10% POSS content performed best. Compared to pure PMMA, a higher electrolyte uptake of 275 wt% was observed and the ionic conductivity was raised to $3.41 \times 10^{-3} \text{ S cm}^{-1}$. The lithium transference number is 0.49. In cell tests (Li/GPE[EC:PC:EMC:DMC 1:1:1:1 v/v/v/v, 1 M LiPF₆]/LiFePO₄), 99.8% capacity retention after 100 cycles at 0.5 C was observed. In addition, the rate capability was improved.

3.1.5. Other Polymers

Cellulose supported poly(propylene carbonate) was synthesized by Zhao et al. and applied as a separator in LiNi_{0.5}Mn_{1.5}O₄ batteries.^[85] Cellulose was utilized to stabilize the mechanically less stable network of polycarbonate. The propylene-carbonate containing separator revealed a large electrochemical stability window of 5 V, a good ionic conductivity of $1.14 \times 10^{-3} \text{ S cm}^{-1}$ and a lithium transference number of 0.68 at room temperature. In cells (Li/GPE[PC, 1 M LiODFB]/LiNi_{0.5}Mn_{1.5}O₄), 91% capacity retention was observed after 100 cycles at 0.5 C, while a commercial separator with liquid electrolyte performed poorly with 78% capacity retention and a lower capacity in rate capability tests at 1 to 5 C. These results were attributed to the good affinity between polycarbonate on the one hand and propylene carbonate and lithium ions on the other.

A novel gel polymer electrolyte was fabricated by Khani and co-workers.^[86] Polypyrrole (PPy) and polyfuran (PFu) were incorporated and in situ crosslinked in a PVdF–HFP support membrane. The hybrid separators were able to accommodate 173 wt% (PVdF–HFP–PFu) and 195 wt% (PVdF–HFP–PPy) of 1 M LiPF₆ in EC:DMC (1:1 w/w). The dendrite suppressing ability was tested in galvanostatic polarization experiments with symmetrical Li/PVdF–HFP–PFu/Li and Na/PVdF–HFP–PPy/Na cells. Compared to Celgard 2500, a high voltage stability

over 500 h was observed, while the commercial separator exhibited an internal short circuit after 233 h. Similar results were observed for Na/Whatman glassfiber/Na cells. In charge/discharge experiments of Li/PVdF–HFP–PFu/LiFePO₄, 78% of the initial capacity were observed after 1000 cycles at 1 C, for Na/PVdF–HFP–PPy/Na₃V₂(PO₄)₃ 94% capacity retention after 1000 cycles at 1 C were observed. SEM imaging of the lithium and sodium anode after cycling revealed no obvious signs of dendrites, compared to electrodes cycled with Celgard and Whatman separators.

He et al. investigated the SEI formation on lithium metal anodes with polyphosphazene GPEs.^[87] It turned out that polyphosphazene GPEs inhibited the dendrite growth compared to common liquid electrolytes. The authors explained this observation can be explained by a more stable and more conductive SEI. A faster SEI formation was observed as well, further reducing dendrite formation.

A triazine-based framework was developed by Shi et al., deposited on polyolefin separators, and applied in Li–S batteries.^[88] The triazine framework exhibited channels that were able to conduct lithium ions and to trap polysulfides, which was proven by UV and X-ray photoelectron spectroscopy. Furthermore, crossover experiments were conducted. The ionic conductivity was hardly affected by coating with triazine; it decreased from 2.9×10^{-4} to $2.7 \times 10^{-4} \text{ S cm}^{-1}$. Due to the high affinity of the triazine to lithium ions, their diffusion coefficient inside the coated membrane was increased. In Li–S batteries, the new membrane exhibited 0.052% capacity decay per cycle over 800 cycles at 1 C (41% capacity retention).

A flame-retarding polymer was synthesized from poly(ethylene glycol-bis-carbamate dimethacrylate), LiTFSI and ethylene carbonate (EC) as plasticizer by Fu et al. (Figure 6).^[89] In inflammation tests, the separator caught fire only after several seconds and extinguished itself due to the high flash point of EC, while common electrolyte mixtures (containing diethyl carbonate (DEC) or dimethylcarbonate (DMC)) catch fire

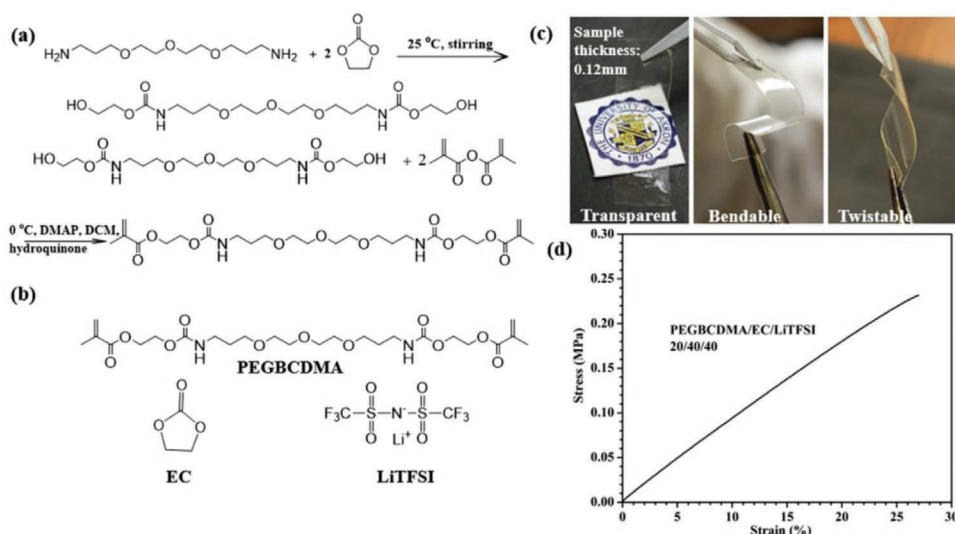


Figure 6. Schematic representation of a) the monomer synthesis, b) the monomer, the applied plasticizer EC and the electrolyte salt LiTFSI and c,d) the mechanical stability and the related stress–strain curve of the flame-retarding polymer membrane. Reproduced with permission.^[89] Copyright 2018, Elsevier.

more easily. An electrolyte, containing 10% of the crosslinked polymer (45% LiTFSI and 45% EC) revealed a high ionic conductivity of $8 \times 10^{-4} \text{ S cm}^{-1}$. In cell tests (Li/SPE/LiFePO₄), 80% capacity retention was achieved after 250 cycles at C/3.

3.1.6. Biopolymers

Beside commercial polymers, biologic and biologically degradable polymers represent a small but interesting niche. They are usually extracted from renewable sources, such as lignin, cellulose, polylactide (PLA) and others.^[90] Advantages of biopolymers are their natural abundance and the independence of fossil resources, they can be extracted from renewable sources, are sometimes biodegradable and usually less toxic and environmentally harmful compared to commercial polymers and separators.^[91]

A crosslinked polymer was prepared using cellulose as well as epichlorohydrin and investigated as GPE by Du et al.^[90a] The free-standing membrane exhibited a good mechanical stability, a high ionic conductivity ($6.34 \times 10^{-3} \text{ S cm}^{-1}$ at room temperature) and a high lithium transference number of 0.82. When utilized in cells (Li/GPE[DMSO, 1 M LiTFSI]/LiNi_{0.5}Co_{0.2}Mn_{0.3}O₂), 90% of the initial capacity was retained after 50 cycles.

Lignin was modified with γ -aminopropyltriethylsiloxane and blended with poly(vinylpyrrolidone) to form a GPE membrane by Liu et al.^[90c] The polymer blend was immersed with electrolyte and characterized by tensile strength tests and SEM. The ionic conductivity was determined to be $2.52 \times 10^{-3} \text{ S cm}^{-1}$ at room temperature, with a lithium-ion transference number of 0.56, both values outperforming the Celgard 2730 separator. In addition, the GPE was tested in lithium cells (Li/GPE[EC:DMC:DEC 1:1:1 w/w/w, 1 M LiPF₆]/LiFePO₄). In cycling tests, 95% of the initial capacity was retained after 100 cycles at 0.2 C.

Perumal et al. reported a potential use of pectin in SPEs applying LiClO₄ as electrolyte salt and small amounts (<0.4 wt%) of EC as plasticizer.^[92] The film revealed a low crystallinity in XRD measurements. In conductivity experiments, ionic conductivities of $3.89 \times 10^{-4} \text{ S cm}^{-1}$ at 30 °C and $1.57 \times 10^{-3} \text{ S cm}^{-1}$ at 90 °C were observed (EC content: 0.3 wt%). Furthermore, a high lithium-ion transference number of 0.97 was reported. The SPE was successfully applied in primary cells (Zn, ZnSO₄/SPE/PbO₂, V₂O₅), to prove its practicability.

3.1.7. Ionic Liquid-Containing Polymeric Separators

Common electrolyte solvents face several challenges when applied in lithium-ion batteries. They are volatile and possess low thermal stabilities and may have a smaller electrochemical stability window.^[93] To overcome these problems, ILs have been applied, which are organic salts with melting points below 100 °C. Low melting points are possible by combining large, bulky, and asymmetrical ions.^[94] ILs are nearly involatile compounds with very low flammabilities, thus improving the safety of the cells.^[95] Furthermore, their conductivities lie within a broad range from 0.1 to $18 \times 10^{-3} \text{ S cm}^{-1}$ at room temperature, which is comparable to organic electrolyte solutions for lithium-ion batteries.^[95a] On the other hand, ILs suffer from high viscosities.^[94a] Nevertheless,

IL-PEs became popular for different battery types, where they simultaneously act as plasticizer, solvent, and electrolyte.^[96] A comprehensive review on the topic of ionic liquids immersed in polymer electrolytes was published by Ye et al.^[96]

Chen et al. reported a PVdF–HFP matrix, incorporating an IL, exhibiting self-healing abilities (Figure 7), which arises from the interactions of the imidazolium cations of the IL and the C-F-dipoles of the polymer.^[97] The ionic conductivity was determined to be $1.5 \times 10^{-3} \text{ S cm}^{-1}$ at 35 °C. In cell tests (Li/IL-PE/LiFePO₄), 97% capacity retention was observed after 200 cycles at 1 C. When applied on bare lithium metal, dendrite growth was suppressed due to a uniform SEI layer. Furthermore, the GPE was applied in Li–S cells, where polysulfide shuttling was decreased and a better cycling performance was achieved compared to a combination of a liquid electrolyte and a Celgard separator.

N-methyl-*N*-propyl pyrrolidinium TFSI was applied in a UV-crosslinked network of polyurethane methacrylate, methyl methacrylate, ethylene glycol dimethacrylate, and LiTFSI by Li et al.^[98] The GPE revealed an ionic conductivity of $1.37 \times 10^{-3} \text{ S cm}^{-1}$ at room temperature and a lithium transference number of 0.22. When applied in Li/IL-PE/LiFePO₄ cells, 86% capacity retention after 80 cycles at 0.5 C was demonstrated.

Different ILs were incorporated in a polyimide matrix and applied in Li/IL-PE/LiFePO₄ cells by Kim^[99] As ILs, *N*-ethyl-, *N*-propyl- and *N*-butyl-*N*-methyl imidazolium TFSI (EMImTFSI, PMImTFSI, and BMImTFSI) were applied. The electrospun membranes exhibit thermal stability up to 400 °C and high anodic stabilities of 5.3 to 5.5 V. The ionic conductivity of the EMImTFSI-based separator was the highest due to its lower viscosity yielding $5.3 \times 10^{-3} \text{ S cm}^{-1}$ at room temperature. The different IL-PEs were applied in Li/IL-PE/LiFePO₄ cells. In cycling tests, all of them demonstrated a capacity decay of less than 1% over 50 cycles at 0.1 C, and EMImTFSI-based IL-PE exhibited the highest coulombic efficiencies.

Metwalli et al. reported on block copolymers of PEO and PS, in which an ionic liquid (*N*-ethyl-*N*-methyl imidazolium trifluoromethanesulfonate) was incorporated.^[100] In the presented study, the morphology of the polymer was correlated to the electrochemical performance. The PEO domain was responsible for the ionic conductivity, while the PS-block increased the mechanical and thermal stability. The incorporation of the IL increased the size of the amorphous regions of PEO and, thus, decreased the *T*_g, which led to better chain mobilities and, thus, a higher conductivity. At 35 °C, $1.98 \times 10^{-3} \text{ S cm}^{-1}$ was achieved, the high ionic conductivity was attributed to the lower crystallinity and higher salt dissociation of LiCF₃SO₃.

Polu et al. prepared an IL-PE from PEO, EMImTFSI and lithium difluoro(oxalate)borate (LiDFOB) with 40 wt% IL.^[101] X-ray diffraction revealed a decreased crystallinity compared to PEO when incorporating the IL, and the interaction between polymer ether bonds and the cations was investigated using FTIR spectroscopy. Compared to the pristine PEO ($5.23 \times 10^{-9} \text{ S cm}^{-1}$) and PEO with LiDFOB ($2.06 \times 10^{-6} \text{ S cm}^{-1}$), the membrane displayed an ionic conductivity of $1.85 \times 10^{-3} \text{ S cm}^{-1}$ at 30 °C, demonstrating an improvement by several orders of magnitudes. After 50 cycles at 0.1 C, 86% of the initial capacity was retained when applied in a Li/IL-PE/LeFePO₄ cell.

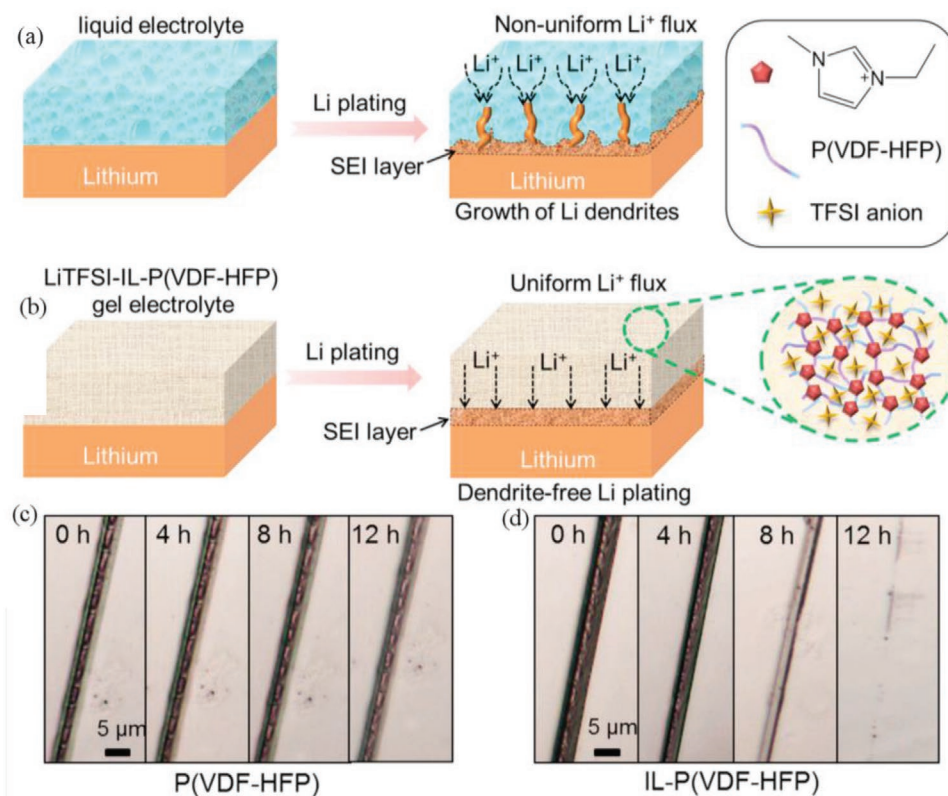


Figure 7. Top: Schematic representation of the dendrite blocking mechanism of the applied self-healing PVdF–HFP-based GPE. Bottom: Self-healing studies on the pristine P(VdF–HFP) and the ionic-liquid-containing separator at room temperature in 1 M electrolyte solution. Reproduced with permission.^[97] Copyright 2018, Elsevier.

3.1.8. Ionic Polymers

Another class of separators is ionic polymers, also called ionomers, namely polycations and polyanions. Both represent interesting candidates for separators and membranes, due to some advantages over charge-neutral polymeric separators. Neutral polymers possess conductivity for both cations and anions. However, because of the strong interactions between Lewis-basic polymers (in particular in the case of PEO) and the lithium ion, the transference number of lithium is less than 0.5 for these separators.^[102] Notably, even if a high overall ionic conductivity is present, the transference number of an electrochemically essential ion (e.g., lithium in a lithium-ion battery) can limit the cell performance. Simulations revealed that single-ion-conducting electrolytes ($t_{\text{ion}} = 1$) outperform systems with low ion transference numbers even if the overall ionic conductivity is one magnitude lower.^[103] When incorporating ionic moieties into polymers, the transference number of the corresponding free counter-ion becomes ≈ 1 . Thus, polyanions possess cation transference numbers of $t_+ = 1$, while $t_- = 1$ applies to polycations. Besides the improved conductivity for specific ions, this effect can also be used to inhibit unwanted shuttling of charged structures, as found for example in lithium–sulfur batteries, where the transfer of negatively charged polysulfides leads to self-discharge.^[104]

Several ionic polymers have been investigated, ranging from the well-known Nafion polymer to sulfonated polystyrenes to the newer field of polymerized ionic liquids.^[93,102]

Polyanions: Negatively charged polymers are permeable for cations—thus, they can be used in CEM.

A copolymer comprised of a TFSI-modified methacrylate (LiMTFSI), poly(ethylene glycol-methacrylate) (PEGM) and poly(ethylene glycol-dimethacrylate) (PEGDM) in different ratios was investigated by Porcarelli et al. (**Figure 8**).^[105] The free-standing film that revealed the highest ionic conductivity contained 50 wt% PC as a plasticizer and the copolymer with 9 wt% LiMTFSI, 36 wt% PEGM and 5 wt% PEGDM. At room temperature, the film exhibited an ionic conductivity of $1.2 \times 10^{-4} \text{ S cm}^{-1}$ and a lithium transference number of 0.86. When applied in cells with Li/GPE/LiFePO₄, the cells exhibited more than 98% and 85% capacity retention at 0.1 C after 100 cycles at 25 and 70 °C, respectively.

Chen et al. synthesized a poly(arylene ether) with sulfonyl imide as part of the backbone and prepared separators using a PVdF–HFP matrix (2:3 w/w poly(arylene ether):PVdF–HFP).^[106] The membrane exhibited a microporous structure and good electrolyte uptake to form a GPE. The ionic conductivity was $0.52 \times 10^{-3} \text{ S cm}^{-1}$ (EC/DMC 1:1 v/v) and the lithium transference number was determined to be 0.83 at room temperature. In cell tests (Li/GPE[EC/DMC 1:1 v/v]/LiFePO₄), no decay of the capacity was observed at 1 C after 100 cycles. Furthermore, dendrite growth of the lithium metal was suppressed by the high lithium transference number and confirmed by long-term square-wave galvanostatic cycling and microscopy images.

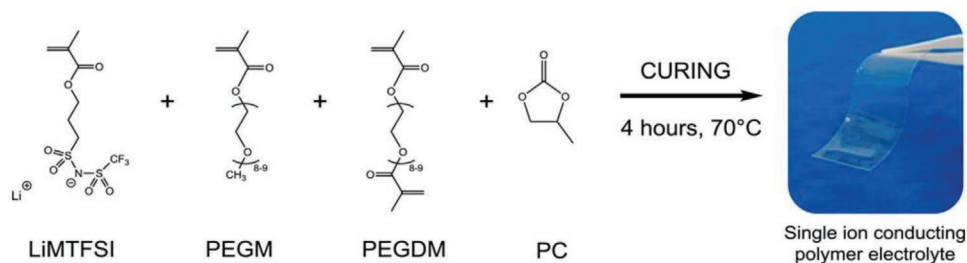


Figure 8. Schematic representation of the applied monomers and plasticizer for the SICP published by Porcarelli et al. Reproduced with permission.^[105] Copyright 2016, American Chemical Society.

Pan et al. prepared a membrane for lithium–sulfur batteries consisting of SPEEK to suppress polysulfide shuttling (**Figure 9**).^[107] The polymer possessed negatively charged nanochannels, which was shown by transmission electron microscopy (TEM) and small-angle X-ray scattering (SAXS). In a lithium–sulfur battery, the newly designed separator enabled very high charge and discharge rates, with stable cycling at high currents of 18 C for 250 cycles and a capacity retention of 91%.

A crosslinked network consisting of lithium bis(allyl malonato) borate and two different thiols, cast on a PVdF support, was presented by Deng et al.^[108] The nearly single-ion-conducting network ($t_+ = 0.92$) was used as a SPE in lithium metal cells, where it was able to suppress dendrite growth due to its high mechanical stability. Furthermore, it demonstrated a good ionic conductivity of $1.32 \times 10^{-3} \text{ S cm}^{-1}$ at 25 °C. In cell tests

(Li/SPE/LiFePO₄), 91% capacity retention after 380 cycles at 1 C was observed (Celgard: 74%).

An ionic-channel-containing separator was produced by Li et al. by mixing hyperbranched PMMA with poly(ether ether ketone) (PEEK) backbone possessing pendant lithium sulfonyl(trifluoromethanesulfonyl)imide groups.^[109] The presence of channels was proven using TEM. The membrane revealed an ionic conductivity of $1.36 \times 10^{-4} \text{ S cm}^{-1}$ at 25 °C and $1.01 \times 10^{-3} \text{ S cm}^{-1}$ at 90 °C, and a high lithium transference number of 0.94 (25 °C), utilizing PC as a plasticizer. In cell tests (Li/GPE[PC]/LiFePO₄) a capacity retention of 92% after 110 cycles at 0.5 C was reported.

Polycations: Mostly anions permeate a membrane made of a polymer containing cationic pendant groups, while cations cannot pass due to repulsion. Thus, such membranes work as AEM.

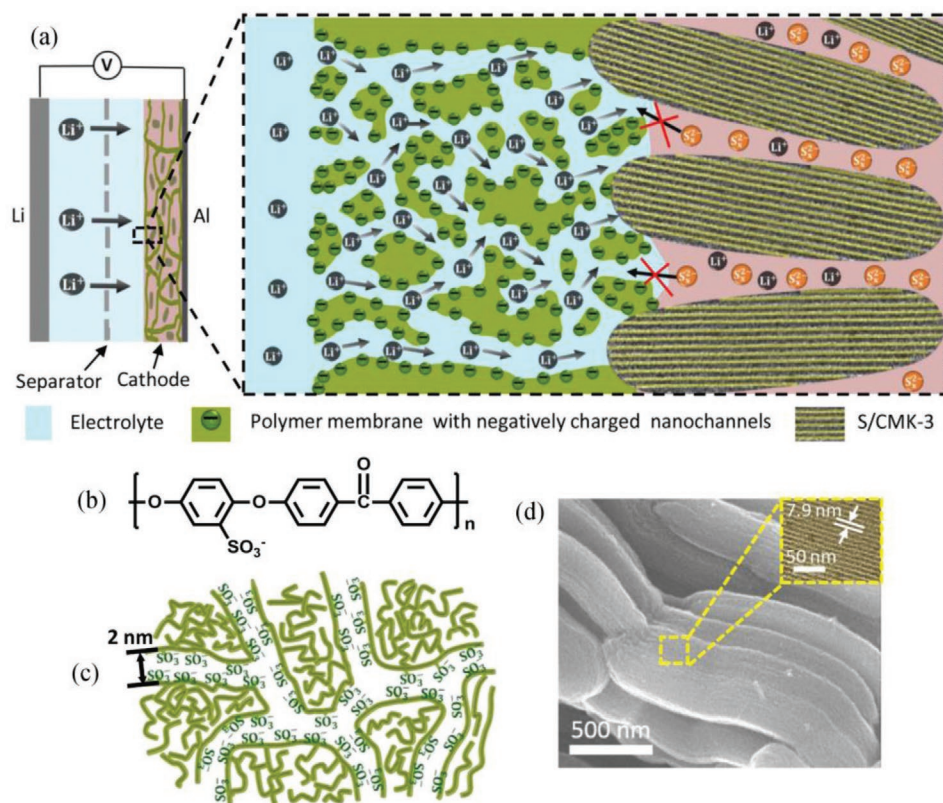
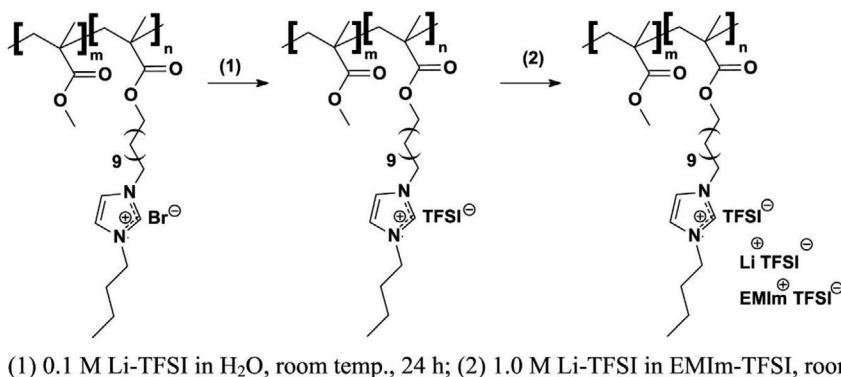


Figure 9. Schematic representation of a) the ion-transport mechanism of the SPEEK membrane, b) the molecular structure of SPEEK, and c) the ionic channels within the SPEEK. d) SEM image of the sulfur–carbon cathode material. Reproduced with permission.^[107] Copyright 2017, Elsevier.



Scheme 8. Schematic representation of the PIL block copolymer and its modification with an ionic liquid to yield the membrane. Reproduced with permission.^[113] Copyright 2016, Elsevier.

Hosseini et al. coated commercial separators with quaternary-ammonia-functionalized polysulfone to improve their performance in alkaline zinc primary batteries.^[59a] When utilizing Whatman GF-A or PallFlex FP separators, a coating with the cationic polymer improved the specific capacity, discharge voltage and utilization of the active material. Furthermore, electrochemical impedance spectroscopy (EIS) measurements confirmed higher ionic conductivities due to the coating of the separators (1.23 S cm^{-1} for coated PallFlex FP, uncoated PallFlex: 0.65 S cm^{-1}).

Abbasi et al. prepared a quaternary-ammonium-functionalized poly(2,6-dimethyl-1,4-phenylene oxide) and applied it in secondary zinc-air batteries.^[110] The separators showed both acceptable ionic conductivity and low zincate crossover. Trimethylamine (TMA) and 1-methylpyrrolidine (MPY) were applied as quaternized ammonium pendant groups. The ionic conductivity was 0.17×10^{-3} and $0.16 \times 10^{-3} \text{ S cm}^{-1}$ for TMA and MPY, respectively. Furthermore, compared to Celgard membranes, zincate crossover was reduced, which resulted in low zincate diffusion coefficients of $1.13 \times 10^{-8} \text{ cm}^2 \text{ min}^{-1}$ (TMA) and $0.28 \times 10^{-8} \text{ cm}^2 \text{ min}^{-1}$ (MPY).

A mixture of PVA and guar hydroxypropyl trimethylammonium chloride was crosslinked with glutaraldehyde and applied as an AEM in supercapacitors and zinc-air secondary cells.^[111] When pyrrole was bound to the separator through an aldehyde group, the hydroxide ionic conductivity reached a high value of 0.12 S cm^{-1} , more than a sevenfold increase compared to a membrane without pyrrole. The Wang group attributed this to the ability of pyrrole to move freely relative to the crosslinked glutaraldehyde and to the formation of hydrophilic clusters, facilitating hydroxide transport. In a supercapacitor, 8000 cycles were performed at 2 A g^{-1} , with a capacity retention of 87%, outperforming the commercially available A201 membrane. The same trend was observed for zinc-air batteries, where the produced separator demonstrated higher discharge capacities compared to the A201 separator.

Polymerized Ionic Liquids: A subclass of ionomers is PIL. For this purpose, a common ionic liquid is chemically bound to a polymer backbone or equipped with a polymerizable group. PILs possess high chemical, electrochemical and thermal stabilities and can prevent electrolyte leakage.^[112] However, even though the solid-state ionic conductivities of PILs are rather

high, they are always lower compared to the conductivities of their nonpolymerized counterparts due to the decreased ion mobility.^[112] Because PILs exhibit high affinities to their corresponding IL, it is of great interest to incorporate ILs into PILs to increase the ionic conductivity and to decrease electrolyte leakage. Furthermore, both PILs and ILs possess low flammability, increasing the safety of the cells.^[113]

Nykaza et al. copolymerized methyl methacrylate with a methacrylate containing 3-butyylimidazolium TFSI as pendant group (**Scheme 8**).^[113] The polymer for the free-standing film was prepared by reversible addition-fragmentation chain-transfer (RAFT) polymerization and soaked with LiTFSI and EMImTFSI. By adding the ionic liquid and the LiTFSI, the conductivity was significantly improved to $1 \times 10^{-3} \text{ S cm}^{-1}$ at room temperature ($3 \times 10^{-7} \text{ S cm}^{-1}$ for the pristine polymer film). The authors attributed this to the better ionic mobility of the IL, compared to the PIL. In lithium cells ($\text{Li}_4\text{Ti}_5\text{O}_{12}/\text{PIL}/\text{LiCoO}_2$), the capacity faded strongly over 100 cycles, maintaining only 27% of the initial capacity. This can be explained with the low electrochemical stability window of the PIL, which was determined to be between 1.7 to 4.4 V (vs Li/Li⁺). However, the cathodic limit rose from 1.0 to 1.7 V (vs Li/Li⁺) for the PIL compared to the IL.

Ma et al. synthesized poly(1-vinyl-3-ethylimidazolium) TFSI and immersed it in a nonwoven PET matrix.^[114] LiTFSI was used as electrolyte salt and $\text{Li}_{1.3}\text{Al}_{0.3}\text{Ti}_{1.7}(\text{PO}_4)_3$ (LATP) as inorganic filler to increase the ionic conductivity. The resulting SPE exhibited an ionic conductivity of $5.92 \times 10^{-4} \text{ S cm}^{-1}$ at $60 \text{ }^\circ\text{C}$ (2 mol kg^{-1} LiTFSI), which was slightly increased by adding 10 wt% LATP to $7.93 \times 10^{-4} \text{ S cm}^{-1}$ at $60 \text{ }^\circ\text{C}$. Higher amounts decreased the conductivity. In test cells ($\text{Li}/\text{SPE}/\text{LiFePO}_4$), a capacity retention of 96% after 250 cycles at $60 \text{ }^\circ\text{C}$ and 1 C (with 10 wt% LATP) was observed.

An ionic-liquid-functionalized polymer was synthesized by Tsao et al. via a sol-gel process, employing Jeffamine ($\text{NH}_2\text{-PPO-PEO-PPO-NH}_2$), 1-methyl-3-propylimidazolium trimethoxysilane and silyl-ether-containing crosslinker.^[115] The hybrid separator was applied as a GPE (1 M LiPF_6 , EC/DEC 1:1 v/v). Excellent thermal stability of up to $412 \text{ }^\circ\text{C}$ was observed, attributed to the incorporated IL. Furthermore, a good ionic conductivity of $6.0 \times 10^{-3} \text{ S cm}^{-1}$ at room temperature for a ratio of 5:1 w/w IL to PPO/PEO and a lithium transference number

of 0.57 could be determined. In cell tests (Li/GPE[1 M LiPF₆, EC/DEC 1:1 v/v]/LiFePO₄), the rate capability was significantly increased compared to the membrane without IL. As well, when cycled over 100 cycles at 0.2 C, over 98% capacity retention was observed.

3.1.9. Inorganic Additives

To further improve the thermal and mechanical properties of separators, many approaches have been reported. One of them is the incorporation or coating of separators with nanoscale inorganic fillers, such as SiO₂,^[116] Al₂O₃,^[117] and TiO₂.^[118] The nanofillers increase the ionic conductivity of polymer membranes by reducing their crystallinity and, thus, increasing the chain mobility.^[119] Another factor improving the ionic conductivity is the interaction of the nanoparticles with the polymer chain and lithium ions. By reducing the interactions between the polymer chains and the cations, the ionic conductivity is raised.^[120] Furthermore, the mechanical stability is enhanced, inhibiting dendrite growth for (lithium) metal anodes, due to higher shear modulus.^[52b,121] In addition, the thermal stability is raised. Porous, ordered structures of nanoparticles reduce the thermal shrinkage of commercially available polymer membranes.^[116] Furthermore, the electrolyte leakage and wettability can be improved by choosing large-surface-area nanoparticles and compatible polymers.^[122]

Nanoparticles can be added to the membrane either by blending them inside the polymer matrix or by coating the membrane with nanoparticles. Blending is more straightforward and easier to process and the properties of the polymer membrane change due to the incorporated particles.^[123] Coating of existing membranes requires an extra step but also enables the modification of commercially available separators. Furthermore, more complex architectures of multilayered sandwich-like structures are accessible.^[124] Coating does not change the intrinsic properties of the polymer but affects the interfaces between separator, electrodes, and electrolyte solvents. This influences the performance of the hybrid separator and results in different ionic conductivities, mechanical stabilities, and electrolyte uptake compared to for the unmodified polymer.^[51]

For more examples of nanofillers in solid polymer electrolytes, the review of Yarmolenko et al. is recommended.^[119] Furthermore, the review of Zhang et al. provides a short paragraph on the topic.^[51]

3.1.10. Concluding Remarks

In summary, several polymers have been applied in lithium batteries. Starting from commercial PP/PE separators, a myriad of possible membranes has been published. Most publications focus on increasing the ionic conductivity and the lithium-ion transference number. Other important parameters that are being investigated are the wettability, the electrolyte uptake, the morphology and pore size and, finally, the overall performance in test cells.

While membrane technology greatly improved and has offered many solutions, some challenges still remain. One

major hurdle is the suppression of lithium dendrites, which might be overcome with a suitable membrane design. Namely, an increase in the mechanical stability, a uniform ion flux and a near-single-ion-conducting character are some approaches to reach this goal. Another challenge that some batteries face is the shuttling of active material, in particular in lithium–sulfur batteries. One solution can be the application of ionomers, which partially block the diffusion of charged species. Solid polymer electrolytes still suffer from low ionic conductivities and a low overall cell performance at room temperature. To improve this type of separator, the polymer and plasticizer have to be modified to yield a low crystallinity and a high ion mobility even at low temperatures. In the more recent field of ionic liquids and polymerized ionic liquids, an important drawback is the low electrochemical stability of some molecular structures. Additionally, the high viscosity of the ionic liquids decreases the ionic mobility and, thus, the ionic conductivity. Through intelligent molecular design, some of the mentioned limitations can be overcome, but the optimum point has yet to be reached.

We are convinced that the development of solid polymer electrolytes has a great potential in terms of cell safety, as dendrite growth of bare lithium anodes can be suppressed and no leakage of potentially flammable electrolyte can take place. Another very promising topic are ionic polymers, which possess high lithium transference numbers and have the potential to suppress unwanted shuttling reactions in some batteries to improve the cycling stability.

3.2. Separators for Organic Thin-Film Batteries

The previous sections focused solely on the separators used in lithium- and other metal-based batteries. However, the emerging field of organic batteries often utilizes commercially available separators, as research mainly focuses on the improvement of the active material. Thus, not many examples for advanced separators can be found in literature. In most cases, polyolefin separators with liquid electrolytes are applied, as they represent the state of the art in commercial lithium battery cells. First examples of organic radical batteries employed Celgard membranes, which was adapted by most of the research community.^[125] However, several publications can be found that demonstrate the usage of glass fibers as separators, but none reported on the influence on the cell performance.^[17,24c,45b,c,126] In some cases, separators based on paper were applied.^[127]

Hatakeyama-Sato et al. produced an all-organic, completely flexible and stretchable, micrometer-thick rechargeable device using PLA as a separator.^[128] PLA was chosen for its biodegradability, mechanical stability, and porosity. The battery, utilizing a TEMPO based cathode and anthraquinone-based anode, was charged and discharged over 40 times at 18 C, yielding a capacity retention of ≈85%.

A poly(3,4-ethylene dioxy thiophene) (PEDOT)–air battery was constructed with sodium poly(styrene sulfonate) (PSSNa) as solid polymer electrolyte by Xuan et al. and by Reyes-Reyes and Lopez-Sandoval.^[129] The anode contained both PEDOT and poly(ethylene imine) (PEI), so that the PEI reduced the oxidized PEDOT⁺⁺ chains back to the neutral state. On the cathodic side, neutral

PEDOT⁰ was oxidized by oxygen to PEDOT⁺. The primary cell was able to maintain an output of 0.8 V for 30 days, while providing a discharge current of 2 μ A for 10 h (1 μ A after 100 h).

In rare cases, other separators are used. Kim et al. investigated the compatibility of a PVdF–HFP GPE with PTMA electrodes.^[130] The applied GPE (EC/DMC 1:1 v/v) performed as good as liquid electrolytes in terms of ionic conductivity and the internal resistance was lowered, compared to the liquid electrolyte. At 1 C, 91% of the initial discharge capacity was observed after 100 cycles. Even at high currents of 50 C, 88% of the discharge capacity at 1 C was reached.

PVdF–HFP was also applied for PTMA-based cathodes and lithium anodes with an ionic liquid by Kim et al.^[131] By incorporating the ionic liquid *N*-butyl-*N*-methyl pyrrolidinium TFSI (Py₁₄TFSI) instead of a common electrolyte solvent mixture (EC/DMC), the solubility of the PTMA was significantly decreased. This led to improved cycling stabilities, as shuttling was strongly suppressed.

A printable, methacrylate-based, ionic-liquid containing GPE for an all-organic battery (PTMA cathode, poly(2-vinyl-11,11,12,12-tetracyano-9,10-anthraquinonodimethane) (TCAQ) anode) was reported very recently by Muench et al.^[132] The copolymer with benzyl methacrylate and poly(ethylene glycol methylether methacrylate) formed free-standing films when it was directly UV-polymerized with the ionic liquid (BMImTFSI). As an additional method, the IL-containing GPE was directly polymerized on a PTMA composite electrode, which led to an improved rate capability and higher overall capacities (24 mAh g⁻¹ at 0.1 C). The authors proposed that the active material was able to swell in both monomers and IL, leading to a better accessibility of the redox active species. In long-term cycling tests a capacity loss of 23% was observed after 1000 charge and discharge cycles at 1 and 5 C were performed, for both free-standing and in situ polymerized films (PTMA/GPE/TCAQ).

Aqil et al. prepared an imidazolium-based polymerized ionic liquid bearing TEMPO redox-active moieties in the side chains, inhibiting the dissolution of active species in the electrolyte solvent and improving the cycling stability as well as rate capability through the good ionic conductivity of the polymerized ionic liquid.^[133] When cast on carbon paper and tested in cells versus lithium metal (Celgard soaked with liquid electrolyte), 1300 cycles at high rates of 60 C were achieved without any capacity fading.

3.3. Membranes for Redox-Flow Batteries

The separator represents an essential component of a flow battery under both economic and performance aspects. Besides the charge-storage materials, it is the greatest cost factor.^[37,134] Due to the use of polymeric active materials, the commonly used, cost-intensive ion-exchange membranes was replaced by affordable size-exclusion membranes.^[31–33,36,38,46,47,135]

Regardless of the type, the separator must feature, on the one hand, a good permeability for the conducting salt ions to enable a high ion conductivity, but on the other hand, a full impermeability for the redox-active material in order to prevent a crosscontamination.^[30b,136] Furthermore, the separator has to display a long lifetime, good mechanical as well as chemical stability in the respective electrolyte system.^[30b,37]

Table 2. Property parameters of commercial ion-exchange membranes for VRFB application.^[138]

	Type	Membrane resistance [Ω cm ⁻²]	Ion conductivity [10^{-2} mS cm ⁻¹]	VO ²⁺ permeability [10^{-6} cm ² min ⁻¹]
APS	AEM	0.85	17.6	0.25
FAP-PE-420	AEM	4.02	0.50	1.16
FAP-PP-475	AEM	3.94	1.78	2.46
Nafion 117	CEM	0.94	20.2	11.4
NEPEM 115	CEM	3.93	2.04	1.93

Generally, there are two different types of separators: Nonionic, porous membranes and dense, ion-conducting membranes, which can be further subdivided into AEMs, CEMs, and amphoteric membranes, which conduct anions and/or cations.^[61b]

Among all investigated flow-battery setups, including the commercially available systems, the all-VRFB is the most studied one and was intensively evolved over the last 30 years.^[137] On that score, the majority of research activities in the field of separators focused on designing membranes for this RFB system.

3.3.1. Ion-Exchange Membranes

Evaluation of Commercial CEMs and AEMs for VRFBs: Hwang et al. studied three AEMs, namely APS, FAP-PE-420, and FAP-PP-475, and two CEMs, Nafion 117 and NEPEM 115.^[138] The membrane resistance, the ionic conductivity and the vanadium-ion permeability were investigated in 1 M H₂SO₄ aqueous solution. The APS AEM featured the lowest membrane resistance and VO²⁺ permeability as well as the highest ion conductivity (Table 2). Based on these results, the APS AEM should be the membrane of choice for a VRFB application. To verify this, VRFB cells with 1.8 M VOSO₄ in 2 M H₂SO₄ aqueous solution were built and the performance (stated values were average values over five cycles) depending on the utilized membrane was examined at a current density of 60 mA cm⁻². The results are shown in Table 3. The achieved VEs (voltage efficiencies) and EEs (energy efficiencies) of all membranes are similar. Only the values of CE (coulomb efficiency) vary notably. Despite its good conductivity and permeability (Table 2), the APS AEM exhibited the lowest CE (89%), whereas the FAP-PP-475 and Nafion 117 exhibited the best values (92%).

Xi et al. investigated the influence of temperature on the performance of different membranes.^[139] The authors investigated

Table 3. Performance parameters of a VRFB depending on the used common ion-exchange membrane.^[138]

	Type	CE [%]	VE [%]	EE [%]
APS	AEM	89	87	78
FAP-PE-420	AEM	91	86	78
FAP-PP-475	AEM	93	85	79
Nafion 117	CEM	92	85	79
NEPEM 115	CEM	89	86	76

Table 4. Specific characteristics of the studied membranes. With the exception of the home-made SPEEK (degree of sulfonation = 0.61) all membranes are commercially available.^[139]

	Type	VO ²⁺ permeability [10 ⁻⁷ cm ² min ⁻¹]	Area resistance [Ω cm ⁻²]	Price [\$ m ⁻²]
Nafion 115	CEM	10.9	0.97	1530
Nafion 212	CEM	5.68	0.26	780
Selemion CMV	CEM	1.10	2.14	390
SPEEK	CEM	0.65	0.46	30
APS	AEM	0.48	0.54	530
Selemion AMV	AEM	0.25	3.76	392

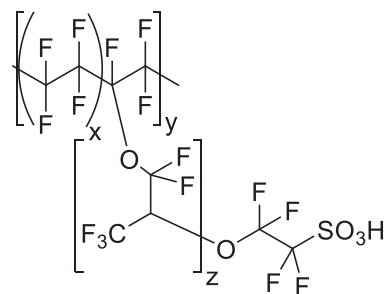
the performance parameters of cells, utilizing four CEMs (Nafion 115 and Nafion 212, Selemion CMV and self-made SPEEK) and two AEMs (APS and Selemion AMV) in a wide temperature range from -20 to 50 °C. Initially, the area resistance, VO²⁺ permeability and costs of the different membranes were compared (Table 4). Both Selemion membranes exhibited a significantly higher area resistance compared to the other membranes. As expected, the AEMs Selemion AMV and APS but also the self-made CEM SPEEK featured the lowest VO²⁺ permeability with values of 0.25, 0.48, and 0.65 10⁻⁷ cm² min⁻¹, respectively, which is five to ten times lower compared to the values of both Nafion-based membranes. To confirm these results, the performance parameters of VRFB cells at room temperature (30 °C) with current densities between 40 and 200 mA cm⁻² were investigated. Independent of the applied current densities, the cells with the Selemion membranes achieved the lowest VE. As a consequence, Selemion AMV and CMV are not suitable for applications in VRFBs. Also, the SPEEK membrane, despite the cost saving aspects, seems to be unsuitable because of its limited mechanical and chemical stability.

Finally, the influence of the temperature in the range from -20 to 50 °C on crucial parameters of the cell was studied (Table 5). Due to the previous results, both Selemion membranes were not included. Nevertheless, the investigations of the capacity retention at -15 °C, room temperature and 50 °C in long-term tests over 300 cycles exhibited that the APS AEM and the SPEEK CEM were not applicable in VRFB due to a significant capacity decay, in particular at temperatures >30 °C (Table 5). Among all, the Nafion 115 seems to be the most suitable membrane for VRFB application at low and ambient temperatures.

Polymeric Cation-Exchange Membranes: Nafion-based membranes are the best-known representatives of CEMs. Due to their chemical stability, excellent ionic conductivity, and ion selectivity, Nafion was originally used as a separator in

Table 5. Capacity decay over 300 cycles at different temperatures.^[139]

	Capacity decay [% per cycle]		
	-15 °C	r.t.	50 °C
Nafion 115	0.064	0.141	0.231
Nafion 212	0.093	0.148	0.251
SPEEK	0.162	0.268	/
APS	0.125	0.301	0.323



Scheme 9. Schematic representation of the chemical structure of Nafion. Adapted with permission.^[140b] Copyright 2004, The American Chemical Society.

electrochemical cells, particularly in context of the chlor-alkali electrolysis,^[140] in metal-ion recovery, sensors,^[141] water electrolysis,^[142] and fuel cells.^[140a,142a]

Nafion is the trade name of a copolymer that was developed by the DuPont Company, more precisely by Walter Grot, in 1962. Perfluorinated (PF) vinyl ether comonomers, which were terminated with sulfonic acid groups (-SO₃H), were implemented as side chains in a tetrafluoroethylene backbone (Scheme 9).^[140a,b,143]

Nafion has been used in membranes for flow-battery application since the middle of the 1980s.^[61a,144] In the course of the development and commercialization of VRFBs, they were well investigated and widely used as benchmark separators.^[30b,61b,137,144a,145] However, due to high material costs (10 to 15% of the overall battery cost or around 40% of the cost of a VRFB cell stack)^[60b] and the known high crossover rate of vanadium ions, the current research focuses on the modification of Nafion as well as on the development of other polymeric membranes in order to overcome these restrictions. Nevertheless, up to now, Nafion membranes are the best choice for large-scale and long-life VRFBs.^[60a,145b]

A possibility to overcome the drawbacks of common Nafion-based membranes is their rational usage and reutilization. Zhou et al. evaluated the recovery of a Nafion 212 membrane via treatment with different aqueous solutions.^[145b] Used in a VRFB, after 1500 h operation time and 12 rounds of assembly and disassembly of the cell, no decisive differences among these three methods and only minor differences to fresh Nafion 212 were observed; it was possible to reuse the Nafion membranes without major capacity loss. With regard to the cycling stability and convenience, the authors declare that treatment with deionized water is the preferred method.

In addition, several studies on the rational use, in particular in order to reduce the costs, were realized. Decreased expenses for the VRFB stack were accomplished by utilizing thinner membranes, like Nafion 212 (50 μm) instead of Nafion 117 (175 μm) or Nafion 115 (125 μm),^[139,146] or by implementation of a pretreatment process that increases the membrane area.^[145b] Since the fabrication method (solution casting) of Nafion 212 is convenient for mass production, the acquisition costs of this membrane can likely decrease from \$225 per m² (2017) to around \$90 per m².^[145b,146d-f,147]

Another approach for the improvement of Nafion-based membranes is their modification by the incorporation of other polymers. To improve the selectivity of Nafion membranes,

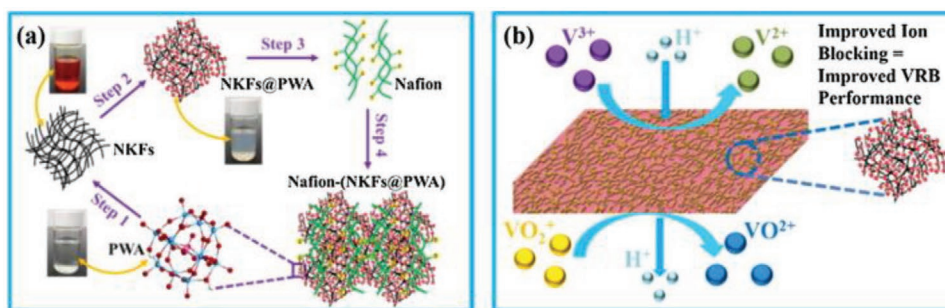


Figure 10. Schematic representation of a) the fabrication process of the composite membrane and b) of the blocking mechanism of the vanadium ions. Reproduced with permission.^[149] Copyright 2019, Elsevier.

conventionally sol-gel or solution casting methods are utilized.^[148]

In 2019, Yang et al. described a vanadium-blocking composite membrane, in which nano Kevlar fibers (NKFs) were immobilized with phosphotungstic acid (PWA) by a solution cast method and finally immersed into a Nafion matrix (**Figure 10a**).^[149] This composite membrane featured remarkable vanadium barrier properties (**Figure 10b**) and provided a proton/vanadium selectivity of 2.48×10^5 S min cm^{-3} at room temperature. This selectivity exceeded 6.3 times the value of recast Nafion. In addition, the VO^{2+} permeability of 2.46×10^{-7} cm^2 min^{-1} was considerably lower compared to recast Nafion with 20.16×10^{-7} cm^2 min^{-1} . Accordingly, utilized in a VRFB, the Nafion membrane with 30 wt% of NKF immobilized on PWA exhibited a better performance in comparison to a recast Nafion separator. In a long-term stability test over 100 cycles at a current density of 80 mA cm^{-2} , the flow cell using the novel composite membrane exhibited a lower capacity fading of 0.175% per cycle, compared to 0.251% per cycle for regular Nafion.

Also in 2019, Liu et al. developed a method for a continuous growth of a 2D hexagonal boron nitride (h-BN) monolayer film to modify common Nafion membranes.^[150] Due to the honeycomb structure with alternating nitrogen and boron atoms, the 2D h-BN films featured a high proton conductivity, good flexibility, as well as an excellent thermal and chemical stability. With a Nafion functional-layer-assisted transfer method, a Nafion/h-BN/SPEEK sandwich membrane was fabricated. Compared to a pristine SPEEK membrane, the Nafion/h-BN/SPEEK sandwich membrane exhibited a three times higher proton selectivity of 3.21×10^5 S min cm^{-3} as well as a lower vanadium ion permeability (1.9×10^{-7} cm^2 min^{-1} vs 8.7×10^{-7} cm^2 min^{-1}). Finally, a VRFB cell utilizing the fabricated membrane was applied at a current density of 120 mA cm^{-2} , showing a CE of over 98% and very similar VEs and EEs, compared to SPEEK, and Nafion/SPEEK membranes (**Table 6**). These values do not indicate a significant improvement toward SPEEK membranes, the sandwich membrane only performs better in VE and EE at low current densities.

Ji et al. prepared SPEEK/TiO₂ composite membranes with different TiO₂ nanoparticle loadings and degrees of sulfonation via a solvent casting method.^[151] Among all prepared composite membranes, a TiO₂ content of 5% led to the highest $\text{H}^+/\text{VO}^{2+}$ ion selectivity (7.26×10^4 S min cm^{-3}) and the lowest VO^{2+} permeability (2.45×10^{-7} cm^2 min^{-1} vs 67.2×10^{-7} cm^2 min^{-1} for Nafion 117). Compared to a Nafion 117 membrane, the detected proton selectivity was 13 times higher. In a VRFB cell, only a

minor decline of the charge and discharge capacity of 0.11% per cycle was observed over 20 cycles at a current density of 50 mA cm^{-2} , which was lower compared to the Nafion-117 cell.

Niu et al. described SPEEK/graphite carbon nitride (g-C₃N₄) hybrid membranes for an application in VRFBs.^[152] The membranes were prepared via a solution-casting method of homogeneously dispersed g-C₃N₄ (in various contents) into a SPEEK matrix. The membrane with 1.5% content of g-C₃N₄ featured a $\text{H}^+/\text{VO}^{2+}$ ion selectivity of 2.15×10^4 S min cm^{-3} , which was significantly higher compared to a common Nafion 117 membrane ($\approx 2 \times 10^3$ S min cm^{-3}), and a good VO^{2+} permeability of 3.7×10^{-7} cm^2 min^{-1} . In a static VRFB, the cell utilizing the 1.5%-hybrid membrane possessed the highest efficiencies and capacities, in comparison to cells utilizing a SPEEK and a Nafion 117 membrane.

In 2019, Ye et al. developed a cost-effective, ecofriendly Nafion-alternative composite membrane, which enabled an excellent VRFB performance.^[153] The authors group incorporated 15 wt% of the biopolymer lignin into a SPEEK polymer to obtain the SPEEK/L15 membrane. This membrane featured a lower VO^{2+} permeability compared to Nafion 212 (0.17×10^{-7} cm^2 min^{-1} vs 1.98×10^{-7} cm^2 min^{-1}) and a significantly higher ion selectivity (173.86×10^4 S min cm^{-3} vs 16.26×10^4 S min cm^{-3}). A VRFB utilizing SPEEK/L15 exhibited a formidable performance. In a long-term cycling test over 350 cycles at a current density of 120 mA cm^{-2} , a capacity retention of 71% after 300 cycles (0.095% capacity decay per cycle), was observed. In contrast, a cell applying the Nafion 212 membrane exhibited a nearly complete capacity decay (equal to a loss of $\approx 0.4\%$ per cycle) within 250 cycles.

Besides SPEEK polymers, polybenzimidazoles (PBIs), which feature a lower vanadium permeability compared to commercial Nafion membranes and, therefore, should enable a better battery performance, were investigated to identify a low-cost alternative.

Table 6. Characteristics of VRFB cells using SPEEK-containing membranes. Charge/discharge experiments were conducted at a current density of 120 mA cm^{-2} .^[150]

	VO^{2+} permeability [$10^{-7} \text{ cm}^2 \text{ min}^{-1}$]	Proton selectivity [$10^4 \text{ S min cm}^{-3}$]	CE [%]	VE [%]	EE [%]
SPEEK	8.7	9.7	≈ 96	≈ 88	≈ 86
Nafion/SPEEK	7.6	11	≈ 97	≈ 88	≈ 86
Nafion/h-BN/SPEEK	1.9	32.1	>98	≈ 87	≈ 85

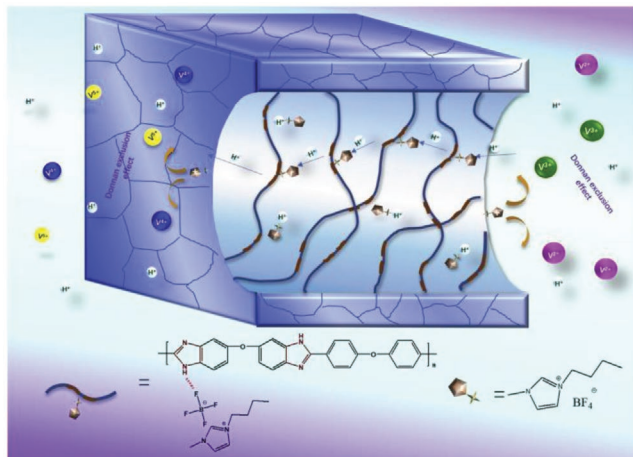


Figure 11. Schematic representation of the proton transfer and the blocking of vanadium-ion crossover in an OPBI membrane by the use of the ionic liquid BMImBF₄. Reproduced with permission.^[155] Copyright 2019, Elsevier.

Xia et al. synthesized various PBI copolymers with different contents of amino groups via a condensation polymerization of 5-aminoisophthalic acid (APTA), 3,3-diaminobenzidine (DAB), and 4,4-dicarboxydiphenyl ether (DCDPE).^[154] A highly sulfonated polybenzimidazole was obtained after post sulfonation. Afterward, covalently crosslinked membranes (CSOPBI) were fabricated with bisphenol A and an epoxy resin via a solution cast technique. Compared to Nafion 117 ($4.23 \times 10^{-6} \text{ cm}^2 \text{ min}^{-1}$) all CSOPBI membranes featured a significantly lower VO²⁺ ion permeability (maximum $5.99 \times 10^{-9} \text{ cm}^2 \text{ min}^{-1}$). In a long-term cycling test over 300 cycles at a current density of 60 mA cm^{-2} , the VRFB cell using a CSOPBI membrane that was based on a DCDPE-to-APTA ratio of 9:1 exhibited CEs up to 99% and EEs of $\approx 85\%$.

Song et al. chose a different approach and described an ion-exchange composite membrane for VRFBs.^[155] For this purpose, the ionic liquid 1-butyl-3-methylimidazolium tetrafluoroborate (BMImBF₄) was embedded in the polymer matrix poly(oxyphenylene benzimidazole) (OPBI) to fabricate membranes via solution casting (Figure 11). Because of the hydrogen bonds that form between BMImBF₄ and OPBI, BMImBF₄ remained in the membrane while cycling the cell. Investigations revealed that an increasing content of the ionic liquid led to a rising proton conductivity and a decreasing vanadium ion permeability. The proton selectivity of a membrane containing 20 wt% ionic liquid was the highest ($1.41 \times 10^6 \text{ S min cm}^{-3}$) and significantly outperformed an unmodified OPBI membrane ($6.06 \times 10^5 \text{ S min cm}^{-3}$) as well as a Nafion 115 membrane ($1.61 \times 10^4 \text{ S min cm}^{-3}$).^[154,155,170] During a long-term stability test of a VRFB cell over 1000 consecutive charge/discharge cycles at a current density of 100 mA cm^{-2} , the cell with the modified OPBI composite membrane achieved a capacity retention of 64% (equal to a capacity fading of 0.036% per cycle), whereas the cell with the Nafion 115 membrane exhibited a low retention of 12%, which corresponded to a decay of 0.088% per cycle.

Polymeric Anion-Exchange Membranes: In contrast to CEMs, AEMs contain positively charged functional groups and can,

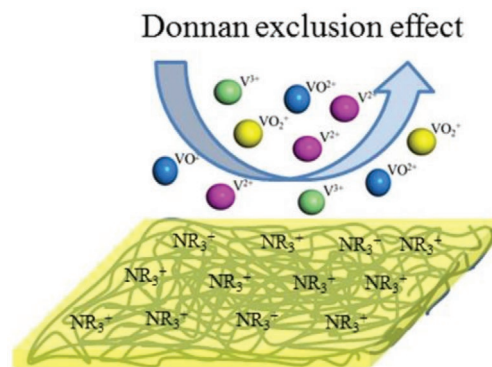


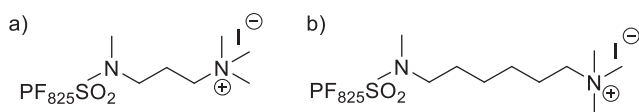
Figure 12. Schematic representation of the Donnan exclusion effect. Reproduced with permission.^[157] Copyright 2017, Elsevier.

therefore, exchange negatively charged ions with the electrolyte solution. As result of the Donnan exclusion effect, the positively charged vanadium ions cannot penetrate the separator (Figure 12).^[156] As a consequence, AEMs feature a lower vanadium-ion permeability compared to CEMs and, thus, improve the CE of VRFBs.^[60]

Up to the beginning of the 2010s, AEMs were rarely examined as separators for commercial RFB systems. However, the few studies on AEMs (e.g., in an iron–chromium RFB by NASA^[158] or in a VRFB by Mohammadi and Skyllas-Kazacos^[159]) indeed demonstrated excellent blocking properties toward cations but a worse chemical stability and battery performance.^[60b,c] Since 2012, due to the progressive development of AEM fuel cells and the improvement of their fabrication process, the number of investigations and studies increased significantly.^[57,60c]

In 2017, Cha et al. fabricated polysulfone-based AEMs by applying chloromethylation and primary diamine-based crosslinkers with various degrees of crosslinking for applications in VRFB.^[156] The membrane with 2.5 mol% crosslinker per chloromethyl group exhibited the best properties of all prepared membranes. Besides an excellent dimensional stability (low degree of swelling in water, only small changes in the size between swollen and dry) and anion (Cl⁻, SO₄²⁻, OH⁻) conductivity, the membrane featured a superior VO²⁺ permeability ($2.72 \times 10^{-8} \text{ cm}^2 \text{ min}^{-1}$ vs $2.88 \times 10^{-6} \text{ cm}^2 \text{ min}^{-1}$ for Nafion 115). In a VRFB cell at a current density of 50 mA cm^{-2} over 30 cycles, a capacity fading of 0.27% per cycle was determined (Nafion 115: 0.93% per cycle).

Park et al. described PF AEMs as an analogue to the widely used Nafion-based CEMs.^[160] Because of the benefits of such CEMs, like the excellent chemical stability, high water mobility, and ionic conductivity, the fabrication of perfluorinated AEMs is of great interest. The authors reported on a new synthesis route to prepare sulfonamide-linked alkyl ammonium perfluorinated AEMs, namely a propyltrimethyl ammonium (Gen 1) and hexyltrimethyl ammonium (Gen 2) PF AEM (Scheme 10). The Gen 2 PF AEM exhibited a more than 50 times better stability against 2 M KOH, even at high temperatures, losing only 10% of the active ionic sites after two weeks (Gen 1: 70% in 24 h). Both membranes featured a good ion-exchange capacity (proportional to the active ionic sites in the membrane) and OH⁻ conductivity of 55×10^{-3} and $43 \times 10^{-3} \text{ S cm}^{-1}$, respectively.



Scheme 10. Schematic representation of the structures of a) Gen 1 and b) Gen 2 PF AEM. Adapted with permission.^[160] Copyright 2017, IOP Science.

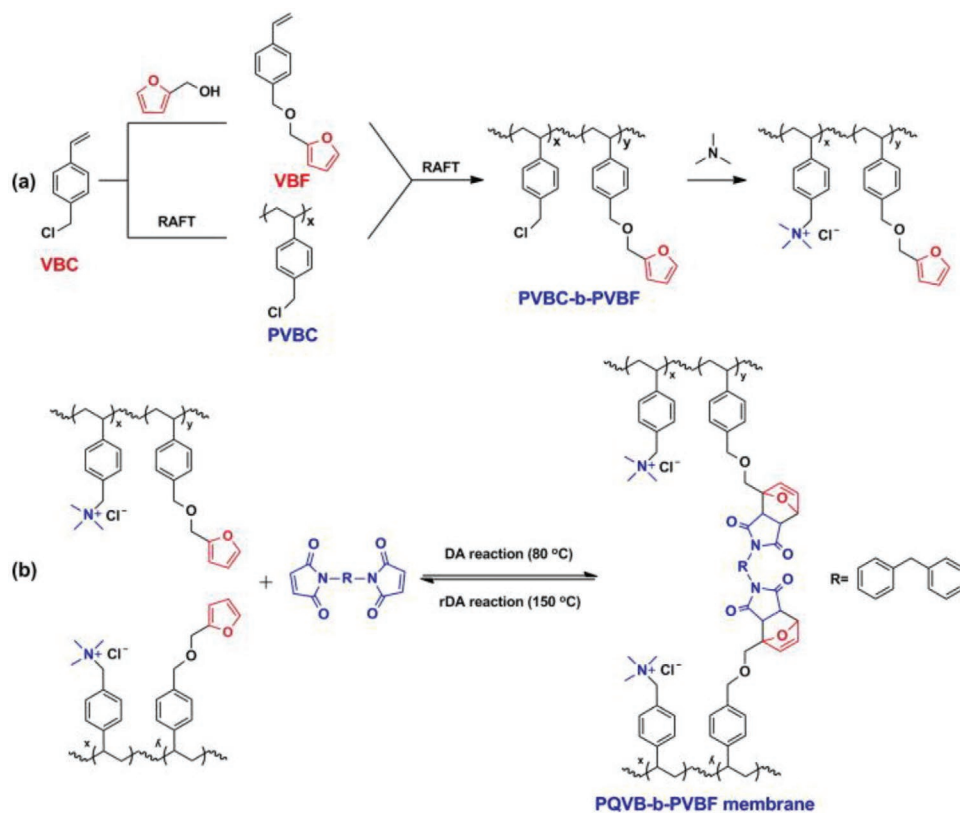
In 2019, Ahn and Kim prepared three poly(arylene ether ketone)-based AEMs with 1-(3-aminopropyl) imidazole pendant groups (PAEK-API) for VRFBs.^[161] All membranes featured a good chemical stability in strongly acidic aqueous media (3 M H₂SO₄) and higher ion-exchange capacities and a lower vanadium-ion permeability in comparison to Nafion 117. Among the three synthesized membranes, the PAEK-API membrane with a PAEK-NHS-to-API molar ratio of 2:1 exhibited the highest ion conductivity of 5.3×10^{-3} S cm⁻¹ (vs 50×10^{-3} S cm⁻¹ for Nafion 117) while maintaining low VO²⁺ permeability of 1.91×10^{-7} cm² min⁻¹ (vs 20.3×10^{-7} cm² min⁻¹ of Nafion 117) (Table 7). In VRFB rate capability tests, the membrane with the 2:1 molar ratio performed better compared to the Nafion 117 membrane in a current-density range from 40 to 100 mA cm⁻². The same PAEK-API membrane exhibited a capacity loss of 0.17% per cycle compared to 0.6% per cycle for Nafion 117 (100 cycles at 40 mA cm⁻²). The better capacity retention is attributed to the low VO²⁺ permeability.

Hou et al. pursued a highly interesting approach with regard to the formation and expansion of cracks, which lower the membrane performance and can lead to a long-term capacity

Table 7. Characteristics of the three PAEK-API AEMs compared to the benchmark Nafion 117 CEM.^[161]

	VO ²⁺ permeability [10 ⁻⁷ cm ² min ⁻¹]	Ion conductivity [×10 ⁻³ S cm ⁻¹]	CE [%]	VE [%]	EE [%]
PAEK-API (3:2)	1.31	4.3	97	82	79
PAEK-API (7:4)	1.57	4.7	97	84	81
PAEK-API (2:1)	1.91	5.3	96	87	83
Nafion 117	20.3	50	90	92	82

loss and self-discharge.^[162] To avoid an expensive replacement of the membrane, the authors developed a self-healing AEM for aqueous, pH-neutral RFBs. To the furan-containing block copolymer PVBC-*b*-PVBF, bismaleimide was added to form crosslinkages via a Diels–Alder reaction. At elevated temperatures, the linkage can be reversibly broken through retro-Diels–Alder reactions (Scheme 11). The resulting self-healing behavior of the membrane was proven via SEM images, which revealed that a crack fully vanished after heating the membrane to 150 °C for 1 h. After the confirmation of the self-healing capability, key parameters of the membrane, such as the ion conductivity (9.5×10^{-3} S cm⁻¹ for Cl⁻ in water) and the ion-exchange capacity (1.69 mmol g⁻¹ in water) were investigated. In particular, the ion conductivity exceeded the values of previously reported AEMs. To validate the applicability of the membrane in flow batteries, an all-organic RFB with 0.1 M 4-hydroxy-2,2,6,6-tetramethylpiperidin-1-oxyl as catholyte and



Scheme 11. Schematic representation of a) the synthesis route to PVBC-*b*-PVBF AEM via RAFT polymerization and b) the integrated self-healing behavior, based on a Diels–Alder reaction. Reproduced with permission.^[162] Copyright 2019, Elsevier.

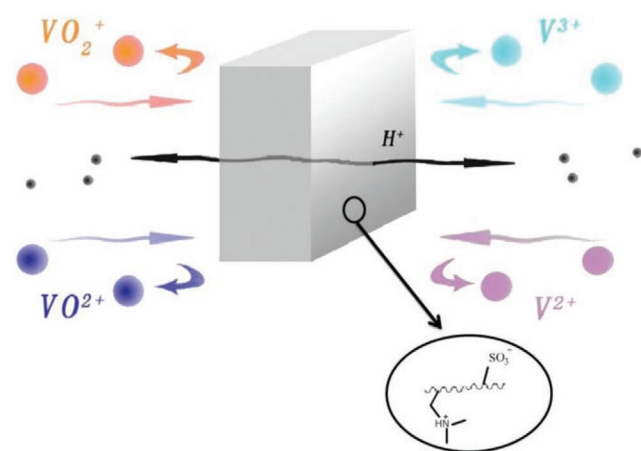


Figure 13. Schematic representation of the working principle of an AIEM in a VRFB. Reproduced with permission.^[164] Copyright 2014, Elsevier.

0.1 M bis(3-trimethylammonio)propyl viologen tetrachloride as anolyte, each in 1 M NaCl aqueous solution, was constructed. At a current density of 10 mA cm⁻², a stability test over 100 charge/discharge cycles was performed. A CE of 97% and a VE and an EE > 80% were achieved.

Amphoteric Polymeric Membranes: The working principle (Figure 13) of amphoteric ion-exchange membranes (AIEMs) was first described by K. Sollner in 1932.^[163] AIEMs feature both cation and anion moieties (e.g., sulfonate and tertiary ammonium groups), which form microscopic channels.^[164] These channels are able to transport the corresponding counter-ions. The macroscopic AIEM reveals different osmotic and electronic properties compared to the separate CEM and AEM.^[165] While large vanadium ions are repelled due to the Donnan effect, protons (and anions) can still permeate the membrane.^[166] Therefore, they combine the benefits of CEMs and AEMs, in particular the high chemical and mechanical stability and the excellent ionic conductivity of the former and the low vanadium-ion permeability of the latter. Notably, AIEMs have not been investigated in depth up to now.^[137]

In 2009, Qiu et al. grafted styrene and dimethyl aminoethyl methacrylate (DMAEMA) on a PVdF film via a γ -irradiation method, followed by a protonation and sulfonation, to develop a new AIEM system.^[167] Compared to the common Nafion 117 CEM (7.93×10^{-7} cm² min⁻¹), the new membrane exhibited a significantly lower vanadium-ion permeability (0.67×10^{-7} cm² min⁻¹). Applied in a VRFB, the AIEM exhibited an improved performance compared to Nafion 117 during an open circuit voltage (OCV) test. Whereas the OCV of the VRFB with Nafion 117 declined to 0.8 V after 14 h, the OCV of the VRFB with the AIEM stayed above 1.2 V (starting from 1.5 V) for about 68 h. This indicates a lower self-discharge for the AIEM, as the permeability for vanadium ions is much lower.

In another study, Sharma and co-workers fabricated an AIEM based on a crosslinked semi-interpenetrating copolymer with a rigid backbone.^[168] In this approach, styrene sulfonate and vinyl benzyl chloride were utilized as anionic and cationic moiety, respectively. The primary amine groups were turned into quarternary ammonium groups via three different quarternizing agents (iodomethane, trimethyl amine, *N*-methyl

morpholine), yielding three different AIEMs (ZWMI, ZWA, and ZWMO) (Scheme 12). All three membranes exhibited a good ion-exchange capacity, chemical and mechanical stability, as well as ionic conductivity (Table 8). Furthermore, the obtained values for the VO²⁺ permeability (Table 8) were one order of magnitude lower than for a common Nafion 117 CEM (3.57×10^{-7} cm² min⁻¹). The values of CE, VE and EE do not improve significantly, compared to Nafion, indicating no actual changes in terms of cell performance.

Dai et al. investigated various bipolar membranes (BPMs).^[169] These possessed an anion-selective layer and a cation-selective layer and were, thus, closely related to AIEMs regarding their working principle and properties (Figure 14).

The BPMs were fabricated from quaternized polysulfone (QAPSF), SPEEK resins and a poly(tetrafluoro ethylene) (PTFE) interlayer by a solution cast method (Figure 14). Several BPMs with different QAPSF-to-SPEEK ratios were obtained, which exhibited good stabilities and ion-exchange capacities.

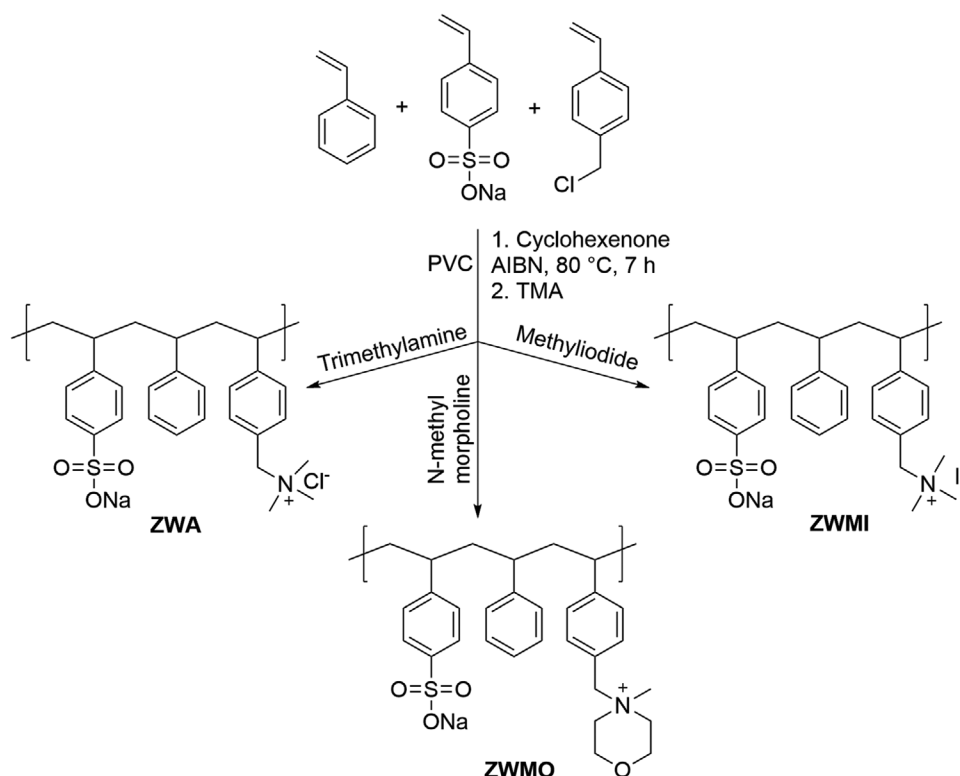
Furthermore, the ionic conductivities and the VO²⁺ permeabilities were significantly enhanced compared to the common Nafion 117 and AIEMs, showing a maximum value of 22.2×10^{-3} S cm⁻¹ for a QAPSF-to-SPEEK ratio of 1:2 (w/w) (Table 9). During a long-term durability test over 100 cycles at a current density of 80 mA cm⁻², the principle applicability of the BPMs was evaluated (Table 9).

3.3.2. Polymeric Porous Membranes

As already discussed, ion-exchange membranes, in particular CEMs such as the perfluorinated Nafion polymers are most frequently applied in commercially available flow batteries like the VRFB due to their excellent chemical stability and proton conductivity. However, the high costs and the high vanadium-ion permeabilities limit an extended commercialization of VRFBs.^[60a,b,145b] As a consequence, the current research focuses on cost-effective alternatives. Polymeric porous membranes, like PTFE/silica (Figure 15), are highly interesting systems, particularly due to the fact that various studies confirmed a similar performance of these membranes in flow cells like the benchmark Nafion-based separators.^[170] In contrast to ion-exchange membranes, porous separators have no ion-blocking capabilities. Instead, the ion separation is accomplished by different transport speeds of different ionic species due to different charge densities or Stokes radii. For example, for protons and vanadium ions, the time required for the diffusion through the membrane differs significantly, enabling the application in VRFBs. Furthermore, it is possible to adapt the membrane to the requirements of the electrolyte by a specific adjustment of the pore size and thickness.^[170,171]

The group of Skyllas-Kazacos performed intensive investigations of different porous separators, such as a modified Daramic PE/silica membrane, for applications in VRFBs.^[159a,172] Montoto et al. showed that it is possible to use commercial PE separators, such as Celgard 2325 and Daramic 175, in pRFBs with ferrocene and viologen containing polymeric active materials.^[41]

In 2011, Zhang et al. successfully demonstrated the synthesis and applicability of nanofiltration membranes by employing a pore-size exclusion to achieve a maximum proton/vanadium



Scheme 12. Schematic representation of the synthesis of AIEMs based on crosslinked semi-interpenetrating copolymers. Adapted with permission.^[168] Copyright 2018, American Chemical Society.

ion selectivity.^[173] Since Wei et al. provided an excellent and detailed overview of polymeric porous separators for RFB applications in their review from 2015, we will confine ourselves to the recently reported research activities.^[170]

Chae et al. developed a hydrophobic dibenzo[1,4]dioxin derived polymer containing nitrile groups with intrinsic microporosity (PIM-1).^[174] Dissolved in chloroform (0.5 wt%), the polymer was deposited on a PAN ultrafiltration membrane to achieve a composite separator. Caused by the Grotthuss or convection mechanism (**Figure 16**), only protons can migrate through the membrane leading to a high proton/vanadium selectivity. In a diffusion cell, the prepared composite membrane (75 μm hydrophobic polymer layer) exhibited a high permeation rate for protons and no detectable permeation of VO^{2+} after 100 h. Due to the absent vanadium ion crossover, a very high EE of 98.7% was achieved in a subsequent battery test at a current density of 1 mA cm^{-2} . In contrast, the observed

EE was nearly 0 when a common Nafion 112 CEM was applied at these low current densities. Likewise at current densities up to 40 mA cm^{-2} , the EE always was above 85%, surpassing the observed values for Nafion 112. Furthermore, during a long-term durability test over 100 cycles at a current density of 20 mA cm^{-2} , the flow cell with the composite membrane exhibited a nearly constant CE of 97%, a VE of 93%, and a EE of 90%.

Peng et al. studied a PBI-based porous membrane.^[171a] Owing to their high stability in acidic media and significantly low vanadium-ion permeability, PBI materials, applied in a VRFB, exhibited a high CE of 99% as well as a low capacity fade of 0.3% per cycle, as shown in different report by Zhou et al.^[175] Therefore, the authors prepared defect-free, ultrathin membranes via casting of a mixture of PBI and dibutyl phthalate (DBP) using different weight ratios. The resulting membranes revealed good mechanical stabilities that are comparable to Nafion 211. The achieved VO^{2+} permeabilities were exceptionally low (down to $8.12 \times 10^{-10} \text{ cm}^2 \text{ min}^{-1}$, in particular compared to Nafion 211 with $2.58 \times 10^{-7} \text{ cm}^2 \text{ min}^{-1}$). The membranes furthermore featured high chemical stabilities in acidic environment, similar to the benchmark Nafion 211. In VRFB cell tests, the performance parameters were explored. Over 20 cycles at a current density of 80 mA cm^{-2} , the PBI membranes exhibited CEs above 98% (Nafion 211: 83%). Among the PBI membranes, the system based on a DBP-to-PBI ratio of 2:1 seems to be the most appropriate one. However, although high values for CE and EE were measured, a large capacity loss of 0.4% per cycle was observed.

Table 8. Characteristics of the three AIEMs in comparison to Nafion 117.^[168]

	VO^{2+} permeability [$10^{-8} \text{ cm}^2 \text{ min}^{-1}$]	Ionic conductivity [$10^{-2} \text{ S cm}^{-1}$]	CE [%]	VE [%]	EE [%]
ZWMI	4.93	2.77	91	87	78
ZWA	4.59	1.84	91	87	79
ZWMO	5.27	3.12	90	85	76
Nafion 117	35.70	/	89	88	79

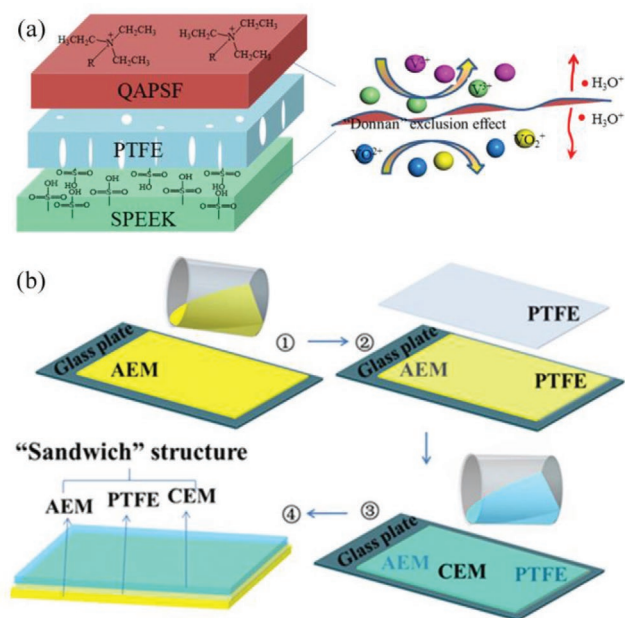


Figure 14. Top: Schematic representation of a) the working principle of BPMs and b) their preparation process. Reproduced with permission.^[169] Copyright 2018, Elsevier.

3.3.3. Concluding Remarks

Several types of polymers have been applied as membranes in RFBs. While Nafion represents the state of the art for commercial VRFB cells, a significant effort has been put into modifying and improving other commercial membranes and to develop superior new membranes. For VRFB applications, research focused mainly on minimizing VO_2^+ crossover and on maximizing the ionic conductivities. Different additives, such as inorganic fillers or ionic liquids, were further able to improve the performance. Moreover, the concept of self-healing could be applied to membranes, to further lengthen their life-time. When utilizing anion exchange membranes, the VO_2^+ permeability was further reduced, however this type of membrane still suffers from lower ionic conductivities, compared to cation exchange membranes. Amphoteric ion exchange membranes offer the advantages of both AEMs and CEMs, but have only recently received an increased attention. The last type of the discussed membranes is porous membranes, a rather new concept in the field of RFB research, which makes the use of ionic polymers redundant.

Table 9. Characteristics of the bipolar membranes.^[169]

QAPSF-to-SPEEK ratio	VO_2^+ permeability [$10^{-7} \text{ cm}^2 \text{ min}^{-1}$]	Ionic conductivity [mS cm^{-1}]	CE [%]	VE [%]	EE [%]
2:1	0.5	3.44	99	73	73
3:2	0.6	10.3	99	80	79
1:1	0.7	11.7	96	77	74
2:3	3.6	16.4	95	64	61
1:2	4.0	22.2	97	70	68

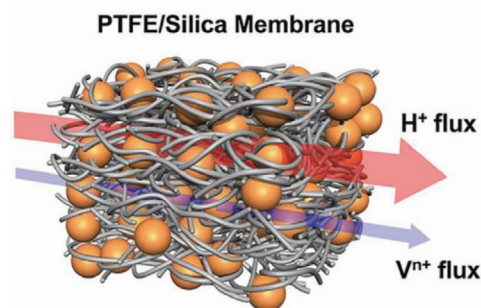


Figure 15. Schematic representation of a PTFE/silica porous membrane and their ion transport in a VRFB. Reproduced with permission.^[170] Copyright 2015, Taylor & Francis Ltd.

As the price plays an important role in developing economically sustainable flow batteries for long-term applications in a wide range of markets, we are convinced that research on cheaper alternatives to Nafion will have a great impact on the future applicability of RFBs. Suitable candidates with similar properties will have to be investigated in detail, to further reduce the price of the full cell. Another major issue is the crossover of active species in VRFBs, which can be mitigated by anion exchange membranes. Further research on this topic might improve membranes in terms of vanadium permeability.

4. Binders

Binders are a medium to keep the different electrode materials of thin-film electrodes in place and prevent the mechanical decay of these electrodes by acting as a sort of glue. Although binders make up only a small proportion of the electrode composite material, they play a crucial role for the battery performance. They increase the mechanical strength and the electrochemical stability of the electrode and ensure electron and ion transport. Furthermore, they improve the dispersity of active material and maximize electric contacts between the electrode components and the current collector.^[176] In general, polymers are used as binders and the molar mass, the concentration of functional groups, and the presence of side chains or branches determine the binding ability.^[177]

This section provides only a short summary of binders in battery applications. For further information, we recommend other, more detailed reviews on the topic, e.g., by Chen et al.,^[176b] Shi et al.,^[176a] and Bresser et al.^[178]

4.1. Binding Mechanisms

The binder processing can ideally be separated in two basic steps. The first step is usually the dissolution of the binder in an appropriate solvent and mixing it with the other components of the electrode. Diffusion of the binder and penetration of porous surfaces determine the structure of the composite material. The second step is the hardening, which can be either drying via evaporating the solvent or chemical hardening by in situ polymerization or postpolymerization

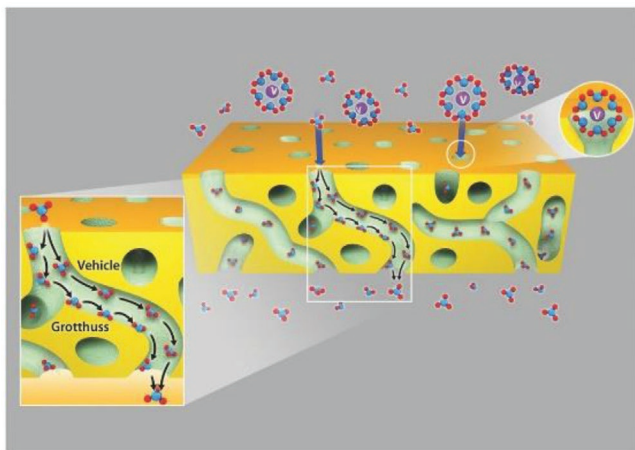


Figure 16. Schematic representation of the proton migration in the PIM-1 membrane due to the Grotthuss or convection mechanism. Reproduced with permission.^[174] Copyright 2016, Wiley.

functionalization (e.g., crosslinking) of the polymers. Depending on the chemical structure of the applied binder and the surface morphology of the other components, different binding mechanisms can be observed. Mechanical interlocking describes the process of the binder penetrating a porous surface and binding to it mechanically after hardening, depicted in **Figure 17**. This largely depends on the surface roughness of the coated material.^[179] In addition, physical intermolecular forces contribute to the binding strength of polymers, mostly van der Waals forces.^[180] Chemical bonding

takes place when the binder possesses functional groups that can interact with other molecules or surface groups. Examples for this type of bond are ionic bonds, hydrogen bonds and, in some cases, covalent bonds.^[181]

4.2. Crucial Binder Properties

In application, binders have to be inert to the processes inside the battery and the formulation process of the electrode. Therefore, high thermal, mechanical, chemical, and electrochemical stabilities are required. Furthermore sufficient electronic and ionic conductivity have to be given, as to not limit the transport processes.

The thermal stability is the most important parameter for the processing of the electrodes, as in the drying process temperatures of up to 120 °C are reached.^[182] The operating temperature window for batteries with common liquid electrolytes in practical use ranges from -20 to 55 °C, for solid state batteries up to 100 °C.^[183]

Regarding the mechanical stability, tensile strength, flexibility, hardness, elasticity and adhesive strength are the most important parameters.^[184] These are largely influenced by the molar mass and the present functional groups of the polymer and determine the stability of the electrode over continued cycling and possible volume changes of the active material, as it is the case for silicon anodes in LIBs.^[184,185]

Furthermore, the binder should be completely inert to the conditions inside the battery. It should not react with the electrolyte, active material and any side- or intermediate product

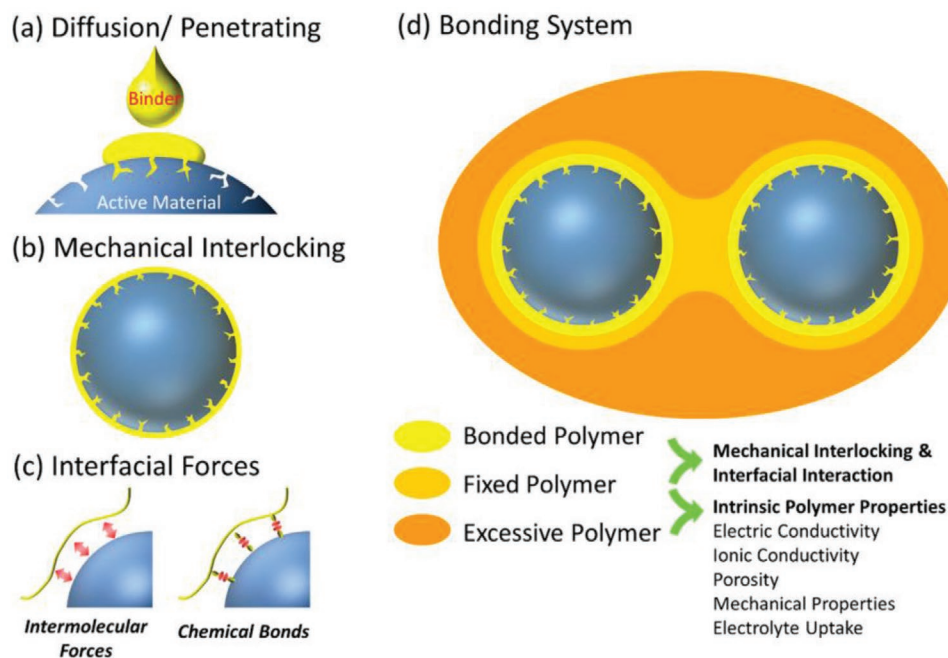


Figure 17. Schematic representation of different binding mechanisms: a) Diffusion and penetration of electrode materials by the binder slurry during electrode processing. b) Mechanical interlocking mechanism between binder and the surface of electrode materials, when the slurry is dried. c) Different chemical binding mechanisms between functional groups of the binder and the particle surface. d) The different states and tasks of the polymer in the bonding system. Reproduced with permission.^[176b] Copyright 2018, American Chemical Society.

of the electrochemical reactions.^[186] As well, the electrochemical stability window has to be in accordance with the cell voltage.

Next to stability issues, the electric and ionic conductivity have to be considered. Using conjugated polymers can raise the conductivity of the binder and might eliminate the necessity of a conductive additive.^[187] Ionic conductivity is mainly dependent on the crystallinity, viscosity, and porosity of the polymer chains and represents an important parameter of a binder.^[188]

4.3. Binders for Lithium- and Other Metal-Based Batteries

The most widely used binder in lithium-battery technology and also for organic batteries is PVdF.^[11b,189] PVdF exhibits good chemical and electrochemical stability, and good processability.^[176c,189a] Still, there are several drawbacks, which have to be overcome to further improve the battery performance. One major problem is the low binding affinity, which is mainly attributed to mechanical interlocking and weak van der Waals forces. Binders containing functional groups, such as alcohols or carboxylic acids, can form stronger interactions with the different materials of the electrode.^[176c] As well, the electrochemical and thermal stability is insufficient. Capacity loss has been attributed to the swelling and dissolution of PVdF in electrolyte solvents. In addition, reactions with graphite and other electrode materials can take place at elevated temperatures, decreasing the cell safety.^[190] Moreover, PVdF is an insulating material; therefore, conductive additives are necessary for an electrode material.^[190b,191] On top of that, the processing is demanding and, therefore, cost intensive. PVdF itself is an expensive polymer and it has to be processed in the toxic and environmentally harmful solvent *N*-methylpyrrolidone (NMP).^[192]

Due to these occurring problems, research focused on identifying new, more stable, cheaper, more environmentally friendly, easily processable, and disposable alternatives to PVdF. Several binders have been developed and tested, mostly in lithium-ion batteries. The most prominent binders are carboxymethyl cellulose (CMC), poly(acrylic acid) (PAA) and sodium-alginate (Na-ALG), which are environmentally friendly and can be processed in water.^[193] Next to these examples, several others have been reported. Electronically and ionically conducting polymers are present in current literature, as well as biological and biologically derived polymers and commercially available polymers. Furthermore, research focuses more and more on improving existing binders, by blending, crosslinking and grafting of different polymers, or by chemical modification of functional groups.

4.3.1. CMC

CMC is one of the most commonly applied binders in research. It was first described by Drogenik et al. in 2003 and has been studied extensively since then.^[193c] It consists of natural cellulose, modified with carboxymethyl groups, which make the material water-soluble. Thus, the processing is more environmentally benign. Compared to PVdF, its price is one magnitude lower. Another advantage is the easy disposal by

pyrolysis.^[192] CMC binds with its carboxylic groups to the surface of the substrates and is able to form strong hydrogen and covalent ester bonds, therefore it is suitable for compounds with surface hydroxyl groups (such as silicon). Furthermore, CMC does not swell in liquid electrolytes, thus maintaining its mechanical properties inside the cell.^[194] Usually, the sodium salt of CMC is applied, but when changing the counter ion to Li⁺, the Li⁺ ion conductivity throughout the binder can be improved.^[195]

Wang et al. studied the degree of substitution of CMC and its influence on the electrochemical performance of silicon anodes.^[196] Very high degrees of substitution do not lead to an improved performance of the electrode. The authors proposed that an intramolecular bonding of the functional groups led to coiling of the polymer and less active binding sites. As well, the overall hydrophobicity of the binder plays an important role. In the study, a substitution degree of 0.55 yielded the highest specific capacity and the best cycling performance, with 46% capacity retention after 100 cycles at 0.1 C, while cells with PVdF lost all capacity after 20 cycles.

Zhang et al. investigated a new, inorganic crosslinker for CMC based on sodium borate for silicon-based lithium ion batteries.^[197] By crosslinking conventional CMC with Na₂B₄O₇ and chemical bonding of CMC and the crosslinker to silicon, the large volume change of silicon during charging/discharging could be accommodated and a long cycle life of 600 cycles at 0.33 C and 34% capacity retention was achieved. Under the same conditions, the control sample of pure CMC nearly lost all capacity after 600 cycles, retaining only 2% of the initial capacity.

Kim et al. compared CMC, alginate and PAA as aqueous binders for LiCoPO₄.^[198] It could be shown that the stiffness of CMC, the uniform distribution and the presence of carboxylate groups prevented the degradation of the electrode material by an attack of HF, which can be generated from the electrolyte salt LiPF₆. Compared to PAA and alginate, CMC possessed superior HF scavenging abilities when used in combination with LiPF₆. In cycling experiments, 68% of the initial capacity was retained after 100 cycles at C/10, which is comparable to other studies on this cathode material.

When mixing CMC with PAA, the performance of the battery can be improved. The addition of PAA leads to an increased ionic conductivity for Li⁺ and a decreased tendency to crack during charge/discharge processes compared to pure CMC. Fei et al. applied the hybrid binder in a ZnMoO₄ × 8H₂O cathode for lithium batteries.^[199] Compared to PVdF and pure CMC as binders, the diffusion coefficient of Li⁺ could be raised by a factor of 1000 and 10, respectively. The manufactured cell maintained 479 mA h g⁻¹ after 50 cycles, when cycled at 100 mA g⁻¹, the capacity fade per cycle was 0.7%. The good stability was attributed to the carboxylic groups of CMC and PAA.

Lee et al. reported a crosslinked mixture of CMC and PAA (1:1) and achieved high mechanical stability and strong binding affinity to Co₃O₄.^[200] The cobalt oxide-nanoparticles showed large volume expansion during charge/discharge cycling, usually leading to domain isolation and a loss of electric conductivity. These drawbacks were successfully prevented by using the cured CMC/PAA hybrid binder.

The SEI formation abilities of PVdF, CMC, PAA, and crosslinked CMC-PAA were compared by Nguyen et al. In this

study, CMC and PAA formed SEIs when applied in silicon electrodes.^[201] It was shown that the pH value of the binder solution strongly affected the formation of a SiO_x layer on the active material, the high pH value of CMC formed thicker SiO_x layers. These will ultimately lower the performance of the cell. In contrary to PVdF, all other polymers formed SEI layers on top of the silicon, thus preventing further decomposition of the electrolyte and leading to slower growing, thinner electrolyte derived SEI in general and higher performance. As well, the HF scavenging ability of CMC was confirmed. In conclusion, crosslinked CMC-PAA and PAA revealed the best electrochemical cycling performance.

4.3.2. PAA

PAA has been applied as binder in several examples, ranging from graphite electrodes, over Sn₃₀Co₃₀C₄₀ to silicon anodes.^[193a,202] It possesses similar properties like CMC in terms of solubility in electrolyte solvents, hardness, and elastic module. Due to the higher concentration of carboxylic groups, a higher binding affinity was achieved for surfaces with large amounts of hydroxyl groups, such as silicon. Other reports attribute PAA the ability to form an artificial SEI and, thus, to stabilize the electrodes.^[203] The binding properties also depend on the degree of substitution. When neutralized with NaOH, a substitution degree of 80% sodium carboxylate and 20% carboxylic acid led to the best performance for silicon anodes.^[203a]

PAA was covalently bound to silicon particles by Jung et al. using a sodium hypophosphite catalyst and thermal annealing, enabling the compensation of large volume changes of the anode during cycling.^[204] The covalent ester bonds exhibited good mechanical and electrochemical stability compared to PAA bound via hydrogen bonds. The use of the catalyst increased the number of ester bonds in comparison to simple thermal annealing. By introducing the covalent bonds, the SEI was stabilized and aggregation of the silicon nanoparticles was suppressed.

Adding ethylenediaminetetraacetic acid (EDTA) to the binder slurry enabled the formation of a stable SEI for silicon anodes, as shown by Lee et al.^[205] Pure PAA exhibited weak HF scavenging abilities, therefore the SEI formed by PAA can be degraded during cycling by in situ formed HF. EDTA suppresses this side reaction by forming an EDTA–water complex and, thus, eliminating the necessary reagent to form HF from PF₅. After 300 cycles, more than 83% of the initial capacity was retained.

Li et al. modified PAA with glycinamide, leading to strong hydrogen bonds to the silicon surface in silicon anodes and inter-chain interactions.^[206] The facile functionalization of the polymer led to a supramolecular self-healing ability, which enabled the accommodation of the large volume changes of the silicon anode during cycling. The prepared electrodes revealed higher capacities compared to electrodes containing unmodified PAA. A high capacity retention of 81% after 285 cycles was observed.

Poly(acrylic acid) was grafted from CMC via free radical graft polymerization by Wei et al., revealing better electrochemical properties in silicon electrodes compared to their linear counterparts.^[207] The grafted polymer revealed better binding affinity to silicon due to the branched structure, leading to multiple point contacts of the 3D network to the substrate. This structure could

withstand the large volumetric changes of the anode through repeated cycling and led to a superior cycling stability, compared to linear CMC, linear PAA and a mixture of PAA and CMC. Furthermore, the grafted polymer assisted in forming an SEI layer.

Cao et al. grafted PAA as sidechains via RAFT from a glycol chitosan backbone and applied it in silicon/graphite composite electrodes.^[208] It was shown that the grafting density as well as the length of the sidechains influenced the mechanical and electrochemical properties of the electrodes. In this report, longer sidechains and higher grafting densities revealed the best cycling stability, which was attributed to a better interaction of the binder with the silicon active material and the higher solution viscosity and, thus, peeling strength of the electrode.

4.3.3. PEI/PEO

PEO is known to dissolve and conduct lithium salts and has therefore been in the focus of battery research for a long time.^[72a] When used as binder material, the electrode benefits from this ability of PEO. It was shown that the cell resistance is dependent not only on the electric conductivity, but mainly on the ionic diffusivity of the electroactive species.^[209] However, plasticized PEO suffers from a low mechanical stability, due to this polymeric additives or copolymers are required to increase the strength.^[210] Due to its similar structure to PEO, PEI is also able to conduct lithium ions and can furthermore form hydrogen bonds both as donor and acceptor.^[211] Other than PEO, PEI can easily be modified at the nitrogen atoms, to decrease the crystallinity and hydrogen bonds or to further create polycations.^[212] PEI is in particular interesting to inhibit polysulfide shuttling in lithium sulfur batteries, because of its high affinity to aforementioned.^[213]

PEI was crosslinked with poly(ethylene glycol diglycidylether) by Chen et al. to synthesize a hydrophilic binder with strong binding sites for lithium–sulfur batteries.^[214] The authors found that an optimum amount of crosslinker improved the performance of the cell. The ideal ratio of glycidylether groups to amino groups was 1:2. In cycling experiments, shuttling of polysulfides was suppressed by strong interactions between polysulfides and the polar groups of the prepared binder. This was proven by Raman spectroscopy and led to a capacity retention of 72% after 400 cycles.

A similar study by Yan et al. reported that a commercial epoxy resin can crosslink PEI and increase the cycling stability.^[215] A stable 3D network was formed, which was able to prevent sulfur shuttling and, thus, increasing the cycle life. When applied in a cell, it proved to be superior to PVdF and exhibited excellent 80% capacity retention at sulfur loadings of 1.9 mg cm⁻² and 0.5 C after 1000 cycles. At high sulfur loadings of 5.4 mg cm⁻² 72% of the initial capacity was retained after 500 cycles at 0.5 C.

Tsao et al. developed a PEO-*b*-PAN copolymer, which was able to increase the rate capability in LiFePO₄ cathodes.^[216] The good dispersion of LiFePO₄ inside the composite material and the ability to conduct Li⁺ ions are the main reasons for improved charge/discharge rates, compared to PVdF.

PEO was investigated as both binder and matrix for the solid electrolyte in a solid-state battery with metallic lithium and

LiFePO₄ by Wan et al.^[217] The PEO was able to mechanically stabilize the solid electrolyte matrix, comprised of Li₇La₃Zr₂O₁₂ nanowires, at high temperatures of 60 °C and improved the ionic conductivity compared to similar systems in the literature. In addition, the battery exhibited a high specific capacity after 80 cycles at 0.1 C, namely 158 mAh g⁻¹.

4.3.4. Comparative Studies of Different Binders

Different binder concentrations of CMC and PAA for silicon anodes were compared by Karkar et al. in a comparative study.^[194] The authors showed that PAA performed better at high binder concentrations, whereas CMC outperformed PAA at low binder concentrations (4 wt%). This finding was attributed to the better bridging properties of CMC, thus functioning better at low concentrations. PAA on the other hand had a higher bulk stability, which resulted in a higher stability at high binder concentrations (12 wt%). At low binder concentrations, ageing of the electrode for 2 to 3 days in a humid atmosphere led to an improved adhesion to the current collector and better cohesion inside the electrode.^[218]

Another study was conducted for different binders and silicon anodes by Xu et al., where commercial PVdF, Na-ALG, Nafion and ion-exchanged Li-Nafion were examined.^[219] In charge/discharge cycling tests of full cells, containing silicon anodes and LiNi_{1/3}Mn_{1/3}Co_{1/3}O₂ (NMC) cathodes, electrodes containing Na-ALG and Li-Nafion exhibited the highest cycling stabilities over 100 cycles. As described before, the superior stabilities compared to PVdF were attributed to the carboxylic acid- and sulfonic acid-groups of Na-ALG and Nafion, respectively, binding well to the silicon surface. The authors also observed that the mechanical properties were not directly proportional to the performance of a binder. Na-ALG featured a high elastic modulus and hardness, whereas Nafion had a very low elastic modulus and hardness. Na-ALG was therefore a rather stiff binder, Nafion softer. As both binders performed very similarly under the same conditions, the mechanical properties do not seem to influence the performance of the binders in the application.

Huang et al. studied the application of CMC, guar gum (GG), Na-ALG and CMC:SBR in silicon anodes and correlated the dispersion homogeneity to the performance of the binders.^[220] An improved dispersion of the single components of the composite material led to a decreased electrical resistance of the films. Of the above mentioned binders, CMC featured the best dispersion efficiency, which also resulted in a lower internal resistance of the electrode film, due a homogeneous distribution of active material and conductive additive. As well, CMC exhibited the best adhesion to the copper substrate in peeling tests. In electrochemical tests, CMC revealed higher capacities compared to Na-ALG and GG, and performed also far better than CMC:SBR. The low performance of the mixture of CMC and SBR was attributed to the migration and, thus, phase separation of SBR inside the composite material.

The tortuosity of different binders (CMC:SBR, Na-ALG, and three different suppliers of PVdF) was measured and correlated to the charge capacities of model cells by Landesfeind et al.^[221] The tortuosity was calculated with the help of EIS and related to the C-rate at which 50% of the capacity can be accessed. Electrodes with lower tortuosity featured better performance as the concentration gradients were lower because of faster ionic transport through the pores. The authors stated that the tortuosity represents a helpful tool for designing new binder systems.

4.3.5. Other

Polyacrylamide (PAM) was crosslinked and applied as a binder in both silicon and sulfur electrodes for lithium-ion batteries by Zhu et al.^[222] Very small amounts of crosslinker (0.1%) produced a hydrogel network with water, which was highly flexible and foldable. In stretch tests, the hydrogel could be stretched to its 6.1-fold length without breaking (Figure 18). The high flexibility stabilized the volume changes during cycling, maintaining the integrity of the electrode. Furthermore, the amido-groups featured high affinities to the silicon surface and to soluble polysulfides, thus preventing shuttling effects. In sulfur electrodes, 98% of the initial capacity was retained after

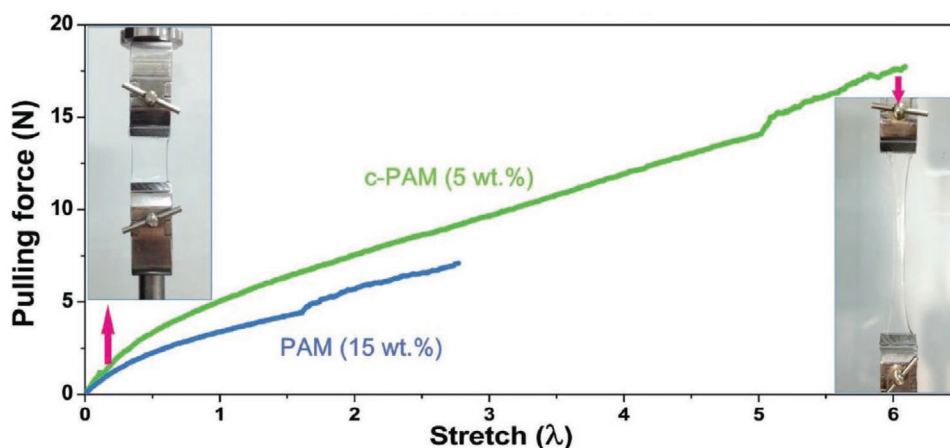


Figure 18. Stretch tests of hydrogels, containing 5% of crosslinked PAM (c-PAM) or 15% of linear PAM. The stretch is stated as the distance between the two clamps divided by the initial distance λ . Reproduced with permission.^[222] Copyright 2018, Wiley.

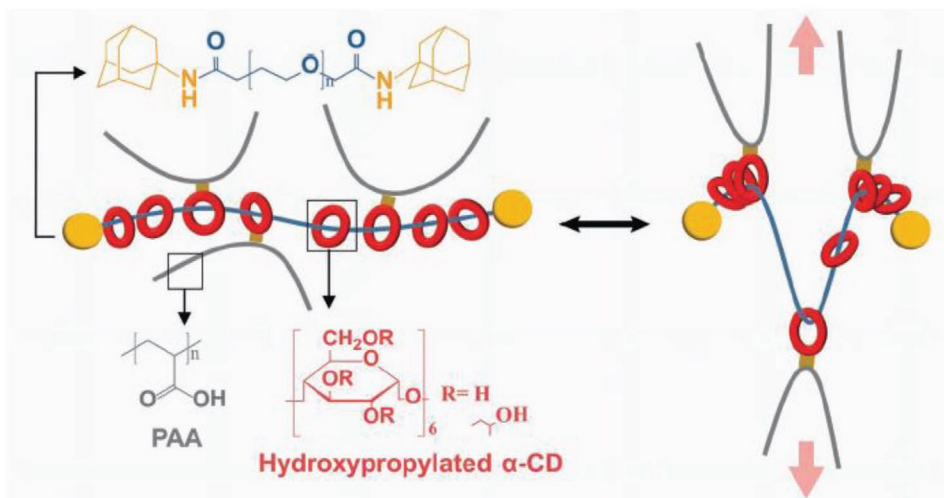


Figure 19. Schematic representation of the polyrotaxane-PEO structure, crosslinked to PAA and its reaction to mechanical stress. Reproduced with permission.^[223] Copyright 2019, Wiley.

200 cycles at 1 C. In silicon anodes, 90% were retained after 100 cycles at 0.1 C, outperforming PVdF and Na-ALG.

Yoo et al. reported a polyrotaxane binder for carbon nanotube (CNT) anodes for lithium-ion batteries (**Figure 19**).^[223] α -Cyclodextrine (α -CD) was wrapped around a PEO-backbone and linked to PAA (5 wt% α -CD and 95 wt% PAA). Because the α -CD-rings were able to move freely along the PEO chain, a high elasticity and stretchability were obtained. In strain tests, the polymer was able to maintain its integrity at up to 570% strain. In a full cell test with a LiFePO_4 cathode, 65% of the initial capacity was retained after 140 cycles at 1 C, outperforming linear PVA.

Supramolecular structures of perylene bisimide (PBI) were investigated by the groups of Cairns and Helms and co-workers^[224] The applicability of supramolecular PBI structures as binders in lithium sulfur batteries was shown in two separate studies. In their first study, a composite binder containing PBI and PVdF exhibited 86% capacity retention after 150 cycles at 1 C. A modified structure of PBI, containing four lithiated carboxylic acid groups, was water-processable and exhibited high affinity toward polysulfides. Compared to the nonlithiated species and to PVdF, superior cycling and high rate stability were observed. After 250 cycles at 1.5 C, 73% of the initial specific capacity was retained.

Lin et al. reported a poly(amic acid) with both free as well as pyrene-functionalized carboxylic acid side groups as a binder for silicon/C anodes.^[225] The free carboxylic acid groups were able to bind to the copper substrate and to the silicon surface via hydrogen bonds and electrostatic interactions, while the pyrene side groups formed π - π interactions to graphite (**Figure 20**). Peeling tests revealed a higher adhesion strength compared to for Na-ALG. In addition, the cycling stability was investigated. After a strong capacity fade during the first five cycles, a capacity retention of 79% from cycle 5 to cycle 300 was obtained, outperforming Na-ALG and polymers without carboxylic acid or pyrene groups.

Applying a mixture of hard and soft polymers in an interweaving network in silicon anodes, Liu et al. were able to

increase the performance and to apply this technique to other electrode materials.^[226] In theory, hard polymers decrease the volumetric changes during cycling, while soft polymers are less likely to crack, act as a better cohesion agent and form stable SEIs. Using poly(furfuryl alcohol) (PFA) as hard component and poly(vinyl alcohol) as the soft part, a mixed binder was prepared and electrochemically tested in silicon anodes. The ratio of 3 PFA to 1 PVA exhibited the best properties. After 300 cycles, 73% capacity retention was observed in silicon anodes. Indentation experiments proved the combined properties of PFA and PVA. Thermoplastic polyurethane (TPU) and SBR were also applied as soft polymers in binder mixtures and investigated for silicon, Sn and Fe_2O_3 electrodes.

Ammonium polyphosphate was applied as an inorganic polymer in lithium-sulfur batteries by Zhou et al.^[227] It was shown that the polyphosphate was able to suppress the shuttling effect of polysulfides and to stabilize the sulfur electrode. As well, the Li^+ -ion mobility was enhanced. Furthermore, polyphosphate acted as a flame retardant and obviously reduced

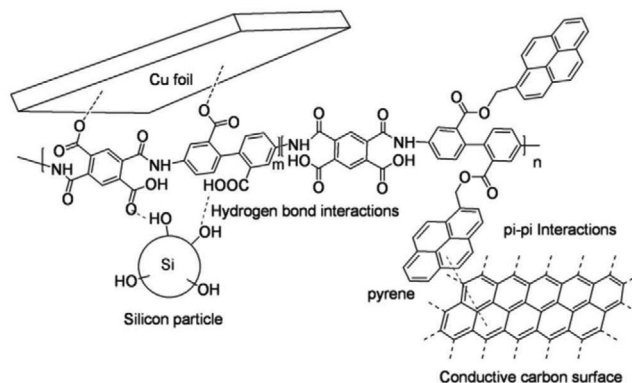


Figure 20. Proposed interactions between poly(amic acid) and Cu foil and silicon, as well as the interactions between pyrene and graphite. Reproduced with permission.^[225] Copyright 2019, Elsevier.

the flammability of the sulfur electrode. In a device, 85% capacity retention was observed after 400 cycles at 0.5 C.

A polyelectrolyte binder, consisting of a poly[(*N,N*-diallyl-*N,N*-dimethylammonium)-*bis*(trifluoromethanesulfonyl)imide] backbone, which was investigated by Li et al., revealed good retention of polysulfides in lithium sulfur batteries and led to an improved cycling stability.^[228] The polycationic backbone featured good affinity to polysulfides causing a higher retention time and preventing shuttling effects. The authors found that the trapped polysulfide chains could be more effectively reoxidized to sulfur or reduced to smaller polysulfide chains during charging/discharging. Cycling stability tests revealed 58% capacity retention after 250 cycles at 0.2 C.

The same polymer was investigated by Chauque et al., who attributed the good electrochemical performance in Li₂TiO₃ electrodes to high Li⁺-ion conductivity and wettability of the electrode material.^[229]

4.3.6. Conducting Binders

Using conducting polymers as binder materials is of interest enabling to avoid the addition of carbonaceous materials. As conducting polymers are usually conjugated, the application of a copolymer or a polymer blend can be mandatory to increase the flexibility and to maintain the mechanical stability.^[230]

Higgins et al. were able to produce a silicon electrode without carbon additives by using the electronically conducting and commercially available poly(3,4-ethylenedioxythiophene) polystyrene sulfonate (PEDOT:PSS) polymer blend.^[231] Electrodes with high loadings of silicon with up to 90 wt% performed well in electrochemical cycling, the optimal loading was 80 wt% of active material. The authors proposed that the main advantages are the commercial availability as well as the easy manufacturing using water-based slurries. Furthermore, they stated that the system can be further improved by adding different polymers to the binder mixture to ensure an improved adhesion to the active material, because PEDOT:PSS does not possess carboxylic groups, nor is it elastomeric.

PEDOT:PSS was crosslinked with PEO and mechanically mixed with PEI by Zeng et al. to yield an electronically and ionically conducting binder for silicon anodes in lithium-ion batteries.^[232] Compared to the commonly used CMC, the resulting binder exhibited a 14 times higher lithium-ion conductivity and a 90 times higher electron conductivity. PEO and PEI are both responsible for the ionic conductivity, while PEDOT:PSS ensures the electronic conductivity. Crosslinking PEO and the sulfonate groups of PSS led to a higher mechanical stability, which can withstand the strain arising from the large volume change of silicon anodes during cycling. The exhibited cycling stability was excellent, maintaining 83% of the initial capacity after 500 cycles.

Another conducting polymer, namely a modified poly(fluorene) with pendant carboxylic groups, was synthesized by Liu et al. and applied in silicon anodes in lithium-ion batteries.^[233] Due to the good electric conductivity of the material, it was possible to construct electrodes without any additional conductive carbon material. The side chains, bearing carboxylic groups, are responsible for the solubility in water during processing and the good stability of the resulting electrode during cycling, as they bind

covalently to the silicon surface. In cycling experiments, over 85% of the initial capacity remained after 100 cycles.

A conducting copolymer consisting of pyrene-functionalized methacrylate and dopamine-substituted methacrylate was synthesized by Zhao et al. and utilized as a binder in silicon anodes.^[234] The pyrene pendant-group containing backbone is responsible for electronic conductivity, whilst the catechol structure has a high binding affinity toward silicon. When cycling the prepared electrode, over 90% of the initial capacity was reached after 120 cycles using a nickel–cobalt–manganese cathode and a silicon anode, proving the good performance of the binder.

Wang et al. prepared doped poly(aniline) (PANI) in the presence of PAA and were able to prepare electrically conducting binders, which did not require further addition of conducting carbon for silicon anodes.^[235] PANI was responsible for the conductivity, PAA ensured a good adhesion to the silicon surface. Different ratios of PANI and PAA were investigated, a content of 30% PAA of the total binder exhibited good mechanical stabilities and the best electrochemical properties. Higher amounts of PAA led to brittle and less flexible binders, which were not able to accommodate large volume changes of the electrode. After 100 cycles at 0.2 C, more than 83% of the capacity was retained and it was charged and discharged for up to 1000 cycles at 1 C with a capacity retention of about 65%.

Another study on PANI as a conductive binder for silicon anodes was performed by Lee and Kim.^[236] The authors copolymerized PANI with anthranilic acid, to introduce a carboxylic acid group to the polymer backbone, which adheres very well to the silicon surface. No additional conductive additives were used in the prepared electrodes. A content of 50% anthranilic acid proved best in terms of cell performance, exhibiting 81% of the initial capacity after 50 cycles. Higher contents of anthranilic acid reduced the conductivity but raised the mechanical stability, while lower contents did vice versa.

Crosslinked PPy was applied in a network with CMC in lithium–sulfur batteries by Liu et al., where the binder could enhance the electronic and ionic conductivity, as well as prevent shuttling effects of polysulfides.^[237] The crosslinker was 4,4'-biphenyldisulfonic acid, which formed bonds through acid–base interactions with poly(pyrrole). The negatively charged sulfonate groups facilitated Li⁺-transport and prevented the dissolution of polysulfides, while the conjugated PPy backbone was responsible for the electronic conductivity. The conducting polymer was in situ polymerized and crosslinked in a CMC matrix, forming a percolating network inside the CMC. Cycling experiments revealed that 76% of the initial capacity was retained after 400 cycles.

4.3.7. Self-Healing Binders

Self-healing polymers are able to form reversible intermolecular bonds, which lead to an intrinsic healing of the polymer if stretched or scratched. Supramolecular interactions and covalent bonds can induce a self-healing behavior. In some cases, energy has to be transferred to the material, usually by heating or light irradiation, to reorganize the polymer chains and reform broken bonds and interactions.^[238] Self-healing

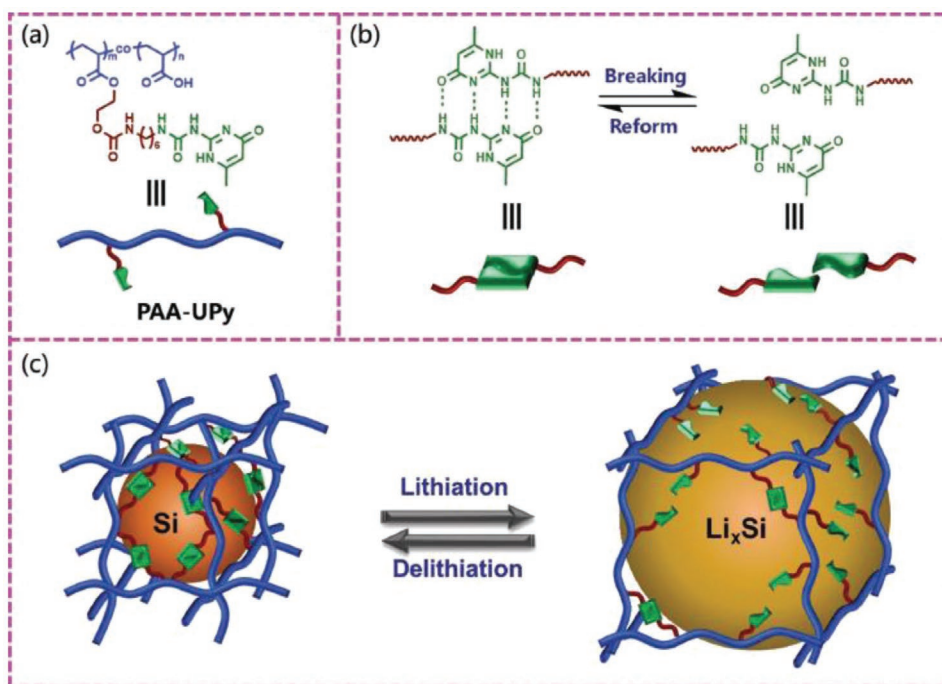


Figure 21. Schematic illustration of the self-healing behavior of polymers with ureido-pyrimidinone pendant groups. Reproduced with permission.^[241] Copyright 2018, Wiley.

polymers are interesting candidates for binder applications as they are able to heal cracks and holes emerging in electrodes due to mechanical stress and/or volume changes during electrochemical cycling, thus prolonging the cycle life of a cell.

Sodium alginate and carboxymethyl chitosan form a self-healing polymer network, which was applied by Wu et al. in silicon anodes.^[239] The resulting water-soluble binders exhibited strong electrostatic interactions between carboxylate and protonated amino groups, which led to the formation of a crosslinked network. This network was able to decrease the capacity fade resulting from large volume changes of silicon during cycling by forming reversible, self-healing bonds between Na-ALG and chitosan and bonds to the hydroxyl groups on the silicon surface. Higher mechanical stability, compared to the single components, was achieved. These findings were supported by the improved charge/discharge cycling stability of the anode employing the polymer network (60% capacity retention after 160 cycles).

An ionically conducting, self-healing polymer on the basis of isocyanate functionalized PEG and PEI was applied in silicon anodes by Munaoka et al.^[240] Self-healing tests revealed the ability of the polymer to heal at room temperature within 3 h. It was shown that 40% crosslinking with 750 g mol⁻¹ PEG yielded the best self-healing abilities. By including PEG into the structure, the ionic resistance was lowered and cycling at higher rates was possible, compared to the polymer without PEG. In long-term cycling experiments, 80% of the initial capacity was retained after 150 cycles.

Another self-healing polymer, based on strong supramolecular interactions among the side groups of a PAA, was investigated by Zhang et al. in silicon electrodes.^[241] As pendant groups, ureido-pyrimidinone was chosen, which can

form quadruple hydrogen bonds between two molecules (Figure 21). Self-healing tests revealed good self-healing abilities at room temperature. In peeling tests, the self-healing binder outperformed both PAA and PVdF, revealing the highest adhesion to silicon, conductive carbon and the current collector. When applied in cycling tests, the electrodes retained high capacities of over 2600 mAh g⁻¹ after 110 cycles (74% of the initial capacity). Moreover, the electrodes showed less and smaller cracks in SEM images after 110 cycles, compared to PAA and CMC electrodes cycled under the same conditions.

4.3.8. Biopolymers

Besides conventionally synthesized polymers, a growing number of natural and naturally derived polymers have been applied as binders. The advantages of biopolymers are their environmental friendliness, water-solubility, and sustainability. While CMC can also be seen as a biopolymer that has been chemically modified, several other polymers have been investigated as binders. Examples range from sodium alginate and chitosan, over starch, lignin, cellulose, guar gum, and xanthan gum (XG) to other polysaccharides.^[193b,242]

The most popular biopolymer binder is alginate, which was described by Kovalenko et al. in 2011 for silicon anodes.^[193b] In contrast to common polysaccharides, it possesses one carboxylate group per repeating unit. Several studies have shown that carboxylic groups strongly contribute to the binding strength of a polymer. Alginate, which is usually won in its sodium salt form, is a copolymer of 1,4-linked β -D-mannuronic acid and α -L-guluronic acid. The ratio and sequence of both co-monomers

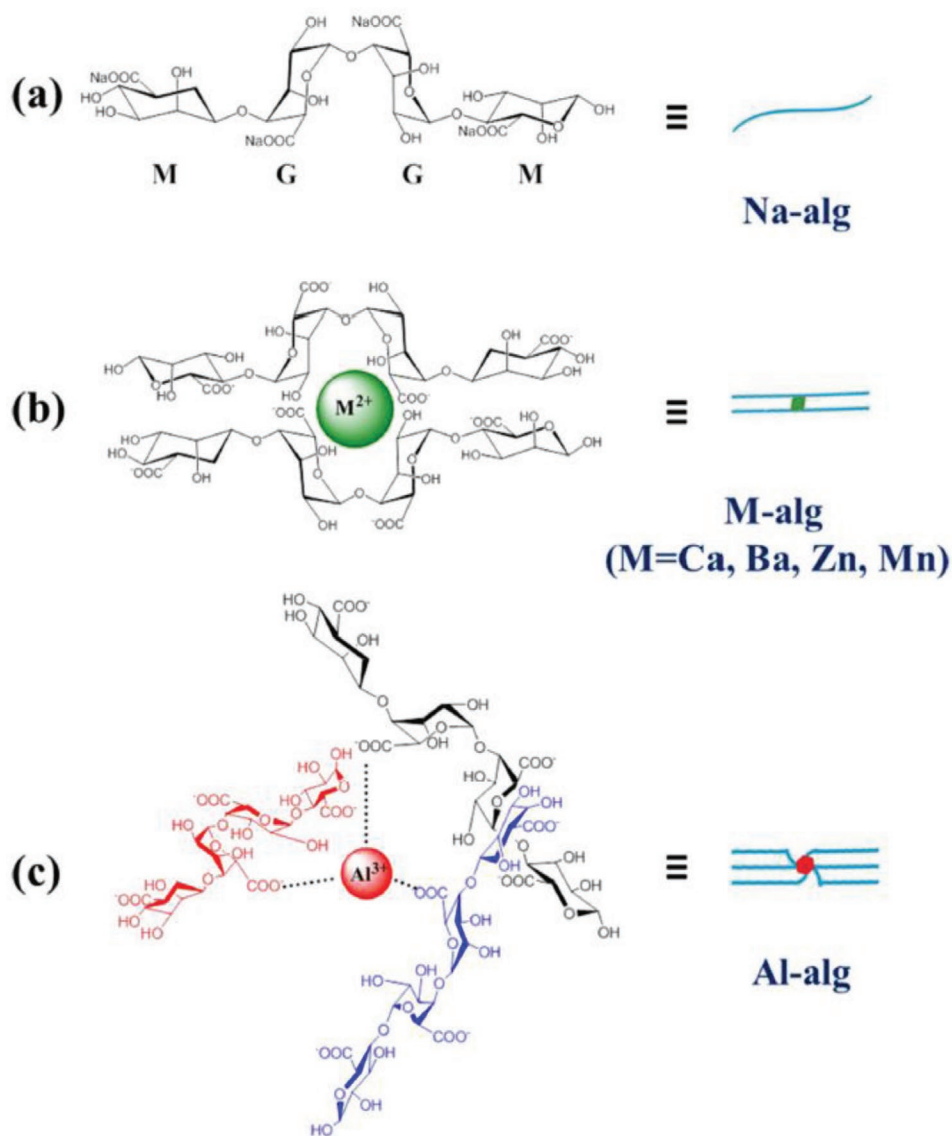


Figure 22. Schematic representation of a) sodium alginate, b) M^{2+} alginate, and c) Al^{3+} alginate. Reproduced with permission.^[245] Copyright 2017, Elsevier.

and, thus, the mechanical properties depend on the conditions under which the algae grew.^[243] Alginate consists of different sequences of mannuronic acid-blocks (MM-blocks), guluronic acid blocks (GG-blocks) and alternating blocks of both monomers (MG-blocks).^[244]

Wu et al. reported alginates with different multivalent metal cations, which crosslinked the alginate chains via coordination and led to a superior performance compared to sodium alginate in silicon anodes (**Figure 22**).^[245] Multiple cations were investigated: Ca^{2+} , Al^{3+} , Ba^{2+} , Mg^{2+} , and Zn^{2+} . Alginate hydrogels containing Al^{3+} and Ba^{2+} revealed the highest viscosities and Vickers hardness values. In addition, the best electrochemical cycling performance was observed, yielding a high initial capacity and capacity retention. When reducing the binder content to 10 wt%, the Ba-ALG electrode still retained 49% of the initial capacity after 200 cycles, showing the best performance among the

investigated cations. These findings were confirmed by Zhang et al., who applied sodium alginate doped with Al^{3+} and Ba^{2+} in $Li_{1.16}Mn_{0.6}Co_{0.12}Ni_{0.12}O_2$ cathodes and were able to increase the cycling stability compared to pristine sodium alginate.^[246]

Zhang et al. prepared an organic cathode material for lithium-ion batteries consisting of terephthalate and using sodium alginate as a binder.^[247] The binder limits the dissolution of the organic molecule inside the liquid electrolyte, due to its strong interactions to the cathode material over hydroxyl and carboxyl-groups. Furthermore, ion and electron transport throughout the electrode were increased as well as the ohmic resistance was decreased, both compared to conventional PVdF binder. The electrode proved to be stable over 1000 cycles, with a capacity decay to 65% of the initial capacity.

Sun et al. prepared a poly(dopamine) electrode material, which acted both as binder and electrochemically active unit

in lithium and sodium batteries.^[248] The catechol group of dopamine featured a strong adhesion to the current collectors and can simultaneously be oxidized to *o*-benzoquinone to yield a redox-active unit. Electrodes were prepared using only poly(dopamine) and a conducting additive, making the use of further binding materials redundant. The electrode showed a high capacity retention of 93% after 580 cycles and further proved to be biodegradable.

Liu et al. applied a mixture of GG and XG in a lithium sulfur battery, which was able to prevent the shuttling of polysulfides.^[181b] Both biopolymers are environmentally friendly and processable in water. Guar gum can interact with the double helix formed by xanthan gum, forming a stable network. Both polymers contain high amounts of oxygen-functional groups, which proved to inhibit shuttling reactions.^[249] As a consequence, high amounts of sulfur in the electrode were possible, namely 19.8 mg cm⁻².

Gelatin was crosslinked with PEI as a bio-derived binder for lithium–sulfur batteries by Akhtar et al.^[250] The authors demonstrated that the good dispersion and adhesion abilities of gelatin were combined with the adsorption abilities for poly(sulfides) of PEI. The latter prevented a shuttling of poly(sulfides). The 3D network structure was able to stabilize a sulfur electrode with 99% capacity retention over 100 cycles at 1C, outperforming pure PEI, gelatin, PVP and PVdF.

Chitosan was crosslinked with glutaraldehyde by Chen et al. and showed improved stability of the silicon anode in lithium ion batteries.^[251] The crosslinked networks exhibited low swelling with electrolyte, a high mechanical stability and a strong chemical bonding to the silicon particles. The optimal content of crosslinker proved to be 3%, as it revealed the best performance, both mechanically and electrochemically. Cells with this crosslinker content retained 70% of the initial capacity after 100 cycles.

Hwang et al. were able to utilize agarose as a binder material for both silicon anode and LiMn₂O₄ (LMO) cathode, revealing good cycling stabilities.^[252] The authors suggested that the hydroxyl and ether groups in agarose contribute to the good binding to silicon and copper surfaces. Agarose was able to suppress the volume expansion of silicon to some extent, while PVdF showed poorer results. When applied in LMO cathodes, agarose was able to chelate Mn²⁺, which is known to dissolve during cycling, thus exhibiting an excellent capacity retention of 99% after 200 cycles at 0.2 C. A full cell, consisting of silicon/hard carbon anode and LMO cathode, both electrodes applying an agarose binder, was fabricated. This cell retained 87% of its initial capacity after 50 cycles at 0.2 C.

Lignin was extracted and thoroughly characterized by Dominguez-Robles et al. and later applied in graphite electrodes.^[253] Although the structure of the lignin extracted from wheat straw depended largely on the extraction technique, the three different investigated lignins were able to compete with PVdF as a binder for graphite electrodes in electrochemical tests.

4.4. Binders for Organic Batteries

As current research for thin film organic batteries mainly focuses on the development of new active materials, the usage

of more advanced binder systems only plays a minor role. In the majority of cases, binders of established lithium battery technology were applied for organic batteries, namely PVdF, PTFE, or PVdF–HFP.^[11,125a,126c,189c,254] Some publications can be found where water-based slurries of CMC are utilized, but none of them investigated the role of the binder on the battery performance.^[126g,254d,255]

TEMPO was covalently bound to a polydopamine derived backbone by Woehlk et al., mimicking strongly adhesive mussel proteins with the help of the catechol group.^[256] The described polymer was able to adhere on several surfaces, ranging from silicon, titanium and alumina to PTFE. Furthermore, CV experiments were conducted, to underline the possible application of the hybrid active binder material in organic batteries.

Komaba et al. applied lithiated poly(acrylic acid) (PAALi) as a binder for PTMA-based cathodes, adding small amounts of CMC as thickener.^[257] The cells possessed a lower charge transfer resistance, than cells with PVdF binder. In cycling experiments, 96% of the initial capacity was retained after 1000 cycles at 20 C.

An azo crosslinked porous organic framework was applied in sodium ion batteries, using an alginate binder by Weeraratne et al.^[258] Here, the azo bonds were reduced and stored Na⁺ as counter ions. This green approach yielded a high capacity retention of over 90% after 150 cycles at 0.3 C. The high capacity retention was attributed to the low solubility of the crosslinked network.

4.5. Concluding Remarks

Binder technology has greatly improved, since the importance of the binding material for the overall performance of the cell was discovered. Many alternatives to commonly used PVdF have been proposed that overcome its drawbacks, such as the use of harmful solvents (NMP) and the large electrolyte uptake and swelling. Ranging from polymers produced in industrial scales, such as poly(acrylic acid), over natural and biologically derived polymers, to conducting polymers, many approaches have been attempted. Current research focuses on increasing the mechanical stability of binders, intelligent functional group design and combinations of different binders for an improved performance.

One of the main challenges of current binder systems is the application in systems with large volume changes during charging/discharging, such as silicon anodes. Usually this leads to a decrease in performance, due to cracks and morphology changes of the electrode, as most of the current binder systems are not yet able to accommodate the volume changes in a satisfactory manner. One approach is the application of highly flexible binders, while at the same time maintaining the mechanical stability. Moreover, the utilization of self-healing polymers represents a promising approach to improve the performance of these electrode materials. Furthermore, the functional groups of the polymers have to interact well with the surface groups of the electrode materials, to ensure a better binding affinity. Crosslinking leads to mechanically more stable binder systems, but higher proportions of crosslinker make the binder prone to cracking. Furthermore, some effort was

devoted into developing conducting binders, as they are able to reduce the amount of conductive additives in an electrode slurry or to make the latter completely redundant. Ionically conducting binders facilitate the ion exchange between electrode and electrolyte and lower the intrinsic resistance of the cell.

In our opinion, the application of concepts like self-healing and the intelligent design of the functional groups have a large potential for future binder systems. Self-healing materials can improve the life-time of electrodes and are more resistant toward volume changes. By tuning the functional groups, the binding affinity to different electrode materials can be optimized to produce more mechanically and electrochemically stable electrode materials. In general, a combination of the aforementioned concepts might further improve the results. Hybrid-binders could simultaneously rely on different binding types and on different mechanisms to accommodate cracks or volume changes during charging/discharging experiments, optimizing existing structures.

5. Conclusion

In summary, polymers are omnipresent in modern day commercial batteries and in battery research activities. One important component of batteries is the separator. While porous separators have been commercially available for a long time, gel-polymer electrolytes and solid polymer electrolytes are emerging areas for lithium-ion battery technology. Here, high lithium ion transference numbers and high ionic conductivities play an important role. For future research the suppression of dendrites through higher mechanical stabilities and the improvement of solid polymer electrolytes in terms of conductivity are essential to enable the goal of a lithium metal anode. In redox-flow applications, ion-exchange membranes play an important role, also size-exclusion membranes have been applied for polymeric active materials and nanoparticle suspensions. In this field of application, the undesired crossover of ions (e.g., VO_2^+) is a major issue. This challenge is addressed by modifying commercial membranes with additional functional groups, by introducing other additives (such as inorganic fillers or ionic liquids) and by utilizing amphoteric membranes.

In solid state batteries, the role of the binder has been put into focus only recently. Here, the compatibility of binder, active material and electrolyte solvent are of great importance. By intelligent design of the binders, their performance has greatly improved. Recent research concentrated more and more on the interactions between functional groups of the binder and the active material, to ensure higher adhesion forces or even covalent bonds. This is particularly important for some electrode materials in current research with large volume changes between the charged and discharged state (e.g., silicon anodes).

Furthermore, polymers are applied as active materials, both in (noncommercial) solid state and redox flow batteries. While some challenges remain, a great progress has been made since the first electrochemically active polymers were developed. In contrast to conventional, metal-based batteries, they are more environmentally benign in both production and disposal, cheaper and can be charged and discharged more quickly.

It has to be noted again that the given values have to be handled with care. Comparability is only given between values in a single study, comparisons between different papers only yield qualitative statements and trends. This is due to changes in experimental setups and utilization of different materials from other sources.

In general, it can be noted that battery technology relies heavily on the development and improvement of the applied polymers. In the past years significant progress was made in polymer research for energy storage, constantly improving existing technologies and developing new concepts in different areas. As polymers are a very versatile class of materials, a large toolbox is at hand for the scientists to further push the limits of lithium-ion, redox-flow, and polymer-organic batteries.

In our eyes, future research should concentrate on enabling even higher capacities in lithium ion batteries, by suppressing dendrites with suitable separators in lithium metal anodes and proper binder design, to accommodate electrode materials with challenging volumetric changes. At the same time, the safety aspect should not be disregarded. By improving the properties of solid polymer electrolytes, leakages of possibly flammable solvents can be reduced to a minimum, minimizing risks for mobile electronic devices or electric vehicles. In terms of flow batteries, the focus should lay on introducing alternatives to expensive and environmentally harmful vanadium active materials, and at the same time developing membranes with lower ionic crossover to increase the lifetime. Polymeric active materials possess the potential to fill the gap between lithium ion technology and supercapacitors, but still lack in long-term stability and suitable large-scale, industrial production methods.

Acknowledgements

The authors would like to thank the priority program “Polymer-based Batteries” (SPP 2248) from the Deutsche Forschungsgesellschaft (DFG), the Regional Innovation Strategy for Smart Specialisation (RIS3), the Thüringer Ministerium für Wirtschaft, Wissenschaft und digitale Gesellschaft (TMWwDG), and DFG project number 328403339 for financial support.

Open access funding enabled and organized by Projekt DEAL.

Conflict of Interest

The authors declare no conflict of interest.

Keywords

active materials, batteries, binders, energy storage, membranes, polymers, separators

Received: June 17, 2020

Revised: August 13, 2020

Published online: September 27, 2020

- [1] International Energy Agency, Paris, Global *Energy & CO₂ Status Report 2018* **2019**.
- [2] REN21, Paris, *Renewables 2019 Global Status Report* **2019**.
- [3] J. I. M. Skea, S. Nishioka, *Clim. Policy* **2008**, *8*, S5.

- [4] X. Luo, J. Wang, M. Dooner, J. Clarke, *Appl. Energy* **2015**, *137*, 511.
- [5] D. Linden, T. B. Reddy, *Handbook of Batteries*, 3rd ed., McGraw-Hill, New York **2002**.
- [6] M. S. Whittingham, *Proc. IEEE* **2012**, *100*, 1518.
- [7] M. S. Whittingham, *Science* **1976**, *192*, 1126.
- [8] K. C. Divya, J. Østergaard, *Electr. Power Syst. Res.* **2009**, *79*, 511.
- [9] G. Martin, L. Rentsch, M. Höck, M. Bertau, *Energy Storage Mater.* **2017**, *6*, 171.
- [10] P. V. Kamat, K. S. Schanze, J. M. Buriak, *ACS Energy Lett.* **2017**, *2*, 1368.
- [11] a) K. Nakahara, S. Iwasa, M. Satoh, Y. Morioka, J. Iriyama, M. Suguro, E. Hasegawa, *Chem. Phys. Lett.* **2002**, *359*, 351; b) H. Nishide, S. Iwasa, Y.-J. Pu, T. Suga, K. Nakahara, M. Satoh, *Electrochim. Acta* **2004**, *50*, 827.
- [12] H. Shirakawa, E. J. Louis, A. G. MacDiarmid, C. K. Chiang, A. J. Heeger, *J. Chem. Soc., Chem. Commun.* **1977**, 578, <https://doi.org/10.1039/C39770000578>.
- [13] a) C. K. Chiang, *Polymer* **1981**, *22*, 1454; b) D. MacInnes, M. A. Druy, P. J. Nigrey, D. P. Nairns, A. G. MacDiarmid, A. J. Heeger, *J. Chem. Soc., Chem. Commun.* **1981**, 317, <https://doi.org/10.1039/C39810000317>; c) J. Caja, R. B. Kaner, A. G. MacDiarmid, *J. Electrochem. Soc.* **1984**, *131*, 2744.
- [14] a) S. Panero, P. Prospero, B. Klapptse, B. Scrosati, *Electrochim. Acta* **1986**, *31*, 1597; b) S. Panero, P. Prospero, F. Bonino, B. Scrosati, A. Corradini, M. Mastragostino, *Electrochim. Acta* **1987**, *32*, 1007.
- [15] J.-L. Brédas, D. Beljonne, V. Coropceanu, J. Cornil, *Chem. Rev.* **2004**, *104*, 4971.
- [16] J. S. Miller, *Adv. Mater.* **1993**, *5*, 671.
- [17] L. Bugnon, C. J. H. Morton, P. Novak, J. Vetter, P. Nesvadba, *Chem. Mater.* **2007**, *19*, 2910.
- [18] K. M. Pelzer, L. Cheng, L. A. Curtiss, *J. Phys. Chem. C* **2017**, *121*, 237.
- [19] Y. Yonekuta, K. Oyaizu, H. Nishide, *Chem. Lett.* **2007**, *36*, 866.
- [20] G. G. Rodríguez-Calero, M. A. Lowe, S. E. Burkhardt, H. D. Abruña, *Langmuir* **2011**, *27*, 13904.
- [21] J. Y. Zhang, L. B. Kong, L. Z. Zhan, J. Tang, H. Zhan, Y. H. Zhou, C. M. Zhan, *J. Power Sources* **2007**, *168*, 278.
- [22] W. Choi, D. Harada, K. Oyaizu, H. Nishide, *J. Am. Chem. Soc.* **2011**, *133*, 19839.
- [23] a) B. Haeupler, R. Burges, T. Janoschka, T. Jaehnert, A. Wild, U. S. Schubert, *J. Mater. Chem. A* **2014**, *2*, 8999; b) P. Sharma, D. Damien, K. Nagarajan, M. M. Shaijumon, M. Hariharan, *J. Phys. Chem. Lett.* **2013**, *4*, 3192.
- [24] a) Y. Takahashi, N. Hayashi, K. Oyaizu, K. Honda, H. Nishide, *Polym. J.* **2008**, *40*, 763; b) S. Sen, J. Saraidaridis, S. Y. Kim, G. T. R. Palmore, *ACS Appl. Mater. Interfaces* **2013**, *5*, 7825; c) G. Li, B. Zhang, J. Wang, H. Zhao, W. Ma, L. Xu, W. Zhang, K. Zhou, Y. Du, G. He, *Angew. Chem., Int. Ed.* **2019**, *58*, 8468.
- [25] C. Friebe, U. S. Schubert, *Top. Curr. Chem.* **2017**, *375*, 1.
- [26] C. Friebe, A. Lex-Balducci, U. S. Schubert, *ChemSusChem* **2019**, *12*, 4093.
- [27] S. Muench, A. Wild, C. Friebe, B. Häupler, T. Janoschka, U. S. Schubert, *Chem. Rev.* **2016**, *116*, 9438.
- [28] M. E. Bhosale, S. Chae, J. M. Kim, J.-Y. Choi, *J. Mater. Chem. A* **2018**, *6*, 19885.
- [29] J. J. Shea, C. Luo, *ACS Appl. Mater. Interfaces* **2020**, *12*, 5361.
- [30] a) T. Janoschka, N. Martin, M. D. Hager, U. S. Schubert, *Angew. Chem., Int. Ed.* **2016**, *55*, 14427; b) J. Winsberg, T. Hagemann, T. Janoschka, M. D. Hager, U. S. Schubert, *Angew. Chem., Int. Ed.* **2017**, *56*, 686.
- [31] J. Winsberg, S. Muench, T. Hagemann, T. Janoschka, S. Morgenstern, M. Billing, F. H. Schacher, G. Hauffman, J.-F. Gohy, S. Hoepfener, M. Hager, U. S. Schubert, *Polym. Chem.* **2016**, *7*, 1711.
- [32] T. Hagemann, M. Strumpf, E. Schröter, C. Stolze, M. Grube, I. Nischang, M. D. Hager, U. S. Schubert, *Chem. Mater.* **2019**, *31*, 7987.
- [33] E. C. Montoto, G. Nagarjuna, J. Hui, M. Burgess, N. M. Sekerak, K. Hernández-Burgos, T.-S. Wei, M. Kneer, J. Grolman, K. J. Cheng, J. A. Lewis, J. S. Moore, J. Rodríguez-López, *J. Am. Chem. Soc.* **2016**, *138*, 13230.
- [34] Y. Y. Lai, X. Li, Y. Zhu, *ACS Appl. Polym. Mater.* **2020**, *2*, 113.
- [35] Y. Ding, C. Zhang, L. Zhang, Y. Zhou, G. Yu, *Chem. Soc. Rev.* **2017**, *47*, 69.
- [36] a) J. Winsberg, T. Janoschka, S. Morgenstern, S. Muench, T. Hagemann, G. Hauffman, J.-F. Gohy, M. D. Hager, U. S. Schubert, *Adv. Mater.* **2016**, *28*, 2238; b) T. Janoschka, N. Martin, U. Martin, C. Friebe, S. Morgenstern, H. Hiller, M. D. Hager, U. S. Schubert, *Nature* **2015**, *527*, 78.
- [37] T. Hagemann, J. Winsberg, M. Grube, I. Nischang, T. Janoschka, N. Martin, M. D. Hager, U. S. Schubert, *J. Power Sources* **2018**, *378*, 546.
- [38] K. Hatakeyama-Sato, T. Nagano, S. Noguchi, Y. Sugai, J. Du, H. Nishide, K. Oyaizu, *ACS Appl. Polym. Mater.* **2019**, *1*, 188.
- [39] T. Saji, Y. Maruyama, S. Aoyagui, *J. Electroanal. Chem.* **1978**, *86*, 219.
- [40] a) Z. Meng, S. Kan, T. Sukegawa, K. Oyaizu, C.-L. Ho, J. Xiang, Y.-H. Feng, Y. H. Lo, H. Nishide, W.-Y. Wong, *J. Organomet. Chem.* **2016**, *812*, 51; b) K. Tamura, N. Akutagawa, M. Satoh, J. Wada, T. Masuda, *Macromol. Rapid Commun.* **2008**, *29*, 1944; c) J. Xiang, S. Kan, H. Tokue, K. Oyaizu, C.-L. Ho, H. Nishide, W.-Y. Wong, M. Wei, *Eur. J. Inorg. Chem.* **2016**, *2016*, 1030.
- [41] E. C. Montoto, G. Nagarjuna, J. S. Moore, J. Rodríguez-López, *J. Electrochem. Soc.* **2017**, *164*, A1688.
- [42] P. S. Borchers, M. Strumpf, C. Friebe, I. Nischang, M. D. Hager, J. Elbert, U. S. Schubert, *Adv. Energy Mater.* **2020**.
- [43] Z. Song, H. Zhan, Y. Zhou, *Angew. Chem., Int. Ed.* **2010**, *49*, 8444.
- [44] a) X. Han, C. Chang, L. Yuan, T. Sun, J. Sun, *Adv. Mater.* **2007**, *19*, 1616; b) M. Armand, S. Grugeon, H. Vezin, S. Laruelle, P. Ribière, P. Poizot, J. M. Tarascon, *Nat. Mater.* **2009**, *8*, 120.
- [45] a) G. Hernandez, N. Casado, A. M. Zamarayeva, J. K. Duet, M. Armand, A. C. Arias, D. Mecerreyes, *ACS Appl. Energy Mater.* **2018**, *1*, 7199; b) H. Wu, S. A. Shevlin, Q. Meng, W. Guo, Y. Meng, K. Lu, Z. Wei, Z. Guo, *Adv. Mater.* **2014**, *26*, 3338; c) F. Xu, H. Wang, J. Lin, X. Luo, S.-a. Cao, H. Yang, *J. Mater. Chem. A* **2016**, *4*, 11491.
- [46] J. Winsberg, S. Benndorf, A. Wild, M. D. Hager, U. S. Schubert, *Macromol. Chem. Phys.* **2018**, *219*, 1700267.
- [47] W. Yan, C. Wang, J. Tian, G. Zhu, L. Ma, Y. Wang, R. Chen, Y. Hu, L. Wang, T. Chen, J. Ma, Z. Jin, *Nat. Commun.* **2019**, *10*, 2513.
- [48] T. Janoschka, S. Morgenstern, H. Hiller, C. Friebe, K. Wolkersdorfer, B. Haeupler, M. D. Hager, U. S. Schubert, *Polym. Chem.* **2015**, *6*, 7801.
- [49] Z. T. Gossage, N. B. Schorr, K. Hernández-Burgos, J. Hui, B. H. Simpson, E. C. Montoto, J. Rodríguez-López, *Langmuir* **2017**, *33*, 9455.
- [50] Z. T. Gossage, K. Hernández-Burgos, J. S. Moore, J. Rodríguez-López, *ChemElectroChem* **2018**, *5*, 3006.
- [51] W. Zhang, Z. Tu, J. Qian, S. Choudhury, L. A. Archer, Y. Lu, *Small* **2018**, *14*, 1703001.
- [52] a) X.-B. Cheng, R. Zhang, C.-Z. Zhao, F. Wei, J.-G. Zhang, Q. Zhang, *Adv. Sci.* **2016**, *3*, 1500213; b) C. Monroe, J. Newman, *J. Electrochem. Soc.* **2005**, *152*, A396.
- [53] a) J. H. Lee, J. K. Hong, D. H. Jang, Y. K. Sun, S. M. Oh, *J. Power Sources* **2000**, *89*, 7; b) Y.-X. Yin, S. Xin, Y.-G. Guo, L.-J. Wan, *Angew. Chem., Int. Ed.* **2013**, *52*, 13186.
- [54] a) M. Yang, J. Hou, *Membranes* **2012**, *2*, 367; b) P. Arora, Z. Zhang, *Chem. Rev.* **2004**, *104*, 4419; c) USABC, Li-Ion Battery Separator Goals **2017**.
- [55] W. Ostwald, *Z. Phys. Chem.* **1890**, *6*, 71.
- [56] a) F. G. Donnan, *Z. Elektrochem. Angew. Phys. Chem.* **1911**, *17*, 572; b) A. Alonso, J. Macanás, G.-L. Davies, Y. Gounko, M. Muñoz, D. Muraviev, in *Advances in Nanocomposite Technology* (Ed.: A. Hashim), InTechOpen, London **2011**.
- [57] H. Prifti, A. Parasuraman, S. Winardi, T. M. Lim, M. Skyllas-Kazacos, *Membranes* **2012**, *2*, 275.
- [58] P. Knauth, M. L. Di Vona, *Adv. Mater. Lett.* **2018**, *9*, 855.
- [59] a) H. Hosseini, D. A. Dornbusch, G. J. Suppes, *Ind. Eng. Chem. Res.* **2016**, *55*, 8557; b) M. Mandal, G. Huang, P. A. Kohl, *J. Membr. Sci.* **2019**, *570–571*, 394.

- [60] a) X. Li, H. Zhang, Z. Mai, H. Zhang, I. Vankelecom, *Energy Environ. Sci.* **2011**, 4, 1147; b) B. Schwenzer, J. Zhang, S. Kim, L. Li, J. Liu, Z. Yang, *ChemSusChem* **2011**, 4, 1388; c) L. Zeng, T. S. Zhao, L. Wei, H. R. Jiang, M. C. Wu, *Appl. Energy* **2019**, 233–234, 622.
- [61] a) Z. Ogumi, Y. Uchimoto, M. Tsujikawa, Z. Takehara, F. R. Foulkes, *J. Electrochem. Soc.* **1990**, 137, 1430; b) D. H. Ruijie Ye, S. J. Yoon, Z. Huang, D. K. Kim, Z. Chang, S. Kim, R. Chen, *J. Electrochem. Energy Convers. Storage* **2018**, 15, 010801.
- [62] D. T. Hallinan, N. P. Balsara, *Annu. Rev. Mater. Res.* **2013**, 43, 503.
- [63] M. F. Lagadec, R. Zahn, V. Wood, *Nat. Energy* **2019**, 4, 16.
- [64] Y. M. Lee, J.-W. Kim, N.-S. Choi, J. A. Lee, W.-H. Seol, J.-K. Park, *J. Power Sources* **2005**, 139, 235.
- [65] a) C. M. Costa, J. L. Gomez Ribelles, S. Lanceros-Mendez, G. B. Appetecchi, B. Scrosati, *J. Power Sources* **2014**, 245, 779; b) V. A. Agubra, D. De la Garza, L. Gallegos, M. Alcoutlabi, *J. Appl. Polym. Sci.* **2016**, 133, n/a; c) C.-Y. Hsu, R.-J. Liu, C.-H. Hsu, P.-L. Kuo, *RSC Adv.* **2016**, 6, 18082; d) L. Li, Y. Ma, W. Wang, Y. Xu, J. You, Y. Zhang, *J. Phys. Chem. Solids* **2016**, 99, 159; e) W. Kang, X. Ma, H. Zhao, J. Ju, Y. Zhao, J. Yan, B. Cheng, *J. Solid State Electrochem.* **2016**, 20, 2791.
- [66] a) J. Amici, C. Francia, J. Zeng, S. Bodoardo, N. Penazzi, *J. Appl. Electrochem.* **2016**, 46, 617; b) J. Liu, C. He, J. He, J. Cui, H. Liu, X. Wu, *J. Solid State Electrochem.* **2017**, 21, 919; c) S. Caimi, H. Wu, M. Morbidelli, *ACS Appl. Energy Mater.* **2018**, 1, 5224.
- [67] D. Wu, L. Deng, Y. Sun, K. S. Teh, C. Shi, Q. Tan, J. Zhao, D. Sun, L. Lin, *RSC Adv.* **2017**, 7, 24410.
- [68] H. Li, Y.-M. Chen, X.-T. Ma, J.-L. Shi, B.-K. Zhu, L.-P. Zhu, *J. Membr. Sci.* **2011**, 379, 397.
- [69] K. Karuppasamy, P. A. Reddy, G. Srinivas, A. Tewari, R. Sharma, X. S. Shajan, D. Gupta, *J. Membr. Sci.* **2016**, 514, 350.
- [70] Y. Ma, L. B. Li, G. X. Gao, X. Y. Yang, J. You, P. X. Yang, *Colloids Surf., A* **2016**, 502, 130.
- [71] Q. Xiao, C. Deng, Q. Wang, Q. Zhang, Y. Yue, S. Ren, *ACS Omega* **2019**, 4, 95.
- [72] a) M. B. Armand, M. J. Duclot, P. Rigaud, *Solid State Ionics* **1981**, 3-4, 429; b) P. V. Wright, *Electrochim. Acta* **1998**, 43, 1137.
- [73] W. Li, Y. Pang, J. Liu, G. Liu, Y. Wang, Y. Xia, *RSC Adv.* **2017**, 7, 23494.
- [74] G. Fu, T. Kyu, *Langmuir* **2017**, 33, 13973.
- [75] K. M. Anilkumar, B. Jinisha, M. Manoj, S. Jayalekshmi, *Eur. Polym. J.* **2017**, 89, 249.
- [76] R. Liu, P. He, Z. Wu, F. Guo, B. Huang, Q. Wang, Z. Huang, C.-a. Wang, Y. Li, *J. Electroanal. Chem.* **2018**, 822, 105.
- [77] a) T.-H. Cho, M. Tanaka, H. Onishi, Y. Kondo, T. Nakamura, H. Yamazaki, S. Tanase, T. Sakai, *J. Power Sources* **2008**, 181, 155; b) A. I. Gopalan, P. Santhosh, K. M. Manesh, J. H. Nho, S. H. Kim, C.-G. Hwang, K.-P. Lee, *J. Membr. Sci.* **2008**, 325, 683; c) X. Ma, P. Kolla, R. Yang, Z. Wang, Y. Zhao, A. L. Smirnova, H. Fong, *Electrochim. Acta* **2017**, 236, 417; d) H. Tsutsumi, A. Matsuo, K. Takase, S. Doi, A. Hisanaga, K. Onimura, T. Oishi, *J. Power Sources* **2000**, 90, 33.
- [78] C. He, J. Liu, J. Li, F. Zhu, H. Zhao, *J. Membr. Sci.* **2018**, 560, 30.
- [79] Y. Huang, Y. Huang, B. Liu, H. Cao, L. Zhao, A. Song, Y. Lin, M. Wang, X. Li, Z. Zhang, *Electrochim. Acta* **2018**, 286, 242.
- [80] a) B. Liu, Y. Huang, H. Cao, L. Zhao, Y. Huang, A. Song, Y. Lin, X. Li, M. Wang, *J. Membr. Sci.* **2018**, 545, 140; b) B. Liu, Y. Huang, Y. X. Huang, X. H. Deng, A. M. Song, Y. H. Lin, M. S. Wang, X. Li, Y. P. Wu, H. J. Cao, *J. Appl. Electrochem.* **2019**, 49, 1167.
- [81] a) T. Chen, Y. Liao, X. Wang, X. Luo, X. Li, W. Li, *Electrochim. Acta* **2016**, 191, 923; b) O. Bohnke, C. Rousselot, P. A. Gillet, C. Truche, *J. Electrochem. Soc.* **1992**, 139, 1862.
- [82] W. Li, M. Yuan, M. Yang, *Eur. Polym. J.* **2006**, 42, 1396.
- [83] X. Huang, D. Xu, W. Chen, H. Yin, C. Zhang, Y. Luo, X. Yu, *J. Electroanal. Chem.* **2017**, 804, 133.
- [84] B. Liu, Y. Huang, L. Zhao, Y. Huang, A. Song, Y. Lin, M. Wang, X. Li, H. Cao, *J. Membr. Sci.* **2018**, 564, 62.
- [85] J. Zhao, J. Zhang, P. Hu, J. Ma, X. Wang, L. Yue, G. Xu, B. Qin, Z. Liu, X. Zhou, G. Cui, *Electrochim. Acta* **2016**, 188, 23.
- [86] H. Khani, S. Kalami, J. B. Goodenough, *Sustainable Energy Fuels* **2020**, 4, 177.
- [87] X. He, S. Schmohl, H. D. Wiemhöfer, *Polym. Test.* **2019**, 76, 505.
- [88] Q. X. Shi, H. J. Pei, N. You, J. Wu, X. Xiang, Q. Xia, X. L. Xie, S. B. Jin, Y. S. Ye, *Chem. Eng. J.* **2019**, 375, 121977.
- [89] G. Fu, M. D. Soucek, T. Kyu, *Solid State Ionics* **2018**, 320, 310.
- [90] a) Z. Du, Y. Su, Y. Qu, L. Zhao, X. Jia, Y. Mo, F. Yu, J. Du, Y. Chen, *Electrochim. Acta* **2019**, 299, 19; b) C. Li, H. Yue, Q. Wang, J. Li, J. Zhang, H. Dong, Y. Yin, S. Yang, *Solid State Ionics* **2018**, 321, 8; c) B. Liu, Y. Huang, H. Cao, A. Song, Y. Lin, M. Wang, X. Li, *J. Solid State Electrochem.* **2018**, 22, 807.
- [91] S. Ramesh, C.-W. Liew, A. K. Arof, *J. Non-Cryst. Solids* **2011**, 357, 3654.
- [92] P. Perumal, P. Christopher Selvin, S. Selvasekarapandian, P. Sivaraj, K. P. Abhilash, V. Moniha, R. Manjula Devi, *Polym. Degrad. Stab.* **2019**, 159, 43.
- [93] G. G. Eshetu, D. Mecerreyes, M. Forsyth, H. Zhang, M. Armand, *Mol. Syst. Des. Eng.* **2019**, 4, 294.
- [94] a) M. Hajime, T. Naohiro, U. Tatsuya, T. Seiji, S. Hikari, A. Kinji, T. Kuniaki, *Chem. Lett.* **2008**, 37, 1020; b) K. Keigo, N. Toshiyuki, H. Rika, M. Hajime, *Chem. Lett.* **2010**, 39, 1303.
- [95] a) M. Galiński, A. Lewandowski, I. Stępnia, *Electrochim. Acta* **2006**, 51, 5567; b) M. Armand, F. Endres, D. R. MacFarlane, H. Ohno, B. Scrosati, *Nat. Mater.* **2009**, 8, 621.
- [96] Y.-S. Ye, J. Rick, B.-J. Hwang, *J. Mater. Chem. A* **2013**, 1, 2719.
- [97] T. Chen, W. Kong, Z. Zhang, L. Wang, Y. Hu, G. Zhu, R. Chen, L. Ma, W. Yan, Y. Wang, J. Liu, Z. Jin, *Nano Energy* **2018**, 54, 17.
- [98] L. Li, X. Yang, J. Li, Y. Xu, *Ionics* **2018**, 24, 735.
- [99] J.-K. Kim, *J. Ind. Eng. Chem.* **2018**, 68, 168.
- [100] E. Metwalli, M. V. Kaepfel, S. J. Schaper, A. Kriele, R. Gilles, K. N. Raftopoulos, P. Mueller-Buschbaum, *ACS Appl. Energy Mater.* **2018**, 1, 666.
- [101] A. R. Polu, H.-W. Rhee, M. Jeevan Kumar Reddy, A. M. Shanmugharaj, S. H. Ryu, D. K. Kim, *J. Ind. Eng. Chem.* **2017**, 45, 68.
- [102] H. Zhang, C. Li, M. Piszcz, E. Coya, T. Rojo, L. M. Rodriguez-Martinez, M. Armand, Z. Zhou, *Chem. Soc. Rev.* **2017**, 46, 797.
- [103] M. Doyle, T. F. Fuller, J. Newman, *Electrochim. Acta* **1994**, 39, 2073.
- [104] D. B. Babu, K. Giribabu, K. Ramesha, *ACS Appl. Mater. Interfaces* **2018**, 10, 19721.
- [105] L. Porcarelli, A. S. Shaplov, F. Bella, J. R. Nair, D. Mecerreyes, C. Gerbaldi, *ACS Energy Lett.* **2016**, 1, 678.
- [106] Y. Chen, Z. Li, X. Liu, D. Zeng, Y. Zhang, Y. Sun, H. Ke, H. Cheng, *J. Membr. Sci.* **2017**, 544, 47.
- [107] Y. Pan, Y. Zhou, Q. Zhao, Y. Dou, S. Chou, F. Cheng, J. Chen, H. K. Liu, L. Jiang, S. X. Dou, *Nano Energy* **2017**, 33, 205.
- [108] K. Deng, J. Qin, S. Wang, S. Ren, D. Han, M. Xiao, Y. Meng, *Small* **2018**, 14, 1801420.
- [109] Z. Li, Q. Yao, Q. Zhang, Y. Zhao, D. Gao, S. Li, S. Xu, *J. Mater. Chem. A* **2018**, 6, 24848.
- [110] A. Abbasi, S. Hosseini, A. Somwangthanaroj, S. Kheawhom, A. Abbasi, S. Hosseini, S. Kheawhom, A. A. Mohamad, *Int. J. Mol. Sci.* **2019**, 20, 3678.
- [111] M. Wang, N. Xu, J. Fu, Y. Liu, J. Qiao, *J. Mater. Chem. A* **2019**, 7, 11257.
- [112] Y. Ye, Y. A. Elabd, *Polymer* **2011**, 52, 1309.
- [113] J. R. Nykaza, A. M. Savage, Q. Pan, S. Wang, F. L. Beyer, M. H. Tang, C. Y. Li, Y. A. Elabd, *Polymer* **2016**, 101, 311.
- [114] F. Ma, Z. Zhang, W. Yan, X. Ma, D. Sun, Y. Jin, X. Chen, K. He, *ACS Sustainable Chem. Eng.* **2019**, 7, 4675.
- [115] C.-H. Tsao, H.-M. Su, H.-T. Huang, P.-L. Kuo, H. Teng, *J. Membr. Sci.* **2019**, 572, 382.
- [116] H.-S. Jeong, S.-Y. Lee, *J. Power Sources* **2011**, 196, 6716.

- [117] P. P. Prosini, P. Villano, M. Carewska, *Electrochim. Acta* **2002**, *48*, 227.
- [118] R. Miao, B. Liu, Z. Zhu, Y. Liu, J. Li, X. Wang, Q. Li, *J. Power Sources* **2008**, *184*, 420.
- [119] O. V. Yarmolenko, A. V. Yudina, K. G. Khatmullina, *Russ. J. Electrochem.* **2018**, *54*, 325.
- [120] a) S. H. Chung, Y. Wang, L. Persi, F. Croce, S. G. Greenbaum, B. Scrosati, E. Plichta, *J. Power Sources* **2001**, *97–98*, 644; b) B. Kumar, L. Scanlon, R. Marsh, R. Mason, R. Higgins, R. Baldwin, *Electrochim. Acta* **2001**, *46*, 1515.
- [121] a) S. Rajendran, O. Mahendran, R. Kannan, *J. Phys. Chem. Solids* **2002**, *63*, 303; b) I. Gurevitch, R. Buonsanti, A. A. Teran, B. Gludovatz, R. O. Ritchie, J. Cabana, N. P. Balsara, *J. Electrochem. Soc.* **2013**, *160*, A1611.
- [122] J.-A. Choi, S. H. Kim, D.-W. Kim, *J. Power Sources* **2010**, *195*, 6192.
- [123] C.-H. Hsu, L.-H. Chien, P.-L. Kuo, *RSC Adv.* **2016**, *6*, 18089.
- [124] W. Zhou, S. Wang, Y. Li, S. Xin, A. Manthiram, J. B. Goodenough, *J. Am. Chem. Soc.* **2016**, *138*, 9385.
- [125] a) J.-K. Kim, G. Cheruvally, J.-W. Choi, J.-H. Ahn, S. H. Lee, D. S. Choi, C. E. Song, *Solid State Ionics* **2007**, *178*, 1546; b) K. Nakahara, J. Iriyama, S. Iwasa, M. Suguro, M. Satoh, E. J. Cairns, *J. Power Sources* **2007**, *165*, 870.
- [126] a) T. Le Gall, K. H. Reiman, M. C. Gossel, J. R. Owen, *J. Power Sources* **2003**, *119–121*, 316; b) E. Bicer, A. Oektemer, *Int. J. Electrochem.* **2013**, *2013*, 732749; c) H. Wu, K. Wang, Y. Meng, K. Lu, Z. Wei, *J. Mater. Chem. A* **2013**, *1*, 6366; d) L. Zhu, X. Cao, *Mater. Lett.* **2015**, *150*, 16; e) D. Nauroozi, M. Pejic, P.-O. Schwartz, M. Wachtler, P. Baeuerle, *RSC Adv.* **2016**, *6*, 111350; f) M. Yao, T. Numoto, H. Ando, R. Kondo, H. T. Takeshita, T. Kiyobayashi, *Energy Procedia* **2016**, *89*, 213; g) D. Mukherjee, G. Gowda Y. K, H. Makri Nimbegondi Kotresh, S. Sampath, *ACS Appl. Mater. Interfaces* **2017**, *9*, 19446; h) P. Gerlach, R. Burges, A. Lex-Balducci, U. S. Schubert, A. Balducci, *J. Power Sources* **2018**, *405*, 142; i) R. Yamamoto, N. Yabuuchi, M. Miyasaka, *J. Electrochem. Soc.* **2018**, *165*, A434.
- [127] a) Y. Dai, Y. Zhang, L. Gao, G. Xu, J. Xie, *J. Electrochem. Soc.* **2011**, *158*, A291; b) R. Emanuelsson, C. Karlsson, H. Huang, C. Kosgei, M. Stroemme, M. Sjoedin, *Russ. J. Electrochem.* **2017**, *53*, 8.
- [128] K. Hatakeyama-Sato, H. Wakamatsu, K. Yamagishi, T. Fujie, S. Takeoka, K. Oyaizu, H. Nishide, *Small* **2019**, *15*, 1805296.
- [129] a) Y. Xuan, M. Sandberg, M. Berggren, X. Crispin, *Org. Electron.* **2012**, *13*, 632; b) M. Reyes-Reyes, R. Lopez-Sandoval, *Org. Electron.* **2018**, *52*, 364.
- [130] J.-K. Kim, G. Cheruvally, J.-W. Choi, J.-H. Ahn, D. S. Choi, C. E. Song, *J. Electrochem. Soc.* **2007**, *154*, A839.
- [131] J.-K. Kim, A. Matic, J.-H. Ahn, P. Jacobsson, *RSC Adv.* **2012**, *2*, 9795.
- [132] S. Muench, R. Burges, A. Lex-Balducci, J. C. Brendel, M. Jäger, C. Friebe, A. Wild, U. S. Schubert, *Energy Storage Mater.* **2020**, *25*, 750.
- [133] M. Aqil, F. Ouhib, A. Aqil, A. El Idrissi, C. Detrembleur, C. Jérôme, *Eur. Polym. J.* **2018**, *106*, 242.
- [134] R. M. Darling, K. G. Gallagher, J. A. Kowalski, S. Ha, F. R. Brushett, *Energy Environ. Sci.* **2014**, *7*, 3459.
- [135] a) T. Sukegawa, I. Masuko, K. Oyaizu, H. Nishide, *Macromolecules* **2014**, *47*, 8611; b) J. Winsberg, T. Hagemann, S. Muench, C. Friebe, B. Häupler, T. Janoschka, S. Morgenstern, M. D. Hager, U. S. Schubert, *Chem. Mater.* **2016**, *28*, 3401.
- [136] a) G. L. Soloveichik, *Chem. Rev.* **2015**, *115*, 11533; b) C. Ponce de León, A. Frías-Ferrer, J. González-García, D. A. Szánto, F. C. Walsh, *J. Power Sources* **2006**, *160*, 716.
- [137] T. N. L. Doan, T. K. A. Hoang, P. Chen, *RSC Adv.* **2015**, *5*, 72805.
- [138] G.-J. Hwang, S.-W. Kim, D.-M. In, D.-Y. Lee, C.-H. Ryu, *J. Ind. Eng. Chem.* **2018**, *60*, 360.
- [139] J. Xi, B. Jiang, L. Yu, L. Liu, *J. Membr. Sci.* **2017**, *522*, 45.
- [140] a) C. Heitner-Wirguin, *J. Membr. Sci.* **1996**, *120*, 1; b) K. A. Mauritz, R. B. Moore, *Chem. Rev.* **2004**, *104*, 4535; c) W. Y. Hsu, T. D. Gierke, *J. Membr. Sci.* **1983**, *13*, 307.
- [141] O. N. T. Osaka, T. Okajima, *Anal. Chem.* **1986**, *58*, 979.
- [142] a) J. L. Weininger, R. R. Russell, *J. Electrochem. Soc.* **1978**, *125*, 1482; b) R. S. Yeo, J. McGreen, G. Kissel, F. Kulesa, S. Srinivasan, *J. Appl. Electrochem.* **1980**, *10*, 741.
- [143] J. Mo, S. Steen, Z. Kang, G. Yang, D. A. Taylor, Y. Li, T. J. Toops, M. P. Brady, S. T. Retterer, D. A. Cullen, J. B. Green, F.-Y. Zhang, *Int. J. Hydrogen Energy* **2017**, *42*, 27343.
- [144] a) M. Rychcik, M. Skyllas-Kazacos, *J. Power Sources* **1988**, *22*, 59; b) K. E. H. Ohya, T. Ohto, Y. Negishi, K. Matsumoto, *Denki Kagaku* **1985**, *53*, 462.
- [145] a) K.-D. Kreuer, *Chem. Mater.* **2014**, *26*, 361; b) Y. Zhou, L. Yu, J. Wang, L. Liu, F. Liang, J. Xi, *RSC Adv.* **2017**, *7*, 19425.
- [146] a) J. Xi, Z. Wu, X. Qiu, L. Chen, *J. Power Sources* **2007**, *166*, 531; b) D. Reed, E. Thomsen, W. Wang, Z. Nie, B. Li, X. Wei, B. Koepfel, V. Sprenkle, *J. Power Sources* **2015**, *285*, 425; c) B. Jiang, L. Wu, L. Yu, X. Qiu, J. Xi, *J. Membr. Sci.* **2016**, *510*, 18; d) V. Viswanathan, A. Crawford, D. Stephenson, S. Kim, W. Wang, B. Li, G. Coffey, E. Thomsen, G. Graff, P. Balducci, M. Kintner-Meyer, V. Sprenkle, *J. Power Sources* **2014**, *247*, 1040; e) A. Crawford, V. Viswanathan, D. Stephenson, W. Wang, E. Thomsen, D. Reed, B. Li, P. Balducci, M. Kintner-Meyer, V. Sprenkle, *J. Power Sources* **2015**, *293*, 388; f) C. Minke, T. Turek, *J. Power Sources* **2015**, *286*, 247.
- [147] S. Naudy, F. Collette, F. Thominette, G. Gebel, E. Espuche, *J. Membr. Sci.* **2014**, *451*, 293.
- [148] J. Dai, Y. Dong, C. Yu, Y. Liu, X. Teng, *J. Membr. Sci.* **2018**, *554*, 324.
- [149] X.-B. Yang, L. Zhao, X.-L. Sui, L.-H. Meng, Z.-B. Wang, *J. Colloid Interface Sci.* **2019**, *542*, 177.
- [150] J. Liu, L. Yu, X. Cai, U. Khan, Z. Cai, J. Xi, B. Liu, F. Kang, *ACS Nano* **2019**, *13*, 2094.
- [151] Y. Ji, Z. Y. Tay, S. F. Y. Li, *J. Membr. Sci.* **2017**, *539*, 197.
- [152] R. Niu, L. Kong, L. Zheng, H. Wang, H. Shi, *J. Membr. Sci.* **2017**, *525*, 220.
- [153] J. Ye, Y. Cheng, L. Sun, M. Ding, C. Wu, D. Yuan, X. Zhao, C. Xiang, C. Jia, *J. Membr. Sci.* **2019**, *572*, 110.
- [154] Z. Xia, L. Ying, J. Fang, Y.-Y. Du, W.-M. Zhang, X. Guo, J. Yin, *J. Membr. Sci.* **2017**, *525*, 229.
- [155] X. Song, L. Ding, L. Wang, M. He, X. Han, *Electrochim. Acta* **2019**, *295*, 1034.
- [156] M. S. Cha, H. Y. Jeong, H. Y. Shin, S. H. Hong, T.-H. Kim, S.-G. Oh, J. Y. Lee, Y. T. Hong, *J. Power Sources* **2017**, *363*, 78.
- [157] J. Ren, Y. Dong, J. Dai, H. Hu, Y. Zhu, X. Teng, *J. Membr. Sci.* **2017**, *544*, 186.
- [158] a) J. S. Ling, J. Charleston, presented at Electrochemical Society Meet., Hollywood, FL, September **1980**; b) R. A. Assink, *J. Membr. Sci.* **1984**, *17*, 205.
- [159] a) T. Mohammadi, M. Skyllas-Kazacos, *J. Membr. Sci.* **1995**, *98*, 77; b) T. Mohammadi, M. S. Kazacos, *J. Power Sources* **1996**, *63*, 179.
- [160] A. M. Park, Z. R. Owczarczyk, L. E. Garner, A. C. Yang-Neyerlin, H. Long, C. M. Antunes, M. R. Sturgeon, M. J. Lindell, S. J. Hamrock, M. Yandrasits, B. S. Pivovar, *ECS Trans.* **2017**, *80*, 957.
- [161] Y. Ahn, D. Kim, *J. Ind. Eng. Chem.* **2019**, *71*, 361.
- [162] J. Hou, Y. Liu, Y. Liu, L. Wu, Z. Yang, T. Xu, *Chem. Eng. Sci.* **2019**, *201*, 167.
- [163] K. Sollner, *Biochem. Z.* **1932**, *244*, 370.
- [164] Y. Wang, S. Wang, M. Xiao, S. Song, D. Han, M. A. Hickner, Y. Meng, *Int. J. Hydrogen Energy* **2014**, *39*, 16123.
- [165] C. W. Carr, K. Sollner, *Biophys. J.* **1964**, *4*, 189.
- [166] a) X. Yan, C. Zhang, Z. Dong, B. Jiang, Y. Dai, X. Wu, G. He, *ACS Appl. Mater. Interfaces* **2018**, *10*, 32247; b) S. Liu, L. Wang, D. Li, B. Liu, J. Wang, Y. Song, *J. Mater. Chem. A* **2015**, *3*, 17590.
- [167] J. Qiu, J. Zhang, J. Chen, J. Peng, L. Xu, M. Zhai, J. Li, G. Wei, *J. Membr. Sci.* **2009**, *334*, 9.
- [168] P. P. Sharma, A. Paul, D. N. Srivastava, V. Kulshrestha, *ACS Omega* **2018**, *3*, 9872.

- [169] J. Dai, Y. Dong, P. Gao, J. Ren, C. Yu, H. Hu, Y. Zhu, X. Teng, *Polymer* **2018**, *140*, 233.
- [170] X. Wei, B. Li, W. Wang, *Polym. Rev.* **2015**, *55*, 247.
- [171] a) S. Peng, X. Yan, X. Wu, D. Zhang, Y. Luo, L. Su, G. He, *RSC Adv.* **2017**, *7*, 1852; b) H. Zhang, C. Ding, J. Cao, W. Xu, X. Li, H. Zhang, *J. Mater. Chem. A* **2014**, *2*, 9524.
- [172] a) S. C. Chieng, M. Kazacos, M. Skyllas-Kazacos, *J. Membr. Sci.* **1992**, *75*, 81; b) S. C. Chieng, M. Kazacos, M. Skyllas-Kazacos, *J. Power Sources* **1992**, *39*, 11; c) T. Mohammadi, M. Skyllas-Kazacos, *J. Appl. Electrochem.* **1997**, *27*, 153.
- [173] H. Zhang, H. Zhang, X. Li, Z. Mai, J. Zhang, *Energy Environ. Sci.* **2011**, *4*, 1676.
- [174] I. S. Chae, T. Luo, G. H. Moon, W. Ogieglo, Y. S. Kang, M. Wessling, *Adv. Energy Mater.* **2016**, *6*, 1600517.
- [175] X. L. Zhou, T. S. Zhao, L. An, L. Wei, C. Zhang, *Electrochim. Acta* **2015**, *153*, 492.
- [176] a) Y. Shi, X. Zhou, G. Yu, *Acc. Chem. Res.* **2017**, *50*, 2642; b) H. Chen, M. Ling, L. Hencz, H. Y. Ling, G. Li, Z. Lin, G. Liu, S. Zhang, *Chem. Rev.* **2018**, *118*, 8936; c) Z. Zhang, T. Zeng, Y. Lai, M. Jia, J. Li, *J. Power Sources* **2014**, *247*, 1; d) H. Zheng, R. Yang, G. Liu, X. Song, V. S. Battaglia, *J. Phys. Chem. C* **2012**, *116*, 4875.
- [177] N. Ohta, T. Sogabe, K. Kuroda, *Carbon* **2001**, *39*, 1434.
- [178] D. Bresser, D. Buchholz, A. Moretti, A. Varzi, S. Passerini, *Energy Environ. Sci.* **2018**, *11*, 3096.
- [179] B. S. Gupta, I. Reiniati, M.-P. G. Laborie, *Colloids Surf., A* **2007**, *302*, 388.
- [180] Q. Shi, S.-C. Wong, W. Ye, J. Hou, J. Zhao, J. Yin, *Langmuir* **2012**, *28*, 4663.
- [181] a) D. Shin, H. Park, U. Paik, *Electrochem. Commun.* **2017**, *77*, 103; b) J. Liu, D. G. D. Galpaya, L. Yan, M. Sun, Z. Lin, C. Yan, C. Liang, S. Zhang, *Energy Environ. Sci.* **2017**, *10*, 750.
- [182] a) W.-J. Song, S. H. Joo, D. H. Kim, C. Hwang, G. Y. Jung, S. Bae, Y. Son, J. Cho, H.-K. Song, S. K. Kwak, S. Park, S. J. Kang, *Nano Energy* **2017**, *32*, 255; b) J. Li, C. Daniel, S. J. An, D. Wood, *MRS Adv.* **2016**, *1*, 1029; c) N. Susarla, S. Ahmed, D. W. Dees, *J. Power Sources* **2018**, *378*, 660.
- [183] a) L. Lu, X. Han, J. Li, J. Hua, M. Ouyang, *J. Power Sources* **2013**, *226*, 272; b) B. Liu, K. Fu, Y. Gong, C. Yang, Y. Yao, Y. Wang, C. Wang, Y. Kuang, G. Pastel, H. Xie, E. D. Wachsman, L. Hu, *Nano Lett.* **2017**, *17*, 4917.
- [184] R. W. Nunes, J. R. Martin, J. F. Johnson, *Polym. Eng. Sci.* **1982**, *22*, 205.
- [185] S.-H. Yook, S.-H. Kim, C.-H. Park, D.-W. Kim, *RSC Adv.* **2016**, *6*, 83126.
- [186] J. Heine, U. Rodehorst, J. Badillo, M. Winter, P. Bieker, *Electrochim. Acta* **2015**, *155*, 110.
- [187] a) Y. Shi, L. Peng, Y. Ding, Y. Zhao, G. Yu, *Chem. Soc. Rev.* **2015**, *44*, 6684; b) M. Ling, J. Qiu, S. Li, C. Yan, M. J. Kiefel, G. Liu, S. Zhang, *Nano Lett.* **2015**, *15*, 4440.
- [188] C. W. Liew, R. Durairaj, S. Ramesh, *PLoS One* **2014**, *9*, 102815.
- [189] a) R. Amin-Sanayei, W. He, in *Advanced Fluoride-Based Materials for Energy Conversion* (Eds: T. Nakajima, H. Groult), Elsevier Inc. **2015**, pp. 225–235, <https://doi.org/10.1016/C2013-0-18650-3>; b) X. Zhao, S. Niketic, C.-H. Yim, J. Zhou, J. Wang, Y. Abu-Lebdeh, *ACS Omega* **2018**, *3*, 11684; c) J.-K. Kim, G. Cheruvally, J.-H. Ahn, Y.-G. Seo, D. S. Choi, S.-H. Lee, C. E. Song, *J. Ind. Eng. Chem.* **2008**, *14*, 371.
- [190] a) M. Osinska-Broniarz, A. Martyla, L. Majchrzycki, M. Nowicki, A. Sierczynska, *Eur. J. Chem.* **2016**, *7*, 182; b) A. M. Grillet, T. Humplik, E. K. Stirrup, S. A. Roberts, D. A. Barringer, C. M. Snyder, M. R. Janvrin, C. A. Appleby, *J. Electrochem. Soc.* **2016**, *163*, A1859; c) H. Maleki, G. Deng, A. Anani, J. Howard, *J. Electrochem. Soc.* **1999**, *146*, 3224; d) H. Maleki, J. R. Selman, R. B. Dinwiddie, H. Wang, *J. Power Sources* **2001**, *94*, 26; e) M. Wang, Q. Tan, L. Liu, J. Li, *ACS Sustainable Chem. Eng.* **2019**, *7*, 12799.
- [191] C. M. Costa, M. M. Silva, S. Lanceros-Méndez, *RSC Adv.* **2013**, *3*, 11404.
- [192] S. F. Lux, F. Schappacher, A. Balducci, S. Passerini, M. Winter, *J. Electrochem. Soc.* **2010**, *157*, A320.
- [193] a) A. Magasinski, B. Zdyrko, I. Kovalenko, B. Hertzberg, R. Burtovoy, C. F. Huebner, T. F. Fuller, I. Luzinov, G. Yushin, *ACS Appl. Mater. Interfaces* **2010**, *2*, 3004; b) I. Kovalenko, B. Zdyrko, A. Magasinski, B. Hertzberg, Z. Milicev, R. Burtovoy, I. Luzinov, G. Yushin, *Science* **2011**, *334*, 75; c) J. Drofenik, M. Gaberscek, R. Dominko, F. W. Poulsen, M. Mogensen, S. Pejovnik, J. Jamnik, *Electrochim. Acta* **2003**, *48*, 883.
- [194] Z. Karkar, D. Guyomard, L. Roue, B. Lestriez, *Electrochim. Acta* **2017**, *258*, 453.
- [195] a) L. Qiu, Z. Shao, W. Wang, F. Wang, D. Wang, Z. Zhou, P. Xiang, C. Xu, *RSC Adv.* **2014**, *4*, 24859; b) H. Park, D. Lee, T. Song, *Ind. Eng. Chem. Res.* **2018**, *57*, 8895.
- [196] X. Wang, J. Liu, Z. Gong, C. Huang, S. He, L. Yu, L. Gan, M. Long, *Electrochemistry* **2019**, *87*, 94.
- [197] L. Zhang, Y. Ding, J. Song, *Chin. Chem. Lett.* **2018**, *29*, 1773.
- [198] E. J. Kim, X. Yue, J. T. S. Irvine, A. R. Armstrong, *J. Power Sources* **2018**, *403*, 11.
- [199] J. Fei, Q. Sun, Y. Cui, J. Li, J. Huang, *J. Electroanal. Chem.* **2017**, *804*, 158.
- [200] M.-H. Lee, T.-H. Kim, C. Hwang, J. Kim, H.-K. Song, *Electrochim. Acta* **2017**, *225*, 78.
- [201] C. C. Nguyen, T. Yoon, D. M. Seo, P. Guduru, B. L. Lucht, *ACS Appl. Mater. Interfaces* **2016**, *8*, 12211.
- [202] a) K. Ui, S. Kikuchi, F. Mikami, Y. Kadoma, N. Kumagai, *J. Power Sources* **2007**, *173*, 518; b) J. Li, D.-B. Le, P. P. Ferguson, J. R. Dahn, *Electrochim. Acta* **2010**, *55*, 2991.
- [203] a) Z.-J. Han, K. Yamagiwa, N. Yabuuchi, J.-Y. Son, Y.-T. Cui, H. Oji, A. Kogure, T. Harada, S. Ishikawa, Y. Aoki, S. Komaba, *Phys. Chem. Chem. Phys.* **2015**, *17*, 3783; b) S. Aoki, Z.-J. Han, K. Yamagiwa, N. Yabuuchi, M. Murase, K. Okamoto, T. Kiyosu, M. Satoh, S. Komaba, *J. Electrochem. Soc.* **2015**, *162*, A2245.
- [204] C.-H. Jung, K.-H. Kim, S.-H. Hong, *ACS Appl. Mater. Interfaces* **2019**, *11*, 26753.
- [205] S.-Y. Lee, Y. Choi, K.-S. Hong, J. K. Lee, J.-Y. Kim, J.-S. Bae, E. D. Jeong, *Appl. Surf. Sci.* **2018**, *447*, 442.
- [206] J. Li, G. Zhang, Y. Yang, D. Yao, Z. Lei, S. Li, Y. Deng, C. Wang, *J. Power Sources* **2018**, *406*, 102.
- [207] L. Wei, C. Chen, Z. Hou, H. Wei, *Sci. Rep.* **2016**, *6*, 19583.
- [208] P.-F. Cao, M. Naguib, Z. Du, E. Stacy, B. Li, T. Hong, K. Xing, D. N. Voylov, J. Li, D. L. Wood, A. P. Sokolov, J. Nanda, T. Saito, *ACS Appl. Mater. Interfaces* **2018**, *10*, 3470.
- [209] S.-E. Cheon, J.-H. Cho, K.-S. Ko, C.-W. Kwon, D.-R. Chang, H.-T. Kim, S.-W. Kim, *J. Electrochem. Soc.* **2002**, *149*, A1437.
- [210] a) D. Guy, B. Lestriez, D. Guyomard, *Adv. Mater.* **2004**, *16*, 553; b) J. M. Tarascon, A. S. Gozdz, C. Schmutz, F. Shokoohi, P. C. Warren, *Solid State Ionics* **1996**, *86–88*, 49; c) B. Tran, I. O. Oladeji, Z. Wang, J. Calderon, G. Chai, D. Atherton, L. Zhai, *Electrochim. Acta* **2013**, *88*, 536.
- [211] H. Dong, J.-K. Hyun, C. Durham, R. A. Wheeler, *Polymer* **2001**, *42*, 7809.
- [212] a) R. A. Sanders, A. G. Snow, R. Frech, D. T. Glatzhofer, *Electrochim. Acta* **2003**, *48*, 2247; b) H. Wang, M. Ling, Y. Bai, S. Chen, Y. Yuan, G. Liu, C. Wu, F. Wu, *J. Mater. Chem. A* **2018**, *6*, 6959.
- [213] a) W. Chen, T. Qian, J. Xiong, N. Xu, X. Liu, J. Liu, J. Zhou, X. Shen, T. Yang, Y. Chen, C. Yan, *Adv. Mater.* **2017**, *29*, 1605160; b) J. Liao, Z. Liu, X. Liu, Z. Ye, *J. Phys. Chem. C* **2018**, *122*, 25917.
- [214] W. Chen, T. Lei, T. Qian, W. Lv, W. He, C. Wu, X. Liu, J. Liu, B. Chen, C. Yan, J. Xiong, *Adv. Energy Mater.* **2018**, *8*, 1702889.
- [215] L. Yan, X. Gao, F. Wahid-Pedro, J. T. Ernest Quinn, Y. Meng, Y. Li, *J. Mater. Chem. A* **2018**, *6*, 14315.
- [216] C.-H. Tsao, C.-H. Hsu, P.-L. Kuo, *Electrochim. Acta* **2016**, *196*, 41.

- [217] Z. Wan, D. Lei, W. Yang, C. Liu, K. Shi, X. Hao, L. Shen, W. Lv, B. Li, Q.-H. Yang, F. Kang, Y.-B. He, *Adv. Funct. Mater.* **2019**, *29*, 1805301.
- [218] Z. Karkar, T. Jaouhari, A. Tranchot, D. Mazouzi, D. Guyomard, B. Lestriez, L. Roué, *J. Power Sources* **2017**, *371*, 136.
- [219] J. Xu, L. Zhang, Y. Wang, T. Chen, M. Al-Shroofy, Y.-T. Cheng, *ACS Appl. Mater. Interfaces* **2017**, *9*, 3562.
- [220] L.-H. Huang, D. Chen, C.-C. Li, Y.-L. Chang, J.-T. Lee, *J. Electrochem. Soc.* **2018**, *165*, A2239.
- [221] J. Landesfeind, A. Eldiven, H. A. Gasteiger, *J. Electrochem. Soc.* **2018**, *165*, A1122.
- [222] X. Zhu, F. Zhang, L. Zhang, L. Zhang, Y. Song, T. Jiang, S. Sayed, C. Lu, X. Wang, J. Sun, Z. Liu, *Adv. Funct. Mater.* **2018**, *28*, 1705015.
- [223] D.-J. Yoo, A. Elabd, S. Choi, Y. Cho, J. Kim, S. J. Lee, S. H. Choi, T.-w. Kwon, K. Char, K. J. Kim, A. Coskun, J. W. Choi, *Adv. Mater.* **2019**, *31*, 1901645.
- [224] a) P. D. Frischmann, Y. Hwa, E. J. Cairns, B. A. Helms, *Chem. Mater.* **2016**, *28*, 7414; b) Y. Hwa, P. D. Frischmann, B. A. Helms, E. J. Cairns, *Chem. Mater.* **2018**, *30*, 685.
- [225] C.-T. Lin, T.-Y. Huang, J.-J. Huang, N.-L. Wu, M.-k. Leung, *J. Power Sources* **2016**, *330*, 246.
- [226] T. Liu, Q. Chu, C. Yan, S. Zhang, Z. Lin, J. Lu, *Adv. Energy Mater.* **2019**, *9*, 1802645.
- [227] G. Zhou, K. Liu, Y. Fan, M. Yuan, B. Liu, W. Liu, F. Shi, Y. Liu, W. Chen, J. Lopez, D. Zhuo, J. Zhao, Y. Tsao, X. Huang, Q. Zhang, Y. Cui, *ACS Cent. Sci.* **2018**, *4*, 260.
- [228] L. Li, L. Ma, D. Prendergast, B. A. Helms, T. A. Pascal, D. Prendergast, B. A. Helms, J. G. Connell, F. Y. Fan, Y.-M. Chiang, S. M. Meckler, *Nat. Commun.* **2017**, *8*, 2277.
- [229] S. Chauque, F. Y. Oliva, O. R. Camara, R. M. Torresi, *J. Solid State Electrochem.* **2018**, *22*, 3589.
- [230] L. Wang, T. Liu, X. Peng, W. Zeng, Z. Jin, W. Tian, B. Gao, Y. Zhou, P. K. Chu, K. Huo, *Adv. Funct. Mater.* **2018**, *28*, 1704858.
- [231] T. M. Higgins, S.-H. Park, P. J. King, C. Zhang, N. McEvoy, N. C. Berner, D. Daly, A. Shmeliov, U. Khan, G. Duesberg, V. Nicolosi, J. N. Coleman, *ACS Nano* **2016**, *10*, 3702.
- [232] W. Zeng, L. Wang, X. Peng, T. Liu, Y. Jiang, F. Qin, L. Hu, P. K. Chu, K. Huo, Y. Zhou, *Adv. Energy Mater.* **2018**, *8*, 1702314.
- [233] D. Liu, Y. Zhao, R. Tan, L.-L. Tian, Y. Liu, H. Chen, F. Pan, *Nano Energy* **2017**, *36*, 206.
- [234] H. Zhao, Y. Wei, C. Wang, R. Qiao, W. Yang, P. B. Messersmith, G. Liu, *ACS Appl. Mater. Interfaces* **2018**, *10*, 5440.
- [235] X. Y. Wang, Y. Zhang, Y. J. Shi, X. Y. Zeng, R. X. Tang, L. M. Wei, *Ionics* **2019**, *25*, 5323.
- [236] K. Lee, T.-H. Kim, *Electrochim. Acta* **2018**, *283*, 260.
- [237] X. Liu, T. Qian, J. Liu, J. Tian, L. Zhang, C. Yan, *Small* **2018**, *14*, 1801536.
- [238] S. Bode, M. Enke, M. Hernandez, R. K. Bose, A. M. Grande, S. van der Zwaag, U. S. Schubert, S. J. Garcia, M. D. Hager, in *Self-healing Materials* (Eds: M. D. Hager, S. van derZwaag, U. S. Schubert), Springer International Publishing, Switzerland **2016**, pp. 113–142.
- [239] Z.-H. Wu, J.-Y. Yang, B. Yu, B.-M. Shi, C.-R. Zhao, Z.-L. Yu, *Rare Met.* **2019**, *38*, 832.
- [240] T. Munaoka, X. Yan, J. Lopez, J. W. F. To, J. Park, J. B. H. Tok, Y. Cui, Z. Bao, *Adv. Energy Mater.* **2018**, *8*, 1703138.
- [241] G. Zhang, Y. Yang, Y. Chen, J. Huang, T. Zhang, H. Zeng, C. Wang, G. Liu, Y. Deng, *Small* **2018**, *14*, 1801189.
- [242] a) L. Chai, Q. Qu, L. Zhang, M. Shen, L. Zhang, H. Zheng, *Electrochim. Acta* **2013**, *105*, 378; b) R. Rohan, T.-C. Kuo, C.-Y. Chiou, Y.-L. Chang, C.-C. Li, J.-T. Lee, *J. Power Sources* **2018**, *396*, 459; c) T. Chen, Q. Zhang, J. Pan, J. Xu, Y. Liu, M. Al-Shroofy, Y.-T. Cheng, *ACS Appl. Mater. Interfaces* **2016**, *8*, 32341; d) B. O. El, D. Beneventi, D. Chaussy, F. Alloin, Y. Bultel, *Nanomaterials* **2018**, *8*, 982; e) Q. Li, H. Yang, L. Xie, J. Yang, Y. Nuli, J. Wang, *Chem. Commun.* **2016**, *52*, 13479; f) Z. Wang, G. Dang, Q. Zhang, J. Xie, *Int. J. Electrochem. Sci.* **2017**, *12*, 7457.
- [243] I. Donati, A. Vetere, A. Gamini, G. Skjaak-Braek, A. Coslovi, C. Campa, S. Paoletti, *Biomacromolecules* **2003**, *4*, 624.
- [244] a) M. Fertah, A. Belfkira, E. m. Dahmane, M. Taourirte, F. Brouillette, *Arabian J. Chem.* **2017**, *10*, S3707; b) S. T. Moe, K. I. Draget, G. Skjak-Braek, O. Smidsrod, *Food Polysaccharides and Their Applications*, Taylor & Francis, Oxfordshire, UK **1995**, pp. 245–286.
- [245] Z.-Y. Wu, L. Deng, J.-T. Li, Q.-S. Huang, Y.-Q. Lu, J. Liu, T. Zhang, L. Huang, S.-G. Sun, *Electrochim. Acta* **2017**, *245*, 371.
- [246] S.-J. Zhang, Y.-P. Deng, Q.-H. Wu, Y. Zhou, J.-T. Li, Z.-Y. Wu, Z.-W. Yin, Y.-Q. Lu, C.-H. Shen, L. Huang, S.-G. Sun, *ChemElectroChem* **2018**, *5*, 1321.
- [247] S. Zhang, S. Ren, D. Han, M. Xiao, S. Wang, Y. Meng, *J. Power Sources* **2019**, *438*, 227007.
- [248] T. Sun, Z.-J. Li, H.-G. Wang, D. Bao, F.-I. Meng, X.-B. Zhang, *Angew. Chem., Int. Ed.* **2016**, *55*, 10662.
- [249] G. Li, M. Ling, Y. Ye, Z. Li, J. Guo, Y. Yao, J. Zhu, Z. Lin, S. Zhang, *Adv. Energy Mater.* **2015**, *5*, 1500878.
- [250] N. Akhtar, H. Shao, F. Ai, Y. Guan, Q. Peng, H. Zhang, W. Wang, A. Wang, B. Jiang, Y. Huang, *Electrochim. Acta* **2018**, *282*, 758.
- [251] C. Chen, S. H. Lee, M. Cho, J. Kim, Y. Lee, *ACS Appl. Mater. Interfaces* **2016**, *8*, 2658.
- [252] G. Hwang, J.-M. Kim, D. Hong, C.-K. Kim, N.-S. Choi, S.-Y. Lee, S. Park, *Green Chem.* **2016**, *18*, 2710.
- [253] J. Dominguez-Robles, R. Sanchez, E. Espinosa, P. Diaz-Carrasco, M. T. Garcia-Dominguez, A. Rodriguez, *Int. J. Biol. Macromol.* **2017**, *104*, 909.
- [254] a) D. Schmidt, B. Haeupler, C. Stolze, M. D. Hager, U. S. Schubert, *J. Polym. Sci., Part A: Polym. Chem.* **2015**, *53*, 2517; b) A. Wild, M. Strumpf, B. Haeupler, M. D. Hager, U. S. Schubert, *Adv. Energy Mater.* **2017**, *7*, 1601415; c) T. Xu, J. Xiong, X. Du, Y. Zhang, S. Song, C. Xiong, L. Dong, *J. Phys. Chem. C* **2018**, *122*, 20057; d) K. Nakahara, J. Iriyama, S. Iwasa, M. Suguro, M. Satoh, E. J. Cairns, *J. Power Sources* **2007**, *165*, 398.
- [255] S. Iwasa, T. Nishi, S. Nakamura, *J. Electroanal. Chem.* **2017**, *805*, 171.
- [256] H. Woehlke, J. Steinkoenig, C. Lang, L. Michalek, V. Trouillet, P. Krolla, A. S. Goldmann, L. Barner, J. P. Blinco, C. Barner-Kowollik, K. E. Fairfull-Smith, *Langmuir* **2018**, *34*, 3264.
- [257] S. Komaba, T. Tanaka, T. Ozeki, T. Taki, H. Watanabe, H. Tachikawa, *J. Power Sources* **2010**, *195*, 6212.
- [258] K. S. Weeraratne, A. A. Alzharani, H. M. El-Kaderi, *ACS Appl. Mater. Interfaces* **2019**, *11*, 23520.



Adrian Saal studied Chemistry at the Friedrich Schiller University Jena and obtained his master's degree in 2017. Since 2018, he has been a Ph.D. student in the group of Prof. Dr. U. S. Schubert, where he is investigating novel active materials for polymer-based organic thin-film batteries.



Tino Hagemann studied Chemistry at the Friedrich Schiller University Jena, Germany. He obtained his diploma degree in Chemistry in the field of metal complexes. He joined the group of Prof. U. S. Schubert as a Ph.D. student in 2013, where he developed organic electrolytes for redox-flow batteries. He completed his Ph.D. in 2018 and has been working since as a postdoc on polymer batteries as alternative battery concepts for the lithium-ion battery.



Ulrich S. Schubert performed his Ph.D. studies at the Universities of Bayreuth and South Florida. After a postdoctoral training at the University of Strasbourg, he moved to the TU Munich and obtained his Habilitation in 1999. In 1999–2000 he was Professor at the University of Munich, and during 2000–2007 Full-Professor at the TU Eindhoven. Since 2007, he is a Full-Professor at the Friedrich Schiller University Jena, Germany. He is founding director of the Center for Energy and Environmental Chemistry Jena (CEEC Jena) and coordinator of the DFG priority program “Polymer-based Batteries” (SPP 2248).